Transcriptional regulation of effector-triggered immunity (ETI) in plants: from tissue to cells

Chhillar, H.

Transcriptional regulation of effector-triggered immunity (ETI) in plants: from tissue to cells

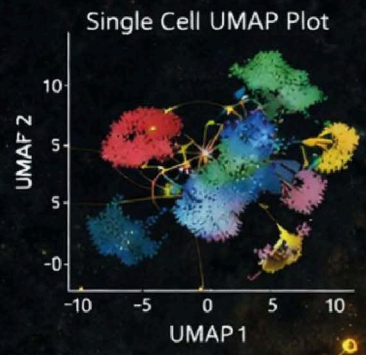

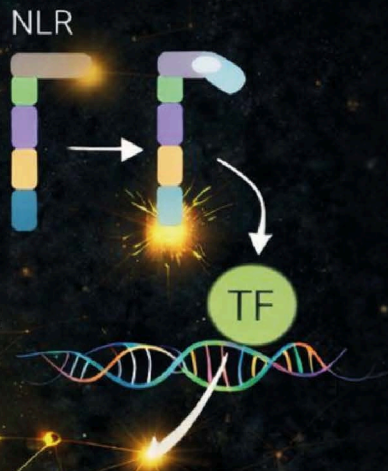

Himanshu Chhillar

Transcriptional regulation of effector-triggered immunity (ETI) in plants: from tissue to cells

Himanshu Chhillar, 2026

A part of this thesis is supported by European Research Council Starting Grant ‘R-ELEVATION’ (grant agreement: 101039824)
Front and back cover: designed by Himanshu Chhillar using Canva AI
Printed by: Proefschrifterij
ISBN number:

Transcriptional regulation of effector-triggered immunity (ETI) in plants: from tissue to cells

Proefschrift

ter verkrijging van
de graad van doctor aan de Universiteit Leiden,
op gezag van rector magnificus prof.dr. S. de Rijcke,
volgens besluit van het college voor promoties
te verdedigen op donderdag 3 juni 2026
klokke 10:00 uur

door

Himanshu Chhillar
geboren te Haryana, India
in 1997

Promotor:

Prof. dr. R. Offringa

Co-promotor:

Dr. P. Ding

Promotiecommissie:

Prof. dr. A.H. Meijer

Prof. dr. T.M. Bezemer

Prof. dr. A.T. Kovács

Prof. dr. G.P. van Wezel

Dr. J.S. Pfeilmeier (University of Amsterdam)

Prof. dr. S. Balazadeh (University of Göttingen)

Table of contents

Chapter 1

General Introduction

Himanshu Chhillar[1], Niels Aerts[2], Saskia CM Van Wees[2], Pingtao Ding[1]

[1]Institute of Biology Leiden, Leiden University, 2333 BE Leiden, The Netherlands
[2]Plant-Microbe Interactions, Department of Biology, Science4Life, Utrecht University, 3508 TB Utrecht, The Netherlands

The sections 3 (Transcriptional regulation of plant innate immunity) and 4 (post-transcriptional regulation) from this chapter are published in review articles: Essays in Biochemistry (2022) Sep 30;66(5):607–620. doi: 10.1042/EBC20210100

Overview of plant immunity

Plants are constantly exposed to a variety of pathogens which pose a serious threat to crop productivity. Plant pathogens have caused major crop disease outbreaks in the past with Great Irish Famine of 19th century being one of the most devastating examples which lead to emigration/death of around 2.5 million people[1]. On top of that, many food and cash crops, such as wheat, rice, maize and others are still under threat of many different types of diseases[2]. According to the Food and Agriculture Organization of the United Nations (FAO) plant diseases lead to approximately 20-40% of global crop loss annually, costing about US$220 billion[3]. In response, global agricultural pesticide use dominated by herbicides has increased steadily over recent decades, nearly doubling since 1990, with associated economic costs rising to almost USD 50 billion annually, reflecting a growing reliance on chemical disease management strategies which pose severe health risks on consumers[4]. These limitations underscore the urgent need for sustainable, disease management strategies that rely on the plant's own innate defense mechanisms. To defend themselves, plants have the inherent capability of responding to the pathogenic cues by eliciting a multitude of defense responses that are mediated through complex signaling networks[5]. Physical barriers on plant surface such as epidermal hairs, wax layers and the cell wall being the first line of defense to prevent pathogen invasion[6]. In addition, anti-microbial molecules in the apoplast acts as chemical barrier to limit pathogen progression[7]. However, some pathogens have evolved to by-bass the physical and chemical barriers to colonize the plants. Plant defense responses can then be initiated by recognition of general pathogen-associated molecular patterns (PAMPs) by cell-surface localized pattern-recognition receptors (PRRs) leading to pattern-triggered immunity (PTI) and that of specific pathogen effector molecules secreted into plant cells recognized by intracellular nucleotide-binding

leucine-rich repeat receptors (NLRs) leading to effector-triggered immunity (ETI)[5]. Conceptually, PTI and ETI in plants share some classical features of innate immune mechanisms in animals, where conserved microbial features and intracellular danger signals are sensed by pattern-recognition receptors and NOD-like receptors, respectively[8,9]. However, unlike animals, plants lack specialized immune cells and adaptive immunity; instead, each cell autonomously perceives pathogens and mounts defense responses. Historically, plant immunity was described using a dichotomous framework of PTI, also termed as PAMP-triggered defense, and ETI, previously referred to as gene-for-gene resistance[10,11]. Emerging evidence has challenged this strict separation, leading to the view that PTI and ETI operate as overlapping, mutually reinforcing modules within a continuum of integrated immune signaling rather than as discrete defense layers[12,13]. These layers of immunity are fine-tuned by spatial, temporal, and molecular contexts. This complexity is further underscored by the roles of transcriptional regulators, calcium signaling, and chromatin dynamics in shaping immune outputs[14–16]. Additionally, recent advances in single-cell and spatial transcriptomics[17] are revealing unprecedented insights into how immunity is executed at the resolution of individual cell types challenging the notion of uniform immune responses across plant tissues.

1. Cell surface immunity

1.1 PRR immune receptor

Plant defense responses can be initiated by recognition of general PAMPs by cell-surface localized PRRs leading to PTI and that of specific pathogen effector molecules secreted into plant cells recognized by intracellular NLRs, activating ETI[10] (**Figure 1**). PRRs can be either receptor-like proteins (RLPs) or receptor-like kinases (RLKs). Both RLPs and RLKs possess an extracellular ectodomain (ECD) and a transmembrane

domain, however RLPs lack a C-terminal intracellular kinase domain[5,18]. Based on their ECD they are classified into different subfamilies: leucine-rich repeat (LRR) domain, lysinemotifs (LysM), lectin domain, or epidermal growth factor (EGF)-like domain[19–21]. PRRs perceive a wide range of PAMPs such as peptides, lipids, peptidoglycans (PGs), and polysaccharides from prokaryotes (bacteria) and chitin and oligo-galacturonides (OGs) from eukaryotes (fungi and oomycetes)[18].

1.2 PRR signaling

Many PRRs acts together with co-receptors to transduce the downstream signaling. Upon ligand perception and binding LRR, RLKs recruit BRI1-ASSOCIATED RECEPTOR 2 KINASE (BAK1), a member of SOMATIC EMBRYOGENESIS RECEPTOR KINASES (SERKs) family[20]. For instance, LRR-RLK FLAGELLIN SENSING2 (FLS2), EF-TU RECEPTOR (EFR), and PEP RECEPTOR 1 (PEPRs) require the coreceptors BAK1 and BAK1-LIKE 1 (BKK1) both of which are members of the SOMATIC EMBRYOGENESIS RECEPTOR KINASE (SERK) family[20,22–24]. On the other hand RLP23 requires BAK1 and SUPPRESSOR OF BIR1 (SOBIR1) as co-receptor for promoting downstream signaling[25]. Additionally RLP23 is suggested being one of the PRR which might require lipase-like protein family to activate some downstream immune responses[26], although this mechanism needs further investigation.

Some RLKs, such as members of the BAK1-INTERACTING RECEPTOR-LIKE KINASE (BIR) family, negatively regulate immune signaling by sequestering SOBIR1 and BAK1, thereby preventing autoactivation[27,28]. Additionally, RLKs like FERONIA have been reported to suppress the interaction between FLS2 and BAK1 by interacting with RAPID ALKALINIZATION FACTORS (RALF23) thereby modulating immune signaling[29]. These findings suggest that PRRs possess both activating and inhibitory roles in modulating downstream responses. Upon ligand

binding, heteromeric receptor complexes form between PRRs and their co-receptors, bringing their cytoplasmic kinase domains into close proximity. This proximity facilitates trans-phosphorylation and subsequent activation of receptor-like cytoplasmic kinases (RLCKs) such as BIK1, initiating downstream signaling cascades[30,31]. Upon PRR activation, a rapid series of cellular events is triggered, including the production of reactive oxygen species (ROS), MAPK cascade activation, cytosolic calcium influx, callose deposition, and extensive transcriptional reprogramming[323334]. Collectively, these physiological and cellular changes constitute pattern-triggered immunity (PTI).

2. Intracellular immunity

2.1 NLRs immune receptors

Adapted pathogens usually deliver a suite of effectors into the plants, which promotes pathogen virulence and results in effector-triggered susceptibility (ETS) in host plants[10]. Plant pathogenic bacteria deliver effectors into host cells using type III secretion systems (TTSS)[35]. Pathogen effectors are recognised by specific disease resistance (R) genes which encode NLR proteins[10,36]. *Arabidopsis thaliana* (Arabidopsis) have around 150 NLR coding genes which are broadly classified into 2 categories[37]. TIR-NB-LRR (TNL) group with an N-terminal Toll and interleukin-1 (TIR)-like domain such as RESISTANT TO PSEUDOMONAS SYRINGAE 4 (RPS4)/RESISTANCE TO RALSTONIA SOLANACEARUM 1 (RRS1) which recognize bacteria carrying AvrRps4[38,39], and CC-NB-LRR (CNL) group with an N-terminal coiled-coil domain such as RESISTANCE TO PSEUDOMONAS SYRINGAE PROTEIN 2 (RPS2) which recognize bacteria carrying AvrRps2[40]. Besides their division into TNLs and CNLs, NLRs can also be distinguished by their functional contribution to immune responses. Certain NLRs act as effector sensors, while helper NLRs (hNLRs) act downstream to relay signaling from these

sensors and promote defense activation. In Arabidopsis most of TNLs and only some CNLs require hNLRs ACTIVATED DISEASE RESISTANCE 1 (ADR1s) and N REQUIREMENT GENE 1 (NRG1s) for mediating downstream immune signaling[41–44]. Downstream signaling also differs between NLR classes, TNLs (e.g., RPS4/RRS1) transmit defense signals through the ENHANCED DISEASE SUSCEPTIBILITY 1 (EDS1) pathway, which involves complex formation with lipase-like proteins PHYTOALEXIN DEFICIENT 4 (PAD4) and SENESCENCE ASSOCIATED GENE 101 (SAG101)[45,46]. On the other hand, classical CNL receptors such as RESISTANCE TO PSEUDOMONAS SYRINGAE PV MACULICOLA (RPM1) and RPS2 require NON-RACE-SPECIFIC DISEASE RESISTANCE 1 (NDR1) for full resistance output[45].

NLRs can detect effectors through direct binding like the TNL RECOGNITION TO PERONOSPORA PARASITICA (RPP1) from Arabidopsis recognizes the *Hyaloperonospora arabidopsidis* (Hpa) effector ARABIDOPSIS THALIANA RECOGNIZED1 (ATR1)[47]. On the other hand NLRs can detect the effectors by guarding host components called guard hypothesis[19]. For instance, Arabidopsis NLRs RPS2 and RPM1 monitor the status of the RPM1-INTERACTING PROTEIN 4 (RIN4) protein[48], which is targeted pathogen effectors. Additionally, the decoy model proposed later by that hosts can evolve alleles or gene copies (paralogs) that don't directly serve essential defense roles[49]. Instead, they act as deceptive copies, resembling real pathogen targets which can also be monitored by NLRs to trigger immune response.

2.2 Key signaling module in ETI: the EDS1 signaling

Upon activation TNLs come in close proximity upon oligomerization which in turn activates the NADase and 2′,3′-cAMP/cGMP synthase activity[9,50–52] which leads to the synthesis of some small molecules like v-cADPR/ADPR/NAM and 2',3'-cNMP that is proposed to activate the

downstream signaling[50,53,54]. Upon TNL activation, the lipase-like proteins SAG101 and EDS1 interact with NRG1[55], while PAD4 and EDS1 associate with ADR1[43] (**Figure 1**). These interactions lead to the formation of heteromeric complexes, which then activate immune responses, including defense-related gene expression and the hypersensitive response (HR). Interestingly, it has been shown that these EDS1-SAG101-NRG1 and EDS1-PAD4-ADR1 have some unequal redundant roles during PTI+ETI activation[56]. More recently, it has been shown that activation and association of helper NLRs and lipase-like protein to form resistosomes, induce calcium influx to promote downstream defense responses[57,58] (**Figure 1**). In addition to these modules, a distinct class of helper NLRs termed NRCs (NLRs required for cell death), predominantly found in Solanaceae species, act as central signaling hubs downstream of multiple sensor NLRs. Upon activation, NRCs oligomerize to form resistosome-like calcium channels that are sufficient to trigger cell death and immune signaling[59,60], highlighting both conserved and lineage-specific strategies for ETI signal execution. Although much progress has been made in dissecting the signaling pathway. However, the contribution of crucial immune regulators in governing the ETI specific responses remains inadequately understood.

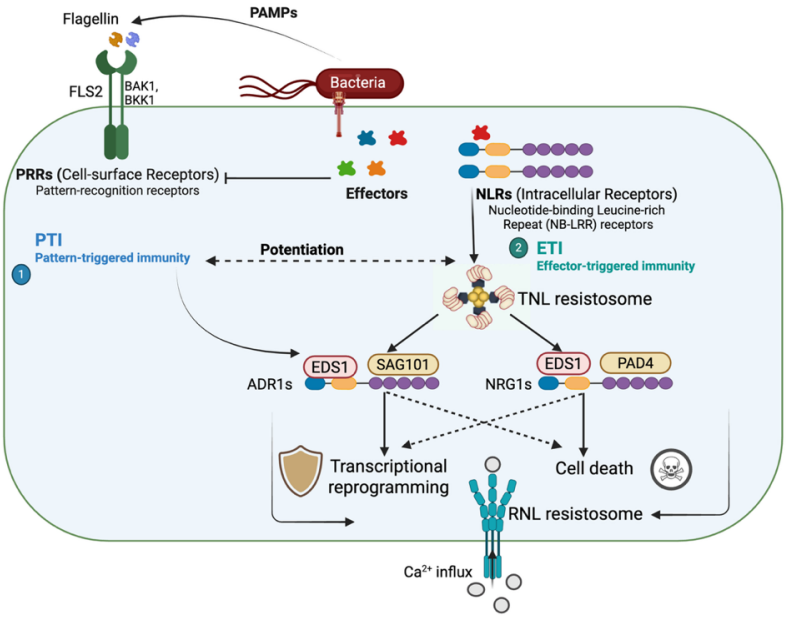

Figure 1. Layered plant immune signaling pathways coordinated by cell-surface and intracellular receptors. The schematic illustration of layered immune system in plants, highlighting how cell-surface and intracellular receptors coordinate immune responses upon pathogen recognition. Pattern-recognition receptors (PRRs), such as FLAGELLIN-SENSING 2 (FLS2), detect conserved pathogen-associated molecular patterns (PAMPs) such as bacterial flagellin and initiate pattern-triggered immunity (PTI). Upon PAMP binding, PRRs form complexes with co-receptors like BRI1-ASSOCIATED RECEPTOR 2 KINASE (BAK1) and BAK1-LIKE 1 (BKK1), leading to activation of early defense responses. To overcome PTI, pathogens deliver effectors into host cells. These effectors are recognized by intracellular nucleotide-binding leucine-rich repeat receptors (NLRs), which activate effector-triggered immunity (ETI). TIR-NLR activation promotes resistosomes that trigger the ENHANCED DISEASE SUSCEPTIBILITY 1 (EDS1) signaling pathway. EDS1 associates with PHYTOALEXIN DEFICIENT 4 (PAD4) and ACTIVATED DISEASE RESISTANCE 1 (ADR1), or with SENESCENCE ASSOCIATED GENE 101 (SAG101) and N REQUIREMENT GENE 1 (NRG1), to form two distinct signaling modules: EDS1-PAD4-ADR1 and EDS1–SAG101–NRG1. Both modules contribute to immune

responses via the formation of helper NLRs (hNLRs) resistosomes, leading to calcium (Ca^{2+}) influx, transcriptional reprogramming, and hypersensitive cell death. The diagram emphasizes that both ADR1 and NRG1 contribute to hNLRs resistosome assembly, with the ADR1 module playing a greater role in defense gene activation, and the NRG1 module being more involved in promoting cell death.

3. Transcriptional regulation of plant innate immunity

3.1 Role of transcription factors

The timing and efficiency of immune transcriptome activation are critical determinants of a plant's ability to mount an effective defense against invading pathogens. Among the various cellular components involved in transcriptional reprogramming, transcription factors (TFs) play a central and well-characterized role. Extensive genetic and functional studies have demonstrated that mutations in key TF families including WRKYs, TGAs, NACs, CALMODULIN-BINDING PROTEIN 60 (CBP60s), ETHYLENE RESPONSE FACTORS (ERFs), BASIC LEUCINE ZIPPER (bZIPs), BASIC HELIX-LOOP-HELIX (bHLHs), MYBs, CALMODULIN-BINDING TRANSCRIPTION ACTIVATOR (CAMTAs), and TCPs can profoundly alter disease resistance phenotypes across a wide range of plant-pathogen interactions[61–67]. These TFs are responsible for activating and fine-tuning the expression of numerous immune-related genes, often integrating upstream signals such as salicylic acid (SA), jasmonic acid (JA), and ethylene (ET) to coordinate context-specific responses.

The central role of TFs in immunity makes them frequent targets of pathogen effectors, which have evolved to manipulate host transcription in order to suppress defense and promote infection[68–70]. Numerous bacterial, fungal, and oomycete pathogens deliver effector proteins directly into host cells to interfere with transcriptional regulators including TFs, transcriptional co-activators, repressors, and components of the

Mediator complex **(Table 1).** Many of these effectors specifically manipulate hormone signaling pathways, especially those involving SA[71,72], JA[73], or the crosstalk between the two[74–77]. By hijacking these signaling hubs, pathogens enhance host susceptibility in a manner tailored to their lifestyle for example, by repressing SA responses to benefit biotrophs or suppressing JA signaling to assist necrotrophs. Overall, this growing body of evidence underscores the vulnerability and importance of transcriptional regulation as both a defensive strength and a strategic weak point in plant pathogen interactions.

Table 1. Pathogen effectors and their host targets that are involved in transcriptional regulation during plant immunity. This table summarizes some well-studied effectors secreted by different pathogens that hijack diverse transcriptional regulators of the host plant, including transcription factors, and transcriptional (co-) activators and repressors, to facilitate infection.

Pathogens	**Effector**	**Function of host target**	**Host target**	**Host species**	**Ref.**
Ralstonia solanacearum	RipAB	Transcription factor (TF)	TGAs	*Arabidopsis thaliana*	[78]
Xanthomonas campestris pv *v esicatoria*	XopD	Transcription factor (TF)	MYB30	*Arabidopsis thaliana*	[79]
Xanthomonas campestris pv *v esicatoria*	XopS	Transcription factor (TF)	WRKY40	*Capsicum annuum*	[77]
Phytoplasma	Phyllogen	Transcription factor (TF)	MADS-box	*Arabidopsis thaliana*, *Oryza sativa*	[80]

Hyaloperonospora arabidopsidis (*Hpa*)	HaRxL44	Mediator complex	MED19a	*Arabidopsis thaliana*	[75]
Hyaloperonospora arabidopsidis (*Hpa*)	HaRxL21	Transcriptional Co-repressor	TOPLESS (TPL)	*Arabidopsis thaliana*	[81]
Pseudomonas syringae	HopZ1 and HopX1	Transcriptional repressor	JASMONA-TE-ZIM DOMAIN (JAZ)	*Arabidopsis thaliana*	[74,76]
Laccaria bicolor	MiSSP7	Transcriptional repressor	JASMONA-TE-ZIM DOMAIN (JAZ)	*Populus trichocarpa*	[73]
Psuedomonas syringae	AvrPtoB	Transcriptional Co-activator	NONEXPR-ESSER OF PR GENES1 (NPR1)	*Arabidopsis thaliana*	[72]
Phytopthora capsici	RxLR48	Transcriptional Co-activator	NONEXPR-ESSER OF PR GENES1 (NPR1)	*Arabidopsis thaliana*	[71]

3.2 Multi-level regulation of transcriptional control

Plant immune transcriptional regulation is orchestrated through a complex, multi-level network involving both general and highly specific responses (**Figure 2**). Early immune responses often involve a general stress response, which is activated by both biotic and abiotic stressors[82–

[85], followed by more tailored transcriptional programs specific to the eliciting pathogen or molecular pattern[82,83,86–92]. This dynamic regulation is mediated by several layers, including post-translational modifications of transcription factors (TFs) such as phosphorylation[93,94], SUMOylation[95,96], and ubiquitination[97–101] which modulate TF activity, DNA binding, and stability. Together, these regulatory strategies provide plants with the flexibility and precision required to interpret diverse immune cues and mount appropriately scaled defense responses.

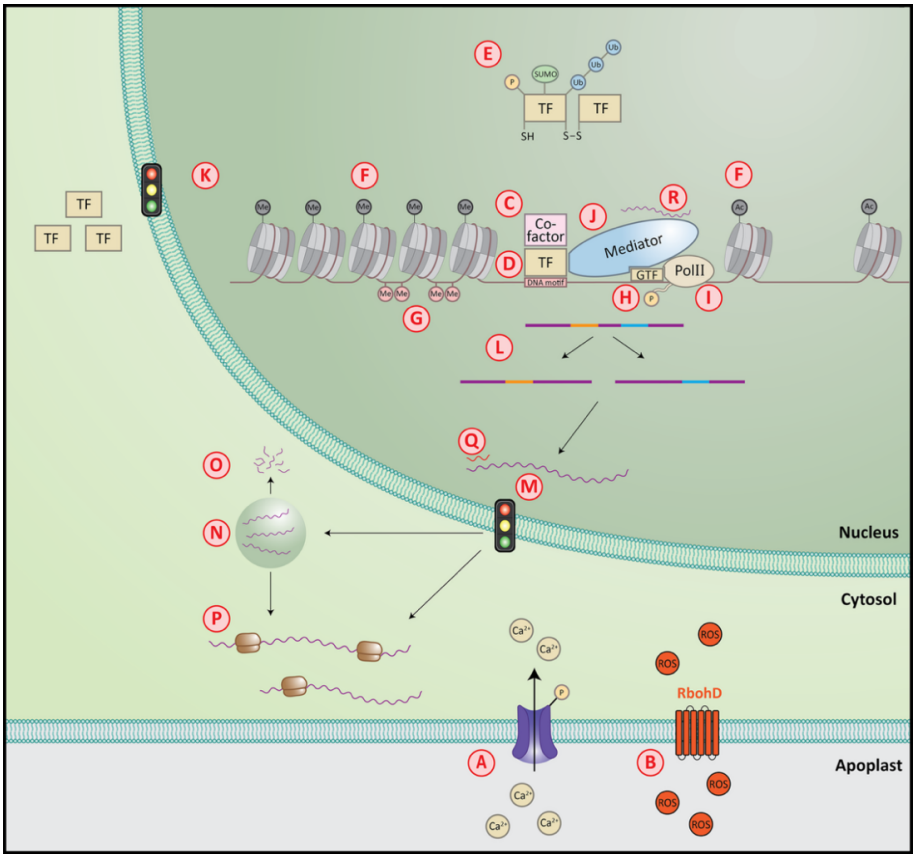

Figure 2. Regulation of transcriptional control occur at multiple levels. Mechanisms involved in the regulation of immune-related transcription. (A) regulation of calcium (Ca^{2+}) influx, which may lead to post-translational modifications of TFs; (B) generation of ROS by RbohD, which may lead to post-translational modifications of TFs (see also Figure 2E); (C) co-factors that may contribute to regulation of transcription; (D) TFs regulate transcription by binding to a motif; (E) post-translational modifications of TFs, such as phosphorylation (P), sumoylation (SUMO), ubiquitination (Ub) and forming of oligomers through S-S bridges depending on the redox state; (F) modifications of histones (methylation [Me] or acetylation [Ac]) to regulate the chromatin state; (G) methylation of DNA; (H) phosphorylation of the C-terminal domain of RNA-polymerase II (PolII) promotes transcription; (I) PolII may initiate transcription at alternative transcription start sites; (J) the Mediator complex forms the bridge between specific TFs, general TFs (GTF) and PolII; (K) selective import of TFs or other proteins; (L) alternative splicing; (M) selective retention of mRNAs in the nucleus; (N) temporary storage of mRNAs in stress granules or P-bodies; (O) degradation of mRNAs from P-bodies; (P) release of mRNAs from stress granules or P-bodies into the cytosol, followed by translation; (Q) post-transcriptional gene silencing by small RNAs; (R) long non-coding RNAs can regulate transcription in different ways, depicted here is modulation of MED19a by ELENA1.

3.3 Chromatin and transcription initiation

Chromatin accessibility plays a critical role in shaping transcriptional outcomes during immune activation. This is governed by histone modifications, nucleosome repositioning, and histone variant exchange, which together influence the accessibility of regulatory DNA regions[102–107]. Notably, compelling evidence shows that transcriptional changes across different immune responses are tightly correlated with chromatin accessibility[16]. In parallel, dynamic DNA methylation and demethylation, mediated by enzymes such as ROS1 and DEMETER (DME), fine-tune promoter accessibility and thereby modulate immune gene expression[108–110]. At the level of the transcriptional machinery, phosphorylation of RNA

Polymerase II's C-terminal domain by immune-activated kinases promotes transcriptional initiation, while phosphatases like CPLs act as negative regulators[111,112]. Additional regulatory precision is achieved through alternative transcription initiation and the activity of the Mediator complex, which can recruit Pol III, Pol IV, or Pol V depending on the transcriptional context and hormonal signaling environment [113–119]. Finally, nuclear import and export mechanisms contribute to the spatial regulation of immune signaling by controlling the localization of key transcriptional regulators such as NPR1, TOPLESS-RELATED1 (TPR1), and CONSTITUTIVE EXPRESSER OF PATHOGENESIS-RELATED GENES 5 (CPR5)-dependent immune factors[120–123].

4. Post-transcriptional regulation

Post-transcriptionally, immune gene expression is fine-tuned by alternative splicing, nuclear retention of mRNAs, and storage or decay in stress granules and P-bodies[124–132]. For instance, P-body components like DECAPPING1 (DCP1) are directly regulated by MPK signaling to promote decay of specific mRNAs during PTI[131,132]. Non-coding RNAs including microRNAs and long non-coding RNAs (lncRNAs) add yet another regulatory dimension. miRNAs participate in post-transcriptional gene silencing and are epigenetically controlled during infection[133,134], while lncRNAs such as ELENA1 enhance immune gene expression by modulating Mediator complex interactions and chromatin dynamics (**Figure 2**)[135,136]. Collectively, these interconnected layers of transcriptional and post-transcriptional regulation enable plants to execute robust, precisely coordinated immune responses while maintaining developmental and metabolic homeostasis.

5. Ca^{2+} signaling and role of CBP60 family in plant immunity

A rapid influx of calcium and a change in redox status are vital parts of plant immunity and they play intertwined roles in PTI and ETI[137]. Calcium

influx is induced immediately upon perception of PAMPs and effectors, which has been coupled to classical calcium channels[15,138], but also to recently identified calcium channels formed by helper NLR-based resistosomes[57,139] (**Figure 1**). Intracellularly, the calcium signal is decoded by calcium-binding proteins like calmodulin (CaM) and Ca^{2+}-dependent protein kinases (CDPKs). These can directly activate TFs, such as the defense-regulating CaM-binding TF family CAMTAs and CBP60s, or WRKY28, WRKY33 and WRKY48, which are phosphorylated by CPK5 and CPK6. This leads to altered defense-related transcription by these TFs, which influences resistance to diverse pathogens[93,94,140,141]. Although in general positive effects of calcium signaling on immunity have been reported, this is not always the case. For example, the Ca^{2+}-activated CAMTA3 (or AtSR1) TF represses SA signaling[142]. Moreover, several other CaM-regulated and CaM-like proteins like CBP60a, CALMODULIN-LIKE 46 (CML46) and CML47 negatively impact SA-related gene expression and accordingly, mutant lines are enhanced resistant to virulent *P. syringae*[143].

The Arabidopsis CBP60 family consists of eight members, several of which have emerged as important regulators of plant defense[62,144]. While most members positively influence immunity, CBP60a is a notable exception, acting as a negative regulator of SA-mediated responses[144]. Among the family, CBP60g and SYSTEMIC ACQUIRED RESISTANCE DEFICIENT 1 (SARD1) are the best characterized and function as central transcriptional hubs in immune signaling. Both are rapidly induced upon pathogen recognition and bind directly to the promoters of numerous defense-related genes[140,145], including those involved in SA and NHP (N-hydroxypipecolic acid) biosynthesis, PTI, ETI-specific genes (**Figure 3**).

Importantly, CBP60g and SARD1 act redundantly, loss of one can be partially compensated by the other, but simultaneous disruption of both

severely compromises immunity[62,140]. Beyond activating positive regulators, emerging evidence suggests that CBP60g and SARD1 also bind to and repress specific negative regulators, enabling them to fine-tune immune output and prevent inappropriate or excessive defense activation. However, a comprehensive study systematically linking the roles of CBP60g and SARD1 to resistance against diverse pathogens and across distinct immune pathways (PTI and ETI) has been lacking. Moreover, a global transcriptional dissection uncoupling their dual roles in activation and repression is needed to fully understand how these transcription factors sit at the heart of a balanced immune regulatory framework, coordinating both pathogen resistance and immune-associated cell death. In addition, it is also important to determine how CBP60g/SARD1-dependent programs are deployed across distinct cellular contexts.

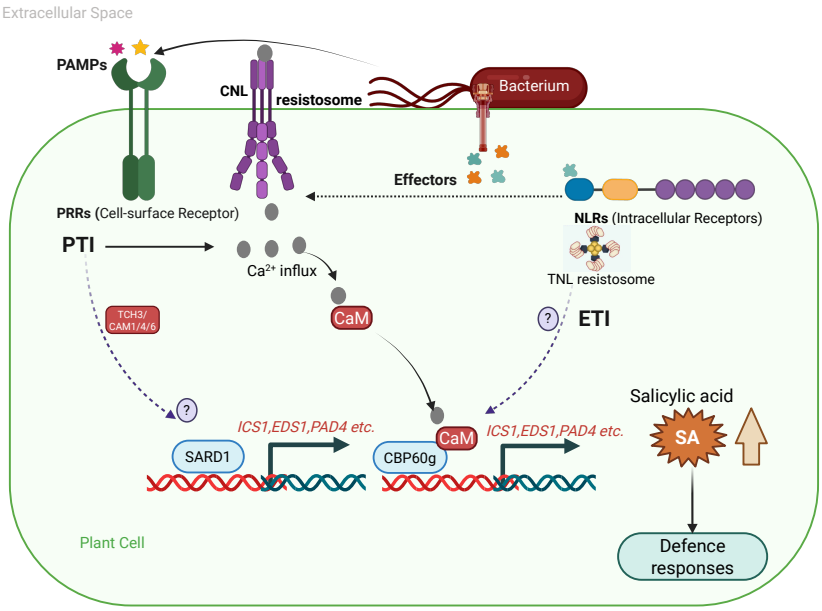

Figure 3. Overview of CBP60g and SARD1 in plant innate immunity. Pathogen recognition by cell-surface receptors and intracellular receptors lead to activation of PTI and ETI. Activation of plant immunity leads to production of reactive oxygen species, callose deposition, cytosolic Ca^{2+} flux, kinase activation, induction of CBP60g and SARD1. CBP60g is activated by Ca^{2+}-dependent calmodulin (CaM) binding (TCH3, CAM1/4/6) and SARD1 is activated by an unknown mechanism, which both activates the expression of *ENHANCED DISEASE SUSCEPTIBILITY 1* (*EDS1*), *PHYTOALEXIN DEFICIENT 4* (*PAD4*), *ISOCHORISMATE synthase 1* (*ICS1*) for promoting SA accumulation and the downstream SA-dependent defense responses.

6. Cell-autonomous immunity across diverse cell states

Understanding how individual plant cells respond to pathogenic threats is essential for unravelling the spatial and functional complexity of plant immunity. Unlike animals, plants lack mobile immune cells and therefore rely on cell-autonomous immune responses. Effector-triggered immunity (ETI), a potent intracellular defense mechanism mediated by nucleotide-binding leucine-rich repeat (NLR) receptors upon effector recognition, is central to this response[11]. However, traditional bulk transcriptomic approaches often obscure the cellular heterogeneity of immune responses, masking how different cells maintain the potential to mount immune activation, and what defines their shared versus cell-type-specific defense responses when pathogen exposure occurs stochastically across a tissue.

The advent of single-cell RNA sequencing (scRNA-seq) has enabled unprecedented resolution in dissecting these responses, revealing that while immune perception can be broadly uniform, the transcriptional execution of ETI is highly shaped by cell identity, developmental context, and chromatin accessibility meaning that the same immune signal may be interpreted differently depending on the cellular landscape in which it is triggered[17]. Importantly, pathogen encounters are rarely synchronized

across all tissues. In natural infections, only a subset of cells perceive pathogen, while surrounding cells experience indirect immune cues. This creates spatially layered immune zones, where infected cells, adjacent bystander cells, and distal tissues may enter distinct transcriptional and metabolic states. Such spatial compartmentalization also highlights the importance of cell-to-cell communication, including local propagation of immune signals and longer-range systemic signaling that primes distal tissues. Recent single-cell studies have revealed that immune activation can organize into “hotspots,” including rare immune-active populations such as PRIMER cells, which occupy the center of immune domains and are surrounded by transcriptionally distinct neighbouring cells[146]. Similar spatial immune patterning has also been observed in other plant species, reinforcing that tissue immunity emerges not only from individual defense responses but also from their coordination across cellular neighborhoods[147].

These findings position scRNA-seq as a transformative tool in plant immunity research, particularly when coupled with spatial omics technologies can help in mapping immune states back to their anatomical context, capturing how immune outputs propagate from infection sites to adjacent and distal tissue regions. In addition, integrating scRNA-seq with other single-cell omics, such as single-cell Assay for transposase-accessible chromatin using sequencing (ATAC-seq), enables the inference of gene regulatory networks (GRNs) that link transcriptional outputs to underlying chromatin accessibility. This multi-omics framework can reveal how cell identity and regulatory state constrain immune competence and shape ETI execution across tissues.

Lastly, disentangling intrinsic immune potential from infection-driven variability remains a major challenge. Synthetic systems that can uniformly activate immune signaling in the absence of pathogens offer a

powerful approach to disentangle intrinsic cell-type immune potential from pathogen-induced variability. By synchronizing immune activation across all cells, these systems enable a controlled view of how different cell types interpret and execute the same immune signal.

Together, these approaches open new avenues to unravel the logic of immune execution across plant tissues and lay the groundwork for designing next-generation strategies to engineer precise, robust, and spatially optimized disease resistance in crops.

7. Thesis outline

Despite extensive knowledge of plant immune signaling, many questions remain unanswered:

1. How are ETI outputs like resistance and cell death genetically separated through EDS1-containing modules?
2. How is effector-triggered immunity executed across distinct leaf cell-types?
3. How do master regulators like CBP60g and SARD1 orchestrate transcriptional dynamics to optimize immune outputs?

To address these questions, this thesis is structured into five chapters:

Chapter 1 provides a general introduction to the field of plant immunity, with a focus on the architecture and signaling logic of effector-triggered immunity (ETI). It outlines how plants, in the absence of mobile immune cells, rely on cell-autonomous defense strategies mediated by intracellular nucleotide-binding leucine-rich repeat (NLR) receptors. The chapter introduces key signaling modules such as EDS1-PAD4 and EDS1-SAG101 and discusses how these modules contribute differently to immune outputs.

Chapter 2 explores how two key EDS1-containing signaling modules EDS1-PAD4 and EDS1-SAG101, acts together with the helper NLRs (hNLRs) and differentially contribute to effector-triggered immunity (ETI) outcomes in plants. Through inducible immune activation, we demonstrate that the EDS1-PAD4-ADR1 module primarily governs disease resistance and immune-associated growth arrest, whereas the EDS1-SAG101-NRG1 module predominantly triggers hypersensitive response (HR)-mediated cell death. These findings reveal that distinct ETI outputs can be genetically uncoupled, offering a framework to investigate their respective transcriptional consequences. Additionally, this chapter introduces the concept of disease priming and discusses its potential application in enhancing plant defense, particularly in cases where immune responses are even partially compromised.

Building on the modular framework of effector-triggered immunity (ETI), **chapter 3** employs single-cell RNA sequencing (scRNA-seq) to profile immune responses across all major cell types in the Arabidopsis leaf, using a synthetic, inducible ETI activation system. We show that while ETI perception is uniform across cells, its execution is highly context-dependent, shaped by cell-type-specific chromatin accessibility and transcription factor networks. Notably, we uncover a spatial organization of immune regulators, with distinct transcriptional modules acting in specific cell types. For example, the transcription factors SARD1 and CBP60g are preferentially expressed in epidermal cells, and we demonstrate their functional necessity in restricting pathogen entry at the leaf surface. These findings highlight the spatial specialization of immune responses and underscore the importance of cell identity in orchestrating effective defense programs.

Chapter 4 centres on the transcription factors CBP60g and SARD1, which serve as master regulators of salicylic acid (SA)-mediated immunity in

plants. Using mutant analyses, inducible ETI systems, and transcriptomic profiling, we reveal that these transcription factors not only promote disease resistance but also play a critical role in fine-tuning the balance between immune activation and cell death. Notably, the *cbp60g sard1* double mutant emerges as a valuable genetic resource for uncoupling resistance from hypersensitive response (HR). These mutants display exaggerated HR yet show compromised disease resistance, all without apparent growth defects challenging the long-held view that HR is a prerequisite for effective immunity. Furthermore, our data indicate that CBP60g and SARD1 modulate both positive and negative regulators of immune signaling, shaping a finely balanced transcriptional network during ETI.

The final **chapter 5** of this thesis summarizes the key findings and conclusions of my research, placing them within the broader context of plant immune regulation. I discuss the significance of these results in advancing our understanding of cell-type-specific immune responses, and reflect on the new questions that have emerged, highlighting areas for future investigation. Additionally, I outline potential applications and future perspectives, emphasizing how insights from this work could contribute to more sustainable and targeted strategies for combating plant diseases.

Together, these studies advance our understanding of the transcriptional and spatial logic underlying plant innate immunity and highlight the modular strategies used by plants to fine-tune defense.

References

1. Gray, P. (2018). The great famine, 1845–1850. In The cambridge history of ireland, J. Kelly and T. Bartlett, eds. (Cambridge University Press), pp. 639–665. 10.1017/9781316335680.027.

2. Ristaino, J.B., Anderson, P.K., Bebber, D.P., Brauman, K.A., Cunniffe, N.J., Fedoroff, N.V., Finegold, C., Garrett, K.A., Gilligan, C.A., Jones, C.M., et al. (2021). The persistent threat of emerging plant disease pandemics to global food security. Proc Natl Acad Sci USA *118*. 10.1073/pnas.2022239118.

3. About | Plant Production and Protection | Food and Agriculture Organization of the United Nations https://www.fao.org/plant-production-protection/about/en.

4. Pesticides use and trade, 1990–2022 (2024). (FAO) 10.4060/cd1486en.

5. Ngou, B.P.M., Jones, J.D.G., and Ding, P. (2022). Plant immune networks. Trends Plant Sci. *27*, 255–273. 10.1016/j.tplants.2021.08.012.

6. Thordal-Christensen, H. (2003). Fresh insights into processes of nonhost resistance. Curr. Opin. Plant Biol. *6*, 351–357. 10.1016/S1369-5266(03)00063-3.

7. Heath, M.C. (2000). Nonhost resistance and nonspecific plant defenses. Curr. Opin. Plant Biol. *3*, 315–319. 10.1016/S1369-5266(00)00087-X.

8. Ausubel, F.M. (2005). Are innate immune signaling pathways in plants and animals conserved? Nat. Immunol. *6*, 973–979. 10.1038/ni1253.

9. Duxbury, Z., Wu, C.-H., and Ding, P. (2021). A comparative overview of the intracellular guardians of plants and animals: nlrs in innate immunity and beyond. Annu. Rev. Plant Biol. *72*, 155–184. 10.1146/annurev-arplant-080620-104948.

10. Jones, J.D.G., and Dangl, J.L. (2006). The plant immune system. Nature *444*, 323–329. 10.1038/nature05286.

11. Jones, J.D.G., Staskawicz, B.J., and Dangl, J.L. (2024). The plant immune system: From discovery to deployment. Cell *187*, 2095–2116. 10.1016/j.cell.2024.03.045.

12. Ngou, B.P.M., Ahn, H.-K., Ding, P., and Jones, J.D.G. (2021). Mutual potentiation of plant immunity by cell-surface and intracellular receptors. Nature *592*, 110–115. 10.1038/s41586-021-03315-7.

13. Yuan, M., Jiang, Z., Bi, G., Nomura, K., Liu, M., Wang, Y., Cai, B., Zhou, J.-M., He, S.Y., and Xin, X.-F. (2021). Pattern-recognition receptors are required for NLR-mediated plant immunity. Nature *592*, 105–109. 10.1038/s41586-021-03316-6.

14. Aerts, N., Chhillar, H., Ding, P., and Van Wees, S.C.M. (2022). Transcriptional regulation of plant innate immunity. Essays Biochem. *66*, 607–620. 10.1042/EBC20210100.

15. Jiang, Y., and Ding, P. (2023). Calcium signaling in plant immunity: a spatiotemporally controlled symphony. Trends Plant Sci. *28*, 74–89. 10.1016/j.tplants.2022.11.001.

16. Ding, P., Sakai, T., Krishna Shrestha, R., Manosalva Perez, N., Guo, W., Ngou, B.P.M., He, S., Liu, C., Feng, X., Zhang, R., et al. (2021). Chromatin accessibility landscapes activated by cell-surface and intracellular immune receptors. J. Exp. Bot. *72*, 7927–7941. 10.1093/jxb/erab373.

17. Zhu, J., Moreno-Pérez, A., and Coaker, G. (2023). Understanding plant pathogen interactions using spatial and single-cell technologies. Commun. Biol. *6*, 814. 10.1038/s42003-023-05156-8.

18. Ngou, B.P.M., Ding, P., and Jones, J.D.G. (2022). Thirty years of resistance: Zig-zag through the plant immune system. Plant Cell *34*, 1447–1478. 10.1093/plcell/koac041.

19. Dangl, J.L., and Jones, J.D. (2001). Plant pathogens and integrated defence responses to infection. Nature *411*, 826–833. 10.1038/35081161.

20. Couto, D., and Zipfel, C. (2016). Regulation of pattern recognition receptor signalling in plants. Nat. Rev. Immunol. *16*, 537–552. 10.1038/nri.2016.77.

21. Tang, D., Wang, G., and Zhou, J.-M. (2017). Receptor Kinases in Plant-Pathogen Interactions: More Than Pattern Recognition. Plant Cell *29*, 618–637. 10.1105/tpc.16.00891.

22. Chinchilla, D., Zipfel, C., Robatzek, S., Kemmerling, B., Nürnberger, T., Jones, J.D.G., Felix, G., and Boller, T. (2007). A flagellin-induced complex of the receptor FLS2 and BAK1 initiates plant defence. Nature *448*, 497–500. 10.1038/nature05999.

23. Heese, A., Hann, D.R., Gimenez-Ibanez, S., Jones, A.M.E., He, K., Li, J., Schroeder, J.I., Peck, S.C., and Rathjen, J.P. (2007). The receptor-like kinase SERK3/BAK1 is a central regulator of innate immunity in plants. Proc Natl Acad Sci USA *104*, 12217–12222. 10.1073/pnas.0705306104.

24. Schulze, B., Mentzel, T., Jehle, A.K., Mueller, K., Beeler, S., Boller, T., Felix, G., and Chinchilla, D. (2010). Rapid heteromerization and phosphorylation of ligand-activated plant transmembrane receptors and their associated kinase BAK1. J. Biol. Chem. *285*, 9444–9451. 10.1074/jbc.M109.096842.

25. Albert, I., Böhm, H., Albert, M., Feiler, C.E., Imkampe, J., Wallmeroth, N., Brancato, C., Raaymakers, T.M., Oome, S., Zhang, H., et al. (2015). An RLP23-SOBIR1-BAK1 complex mediates NLP-triggered immunity. Nat. Plants *1*, 15140. 10.1038/nplants.2015.140.

26. Pruitt, R.N., Locci, F., Wanke, F., Zhang, L., Saile, S.C., Joe, A., Karelina, D., Hua, C., Fröhlich, K., Wan, W.-L., et al. (2021). The EDS1-PAD4-ADR1 node mediates Arabidopsis pattern-triggered immunity. Nature *598*, 495–499. 10.1038/s41586-021-03829-0.

27. Halter, T., Imkampe, J., Mazzotta, S., Wierzba, M., Postel, S., Bücherl, C., Kiefer, C., Stahl, M., Chinchilla, D., Wang, X., et al. (2014). The leucine-rich repeat receptor kinase BIR2 is a negative

regulator of BAK1 in plant immunity. Curr. Biol. *24*, 134–143. 10.1016/j.cub.2013.11.047.

28. Ma, C., Liu, Y., Bai, B., Han, Z., Tang, J., Zhang, H., Yaghmaiean, H., Zhang, Y., and Chai, J. (2017). Structural basis for BIR1-mediated negative regulation of plant immunity. Cell Res. *27*, 1521–1524. 10.1038/cr.2017.123.

29. Stegmann, M., Monaghan, J., Smakowska-Luzan, E., Rovenich, H., Lehner, A., Holton, N., Belkhadir, Y., and Zipfel, C. (2017). The receptor kinase FER is a RALF-regulated scaffold controlling plant immune signaling. Science *355*, 287–289. 10.1126/science.aal2541.

30. Lu, D., Wu, S., He, P., and Shan, L. (2010). Phosphorylation of receptor-like cytoplasmic kinases by bacterial flagellin. Plant Signal. Behav. *5*, 598–600. 10.4161/psb.11500.

31. Zhang, J., Li, W., Xiang, T., Liu, Z., Laluk, K., Ding, X., Zou, Y., Gao, M., Zhang, X., Chen, S., et al. (2010). Receptor-like cytoplasmic kinases integrate signaling from multiple plant immune receptors and are targeted by a Pseudomonas syringae effector. Cell Host Microbe *7*, 290–301. 10.1016/j.chom.2010.03.007.

32. Macho, A.P., and Zipfel, C. (2014). Plant PRRs and the activation of innate immune signaling. Mol. Cell *54*, 263–272. 10.1016/j.molcel.2014.03.028.

33. Boller, T., and Felix, G. (2009). A renaissance of elicitors: perception of microbe-associated molecular patterns and danger

signals by pattern-recognition receptors. Annu. Rev. Plant Biol. *60*, 379–406. 10.1146/annurev.arplant.57.032905.105346.

34. Kadota, Y., Sklenar, J., Derbyshire, P., Stransfeld, L., Asai, S., Ntoukakis, V., Jones, J.D.G., Shirasu, K., Menke, F., Jones, A., et al. (2014). Direct regulation of the NADPH oxidase RBOHD by the PRR-associated kinase BIK1 during plant immunity. Mol. Cell *54*, 43–55. 10.1016/j.molcel.2014.02.021.

35. Büttner, D., and He, S.Y. (2009). Type III protein secretion in plant pathogenic bacteria. Plant Physiol. *150*, 1656–1664. 10.1104/pp.109.139089.

36. Kourelis, J., and van der Hoorn, R.A.L. (2018). Defended to the nines: 25 years of resistance gene cloning identifies nine mechanisms for R protein function. Plant Cell *30*, 285–299. 10.1105/tpc.17.00579.

37. Meyers, B.C., Kozik, A., Griego, A., Kuang, H., and Michelmore, R.W. (2003). Genome-wide analysis of NBS-LRR-encoding genes in Arabidopsis. Plant Cell *15*, 809–834. 10.1105/tpc.009308.

38. Gassmann, W., Hinsch, M.E., and Staskawicz, B.J. (1999). The Arabidopsis RPS4 bacterial-resistance gene is a member of the TIR-NBS-LRR family of disease-resistance genes. Plant J. *20*, 265–277. 10.1046/j.1365-313X.1999.00600.x.

39. Narusaka, M., Shirasu, K., Noutoshi, Y., Kubo, Y., Shiraishi, T., Iwabuchi, M., and Narusaka, Y. (2009). RRS1 and RPS4 provide a dual Resistance-gene system against fungal and bacterial

pathogens. Plant J. *60*, 218–226. 10.1111/j.1365-313X.2009.03949.x.

40. Mindrinos, M., Katagiri, F., Yu, G.-L., and Ausubel, F.M. (1994). The A. thaliana disease resistance gene *RPS2* encodes a protein containing a nucleotide-binding site and leucine-rich repeats. Cell *78*, 1089–1099. 10.1016/0092-8674(94)90282-8.

41. Bonardi, V., Tang, S., Stallmann, A., Roberts, M., Cherkis, K., and Dangl, J.L. (2011). Expanded functions for a family of plant intracellular immune receptors beyond specific recognition of pathogen effectors. Proc Natl Acad Sci USA *108*, 16463–16468. 10.1073/pnas.1113726108.

42. Castel, B., Ngou, P.-M., Cevik, V., Redkar, A., Kim, D.-S., Yang, Y., Ding, P., and Jones, J.D.G. (2019). Diverse NLR immune receptors activate defence via the RPW8-NLR NRG1. New Phytol. *222*, 966–980. 10.1111/nph.15659.

43. Wu, Z., Li, M., Dong, O.X., Xia, S., Liang, W., Bao, Y., Wasteneys, G., and Li, X. (2019). Differential regulation of TNL-mediated immune signaling by redundant helper CNLs. New Phytol. *222*, 938–953. 10.1111/nph.15665.

44. Saile, S.C., Jacob, P., Castel, B., Jubic, L.M., Salas-Gonzáles, I., Bäcker, M., Jones, J.D.G., Dangl, J.L., and El Kasmi, F. (2020). Two unequally redundant "helper" immune receptor families mediate Arabidopsis thaliana intracellular "sensor" immune receptor functions. PLoS Biol. *18*, e3000783. 10.1371/journal.pbio.3000783.

45. Aarts, N., Metz, M., Holub, E., Staskawicz, B.J., Daniels, M.J., and Parker, J.E. (1998). Different requirements for EDS1 and NDR1 by disease resistance genes define at least two R gene-mediated signaling pathways in Arabidopsis. Proc Natl Acad Sci USA *95*, 10306–10311. 10.1073/pnas.95.17.10306.

46. Feys, B.J., Wiermer, M., Bhat, R.A., Moisan, L.J., Medina-Escobar, N., Neu, C., Cabral, A., and Parker, J.E. (2005). Arabidopsis SENESCENCE-ASSOCIATED GENE101 stabilizes and signals within an ENHANCED DISEASE SUSCEPTIBILITY1 complex in plant innate immunity. Plant Cell *17*, 2601–2613. 10.1105/tpc.105.033910.

47. Krasileva, K.V., Dahlbeck, D., and Staskawicz, B.J. (2010). Activation of an Arabidopsis resistance protein is specified by the in planta association of its leucine-rich repeat domain with the cognate oomycete effector. Plant Cell *22*, 2444–2458. 10.1105/tpc.110.075358.

48. Chung, E.-H., da Cunha, L., Wu, A.-J., Gao, Z., Cherkis, K., Afzal, A.J., Mackey, D., and Dangl, J.L. (2011). Specific threonine phosphorylation of a host target by two unrelated type III effectors activates a host innate immune receptor in plants. Cell Host Microbe *9*, 125–136. 10.1016/j.chom.2011.01.009.

49. van der Hoorn, R.A.L., and Kamoun, S. (2008). From Guard to Decoy: a new model for perception of plant pathogen effectors. Plant Cell *20*, 2009–2017. 10.1105/tpc.108.060194.

50. Wan, L., Essuman, K., Anderson, R.G., Sasaki, Y., Monteiro, F., Chung, E.-H., Osborne Nishimura, E., DiAntonio, A., Milbrandt, J.,

Dangl, J.L., et al. (2019). TIR domains of plant immune receptors are NAD+-cleaving enzymes that promote cell death. Science *365*, 799–803. 10.1126/science.aax1771.

51. Ma, S., Lapin, D., Liu, L., Sun, Y., Song, W., Zhang, X., Logemann, E., Yu, D., Wang, J., Jirschitzka, J., et al. (2020). Direct pathogen-induced assembly of an NLR immune receptor complex to form a holoenzyme. Science *370*. 10.1126/science.abe3069.

52. Martin, R., Qi, T., Zhang, H., Liu, F., King, M., Toth, C., Nogales, E., and Staskawicz, B.J. (2020). Structure of the activated ROQ1 resistosome directly recognizing the pathogen effector XopQ. Science *370*. 10.1126/science.abd9993.

53. Horsefield, S., Burdett, H., Zhang, X., Manik, M.K., Shi, Y., Chen, J., Qi, T., Gilley, J., Lai, J.-S., Rank, M.X., et al. (2019). NAD+ cleavage activity by animal and plant TIR domains in cell death pathways. Science *365*, 793–799. 10.1126/science.aax1911.

54. Yu, D., Song, W., Tan, E.Y.J., Liu, L., Cao, Y., Jirschitzka, J., Li, E., Logemann, E., Xu, C., Huang, S., et al. (2022). TIR domains of plant immune receptors are 2',3'-cAMP/cGMP synthetases mediating cell death. Cell *185*, 2370-2386.e18. 10.1016/j.cell.2022.04.032.

55. Sun, X., Lapin, D., Feehan, J.M., Stolze, S.C., Kramer, K., Dongus, J.A., Rzemieniewski, J., Blanvillain-Baufumé, S., Harzen, A., Bautor, J., et al. (2021). Pathogen effector recognition-dependent association of NRG1 with EDS1 and SAG101 in TNL receptor immunity. Nat. Commun. *12*, 3335. 10.1038/s41467-021-23614-x.

56. Lapin, D., Kovacova, V., Sun, X., Dongus, J.A., Bhandari, D., von Born, P., Bautor, J., Guarneri, N., Rzemieniewski, J., Stuttmann, J., et al. (2019). A Coevolved EDS1-SAG101-NRG1 Module Mediates Cell Death Signaling by TIR-Domain Immune Receptors. Plant Cell *31*, 2430–2455. 10.1105/tpc.19.00118.

57. Jacob, P., Kim, N.H., Wu, F., El-Kasmi, F., Chi, Y., Walton, W.G., Furzer, O.J., Lietzan, A.D., Sunil, S., Kempthorn, K., et al. (2021). Plant “helper” immune receptors are Ca2+-permeable nonselective cation channels. Science *373*, 420–425. 10.1126/science.abg7917.

58. Feehan, J.M., Wang, J., Sun, X., Choi, J., Ahn, H.-K., Ngou, B.P.M., Parker, J.E., and Jones, J.D.G. (2023). Oligomerization of a plant helper NLR requires cell-surface and intracellular immune receptor activation. Proc Natl Acad Sci USA *120*, e2210406120. 10.1073/pnas.2210406120.

59. Liu, F., Yang, Z., Wang, C., You, Z., Martin, R., Qiao, W., Huang, J., Jacob, P., Dangl, J.L., Carette, J.E., et al. (2024). Activation of the helper NRC4 immune receptor forms a hexameric resistosome. Cell *187*, 4877-4889.e15. 10.1016/j.cell.2024.07.013.

60. Madhuprakash, J., Toghani, A., Contreras, M.P., Posbeyikian, A., Richardson, J., Kourelis, J., Bozkurt, T.O., Webster, M.W., and Kamoun, S. (2024). A disease resistance protein triggers oligomerization of its NLR helper into a hexameric resistosome to mediate innate immunity. Sci. Adv. *10*, eadr2594. 10.1126/sciadv.adr2594.

61. Tsuda, K., and Somssich, I.E. (2015). Transcriptional networks in plant immunity. New Phytol. *206*, 932–947. 10.1111/nph.13286.

62. Zhang, Y., Xu, S., Ding, P., Wang, D., Cheng, Y.T., He, J., Gao, M., Xu, F., Li, Y., Zhu, Z., et al. (2010). Control of salicylic acid synthesis and systemic acquired resistance by two members of a plant-specific family of transcription factors. Proc Natl Acad Sci USA *107*, 18220–18225. 10.1073/pnas.1005225107.

63. Fernández-Calvo, P., Chini, A., Fernández-Barbero, G., Chico, J.M., Gimenez-Ibanez, S., Geerinck, J., Eeckhout, D., Schweizer, F., Godoy, M., Franco-Zorrilla, J.M., et al. (2011). The *Arabidopsis* bHLH transcription factors MYC3 and MYC4 are targets of JAZ repressors and act additively with MYC2 in the activation of jasmonate responses. Plant Cell *23*, 701–715. 10.1105/tpc.110.080788.

64. Li, S. (2015). The Arabidopsis thaliana TCP transcription factors: A broadening horizon beyond development. Plant Signal. Behav. *10*, e1044192. 10.1080/15592324.2015.1044192.

65. Amorim, L.L.B., da Fonseca Dos Santos, R., Neto, J.P.B., Guida-Santos, M., Crovella, S., and Benko-Iseppon, A.M. (2017). Transcription factors involved in plant resistance to pathogens. Curr. Protein Pept. Sci. *18*, 335–351. 10.2174/1389203717666160619185308.

66. Yuan, X., Wang, H., Cai, J., Li, D., and Song, F. (2019). NAC transcription factors in plant immunity. Phytopathol. Res. *1*, 3. 10.1186/s42483-018-0008-0.

67. Kim, Y., Gilmour, S.J., Chao, L., Park, S., and Thomashow, M.F. (2020). Arabidopsis CAMTA transcription factors regulate pipecolic acid biosynthesis and priming of immunity genes. Mol. Plant *13*, 157–168. 10.1016/j.molp.2019.11.001.

68. Ding, P., and Redkar, A. (2018). Pathogens suppress host transcription factors for rampant proliferation. Trends Plant Sci. *23*, 950–953. 10.1016/j.tplants.2018.08.010.

69. Han, X., and Kahmann, R. (2019). Manipulation of phytohormone pathways by effectors of filamentous plant pathogens. Front. Plant Sci. *10*, 822. 10.3389/fpls.2019.00822.

70. Wang, Y., Pruitt, R.N., Nürnberger, T., and Wang, Y. (2022). Evasion of plant immunity by microbial pathogens. Nat. Rev. Microbiol. *20*, 449–464. 10.1038/s41579-022-00710-3.

71. Li, Q., Chen, Y., Wang, J., Zou, F., Jia, Y., Shen, D., Zhang, Q., Jing, M., Dou, D., and Zhang, M. (2019). A Phytophthora capsici virulence effector associates with NPR1 and suppresses plant immune responses. Phytopathol. Res. *1*, 6. 10.1186/s42483-019-0013-y.

72. Chen, H., Chen, J., Li, M., Chang, M., Xu, K., Shang, Z., Zhao, Y., Palmer, I., Zhang, Y., McGill, J., et al. (2017). A bacterial type III effector targets the master regulator of salicylic acid signaling, NPR1, to subvert plant immunity. Cell Host Microbe *22*, 777-788.e7. 10.1016/j.chom.2017.10.019.

73. Plett, J.M., Daguerre, Y., Wittulsky, S., Vayssières, A., Deveau, A., Melton, S.J., Kohler, A., Morrell-Falvey, J.L., Brun, A., Veneault-

Fourrey, C., et al. (2014). Effector MiSSP7 of the mutualistic fungus Laccaria bicolor stabilizes the Populus JAZ6 protein and represses jasmonic acid (JA) responsive genes. Proc Natl Acad Sci USA *111*, 8299–8304. 10.1073/pnas.1322671111.

74. Jiang, S., Yao, J., Ma, K.-W., Zhou, H., Song, J., He, S.Y., and Ma, W. (2013). Bacterial effector activates jasmonate signaling by directly targeting JAZ transcriptional repressors. PLoS Pathog. *9*, e1003715. 10.1371/journal.ppat.1003715.

75. Caillaud, M.C., Asai, S., Rallapalli, G., Piquerez, S., Fabro, G., and Jones, J.D.G. (2013). A downy mildew effector attenuates salicylic acid-triggered immunity in Arabidopsis by interacting with the host Mediator complex. PLoS Biol. *11*, e1001732. 10.1371/journal.pbio.1001732.

76. Gimenez-Ibanez, S., Boter, M., Fernández-Barbero, G., Chini, A., Rathjen, J.P., and Solano, R. (2014). The bacterial effector HopX1 targets JAZ transcriptional repressors to activate jasmonate signaling and promote infection in Arabidopsis. PLoS Biol. *12*, e1001792. 10.1371/journal.pbio.1001792.

77. Raffeiner, M., Üstün, S., Guerra, T., Spinti, D., Fitzner, M., Sonnewald, S., Baldermann, S., and Börnke, F. (2022). The Xanthomonas type-III effector XopS stabilizes CaWRKY40a to regulate defense responses and stomatal immunity in pepper (Capsicum annuum). Plant Cell *34*, 1684–1708. 10.1093/plcell/koac032.

78. Qi, P., Huang, M., Hu, X., Zhang, Y., Wang, Y., Li, P., Chen, S., Zhang, D., Cao, S., Zhu, W., et al. (2022). A Ralstonia

solanacearum effector targets TGA transcription factors to subvert salicylic acid signaling. Plant Cell *34*, 1666–1683. 10.1093/plcell/koac015.

79. Canonne, J., Marino, D., Jauneau, A., Pouzet, C., Brière, C., Roby, D., and Rivas, S. (2011). The Xanthomonas type III effector XopD targets the Arabidopsis transcription factor MYB30 to suppress plant defense. Plant Cell *23*, 3498–3511. 10.1105/tpc.111.088815.

80. Kitazawa, Y., Iwabuchi, N., Maejima, K., Sasano, M., Matsumoto, O., Koinuma, H., Tokuda, R., Suzuki, M., Oshima, K., Namba, S., et al. (2022). A phytoplasma effector acts as a ubiquitin-like mediator between floral MADS-box proteins and proteasome shuttle proteins. Plant Cell *34*, 1709–1723. 10.1093/plcell/koac062.

81. Harvey, S., Kumari, P., Lapin, D., Griebel, T., Hickman, R., Guo, W., Zhang, R., Parker, J.E., Beynon, J., Denby, K., et al. (2020). Downy Mildew effector HaRxL21 interacts with the transcriptional repressor TOPLESS to promote pathogen susceptibility. PLoS Pathog. *16*, e1008835. 10.1371/journal.ppat.1008835.

82. Bjornson, M., Pimprikar, P., Nürnberger, T., and Zipfel, C. (2021). The transcriptional landscape of Arabidopsis thaliana pattern-triggered immunity. Nat. Plants *7*, 579–586. 10.1038/s41477-021-00874-5.

83. Maier, B.A., Kiefer, P., Field, C.M., Hemmerle, L., Bortfeld-Miller, M., Emmenegger, B., Schäfer, M., Pfeilmeier, S., Sunagawa, S., Vogel, C.M., et al. (2021). A general non-self response as part of

plant immunity. Nat. Plants *7*, 696–705. 10.1038/s41477-021-00913-1.

84. Walley, J.W., Coughlan, S., Hudson, M.E., Covington, M.F., Kaspi, R., Banu, G., Harmer, S.L., and Dehesh, K. (2007). Mechanical stress induces biotic and abiotic stress responses via a novel cis-element. PLoS Genet. *3*, 1800–1812. 10.1371/journal.pgen.0030172.

85. Benn, G., Wang, C.-Q., Hicks, D.R., Stein, J., Guthrie, C., and Dehesh, K. (2014). A key general stress response motif is regulated non-uniformly by CAMTA transcription factors. Plant J. *80*, 82–92. 10.1111/tpj.12620.

86. Windram, O., Madhou, P., McHattie, S., Hill, C., Hickman, R., Cooke, E., Jenkins, D.J., Penfold, C.A., Baxter, L., Breeze, E., et al. (2012). Arabidopsis defense against Botrytis cinerea: chronology and regulation deciphered by high-resolution temporal transcriptomic analysis. Plant Cell *24*, 3530–3557. 10.1105/tpc.112.102046.

87. Lewis, L.A., Polanski, K., de Torres-Zabala, M., Jayaraman, S., Bowden, L., Moore, J., Penfold, C.A., Jenkins, D.J., Hill, C., Baxter, L., et al. (2015). Transcriptional Dynamics Driving MAMP-Triggered Immunity and Pathogen Effector-Mediated Immunosuppression in Arabidopsis Leaves Following Infection with Pseudomonas syringae pv tomato DC3000. Plant Cell *27*, 3038–3064. 10.1105/tpc.15.00471.

88. Hickman, R., Van Verk, M.C., Van Dijken, A.J.H., Mendes, M.P., Vroegop-Vos, I.A., Caarls, L., Steenbergen, M., Van der Nagel, I.,

Wesselink, G.J., Jironkin, A., et al. (2017). Architecture and dynamics of the jasmonic acid gene regulatory network. Plant Cell *29*, 2086–2105. 10.1105/tpc.16.00958.

89. Hickman, R., Mendes, M.P., Van Verk, M.C., Van Dijken, A.J.H., Di Sora, J., Denby, K., Pieterse, C.M.J., and Van Wees, S.C.M. (2019). Transcriptional Dynamics of the Salicylic Acid Response and its Interplay with the Jasmonic Acid Pathway. BioRxiv. 10.1101/742742.

90. Zander, M., Lewsey, M.G., Clark, N.M., Yin, L., Bartlett, A., Saldierna Guzmán, J.P., Hann, E., Langford, A.E., Jow, B., Wise, A., et al. (2020). Integrated multi-omics framework of the plant response to jasmonic acid. Nat. Plants *6*, 290–302. 10.1038/s41477-020-0605-7.

91. Tang, B., Liu, C., Li, Z., Zhang, X., Zhou, S., Wang, G.-L., Chen, X.-L., and Liu, W. (2021). Multilayer regulatory landscape during pattern-triggered immunity in rice. Plant Biotechnol. J. *19*, 2629–2645. 10.1111/pbi.13688.

92. Winkelmüller, T.M., Entila, F., Anver, S., Piasecka, A., Song, B., Dahms, E., Sakakibara, H., Gan, X., Kułak, K., Sawikowska, A., et al. (2021). Gene expression evolution in pattern-triggered immunity within Arabidopsis thaliana and across Brassicaceae species. Plant Cell *33*, 1863–1887. 10.1093/plcell/koab073.

93. Gao, X., and He, P. (2013). Nuclear dynamics of Arabidopsis calcium-dependent protein kinases in effector-triggered immunity. Plant Signal. Behav. *8*, e23868. 10.4161/psb.23868.

94. Zhou, J., Wang, X., He, Y., Sang, T., Wang, P., Dai, S., Zhang, S., and Meng, X. (2020). Differential phosphorylation of the transcription factor WRKY33 by the protein kinases CPK5/CPK6 and MPK3/MPK6 cooperatively regulates camalexin biosynthesis in arabidopsis. Plant Cell *32*, 2621–2638. 10.1105/tpc.19.00971.

95. Sharma, M., Fuertes, D., Perez-Gil, J., and Lois, L.M. (2021). Sumoylation in phytopathogen interactions: balancing invasion and resistance. Front. Cell Dev. Biol. *9*, 703795. 10.3389/fcell.2021.703795.

96. Verma, V., Srivastava, A.K., Gough, C., Campanaro, A., Srivastava, M., Morrell, R., Joyce, J., Bailey, M., Zhang, C., Krysan, P.J., et al. (2021). SUMO enables substrate selectivity by mitogen-activated protein kinases to regulate immunity in plants. Proc Natl Acad Sci USA *118*. 10.1073/pnas.2021351118.

97. Van der Does, D., Leon-Reyes, A., Koornneef, A., Van Verk, M.C., Rodenburg, N., Pauwels, L., Goossens, A., Körbes, A.P., Memelink, J., Ritsema, T., et al. (2013). Salicylic acid suppresses jasmonic acid signaling downstream of SCFCOI1-JAZ by targeting GCC promoter motifs via transcription factor ORA59. Plant Cell *25*, 744–761. 10.1105/tpc.112.108548.

98. Furniss, J.J., and Spoel, S.H. (2015). Cullin-RING ubiquitin ligases in salicylic acid-mediated plant immune signaling. Front. Plant Sci. *6*, 154. 10.3389/fpls.2015.00154.

99. Chico, J.M., Lechner, E., Fernandez-Barbero, G., Canibano, E., García-Casado, G., Franco-Zorrilla, J.M., Hammann, P., Zamarreño, A.M., García-Mina, J.M., Rubio, V., et al. (2020).

CUL3BPM E3 ubiquitin ligases regulate MYC2, MYC3, and MYC4 stability and JA responses. Proc Natl Acad Sci USA *117*, 6205–6215. 10.1073/pnas.1912199117.

100. Ban, Z., and Estelle, M. (2021). CUL3 E3 ligases in plant development and environmental response. Nat. Plants *7*, 6–16. 10.1038/s41477-020-00833-6.

101. Zavaliev, R., Mohan, R., Chen, T., and Dong, X. (2020). Formation of NPR1 Condensates Promotes Cell Survival during the Plant Immune Response. Cell *182*, 1093-1108.e18. 10.1016/j.cell.2020.07.016.

102. Cai, H., Huang, Y., Chen, F., Liu, L., Chai, M., Zhang, M., Yan, M., Aslam, M., He, Q., and Qin, Y. (2021). ERECTA signaling regulates plant immune responses via chromatin-mediated promotion of WRKY33 binding to target genes. New Phytol. *230*, 737–756. 10.1111/nph.17200.

103. Pardal, A.J., Piquerez, S.J.M., Dominguez-Ferreras, A., Frungillo, L., Mastorakis, E., Reilly, E., Latrasse, D., Concia, L., Gimenez-Ibanez, S., Spoel, S.H., et al. (2021). Immunity onset alters plant chromatin and utilizes EDA16 to regulate oxidative homeostasis. PLoS Pathog. *17*, e1009572. 10.1371/journal.ppat.1009572.

104. Han, S.-K., Wu, M.-F., Cui, S., and Wagner, D. (2015). Roles and activities of chromatin remodeling ATPases in plants. Plant J. *83*, 62–77. 10.1111/tpj.12877.

105. Huang, C.-Y., Rangel, D.S., Qin, X., Bui, C., Li, R., Jia, Z., Cui, X., and Jin, H. (2021). The chromatin-remodeling protein

BAF60/SWP73A regulates the plant immune receptor NLRs. Cell Host Microbe *29*, 425-434.e4. 10.1016/j.chom.2021.01.005.

106. Zhang, X., Bernatavichute, Y.V., Cokus, S., Pellegrini, M., and Jacobsen, S.E. (2009). Genome-wide analysis of mono-, di- and trimethylation of histone H3 lysine 4 in Arabidopsis thaliana. Genome Biol. *10*, R62. 10.1186/gb-2009-10-6-r62.

107. Dvořák Tomaštíková, E., Hafrén, A., Trejo-Arellano, M.S., Rasmussen, S.R., Sato, H., Santos-González, J., Köhler, C., Hennig, L., and Hofius, D. (2021). Polycomb Repressive Complex 2 and KRYPTONITE regulate pathogen-induced programmed cell death in Arabidopsis. Plant Physiol. *185*, 2003–2021. 10.1093/plphys/kiab035.

108. Erdmann, R.M., and Picard, C.L. (2020). RNA-directed DNA Methylation. PLoS Genet. *16*, e1009034. 10.1371/journal.pgen.1009034.

109. Dowen, R.H., Pelizzola, M., Schmitz, R.J., Lister, R., Dowen, J.M., Nery, J.R., Dixon, J.E., and Ecker, J.R. (2012). Widespread dynamic DNA methylation in response to biotic stress. Proc Natl Acad Sci USA *109*, E2183-91. 10.1073/pnas.1209329109.

110. Huang, M., Zhang, Y., Wang, Y., Xie, J., Cheng, J., Fu, Y., Jiang, D., Yu, X., and Li, B. (2022). Active DNA demethylation regulates MAMP-triggered immune priming in Arabidopsis. J. Genet. Genomics. 10.1016/j.jgg.2022.02.021.

111. Li, F., Cheng, C., Cui, F., de Oliveira, M.V.V., Yu, X., Meng, X., Intorne, A.C., Babilonia, K., Li, M., Li, B., et al. (2014). Modulation

of RNA polymerase II phosphorylation downstream of pathogen perception orchestrates plant immunity. Cell Host Microbe *16*, 748–758. 10.1016/j.chom.2014.10.018.

112. Thatcher, L.F., Foley, R., Casarotto, H.J., Gao, L.-L., Kamphuis, L.G., Melser, S., and Singh, K.B. (2018). The Arabidopsis RNA Polymerase II Carboxyl Terminal Domain (CTD) Phosphatase-Like1 (CPL1) is a biotic stress susceptibility gene. Sci. Rep. *8*, 13454. 10.1038/s41598-018-31837-0.

113. Thieffry, A., López-Márquez, D., Bornholdt, J., Malekroudi, M.G., Bressendorff, S., Barghetti, A., Sandelin, A., and Brodersen, P. (2022). PAMP-triggered genetic reprogramming involves widespread alternative transcription initiation and an immediate transcription factor wave. Plant Cell. 10.1093/plcell/koac108.

114. Zhai, Q., and Li, C. (2019). The plant Mediator complex and its role in jasmonate signaling. J. Exp. Bot. *70*, 3415–3424. 10.1093/jxb/erz233.

115. Nomoto, M., Skelly, M.J., Itaya, T., Mori, T., Suzuki, T., Matsushita, T., Tokizawa, M., Kuwata, K., Mori, H., Yamamoto, Y.Y., et al. (2021). Suppression of MYC transcription activators by the immune cofactor NPR1 fine-tunes plant immune responses. Cell Rep. *37*, 110125. 10.1016/j.celrep.2021.110125.

116. Zhang, F., Yao, J., Ke, J., Zhang, L., Lam, V.Q., Xin, X.-F., Zhou, X.E., Chen, J., Brunzelle, J., Griffin, P.R., et al. (2015). Structural basis of JAZ repression of MYC transcription factors in jasmonate signalling. Nature *525*, 269–273. 10.1038/nature14661.

117. Zhang, Y., Shi, C., Fu, W., Gu, X., Qi, Z., Xu, W., and Xia, G. (2021). Arabidopsis MED18 interaction with RNA pol IV and V subunit nrpd2a in transcriptional regulation of plant immune responses. Front. Plant Sci. *12*, 692036. 10.3389/fpls.2021.692036.

118. Lai, Z., Schluttenhofer, C.M., Bhide, K., Shreve, J., Thimmapuram, J., Lee, S.Y., Yun, D.-J., and Mengiste, T. (2014). MED18 interaction with distinct transcription factors regulates multiple plant functions. Nat. Commun. *5*, 3064. 10.1038/ncomms4064.

119. Haag, J.R., and Pikaard, C.S. (2011). Multisubunit RNA polymerases IV and V: purveyors of non-coding RNA for plant gene silencing. Nat. Rev. Mol. Cell Biol. *12*, 483–492. 10.1038/nrm3152.

120. Wang, S., Gu, Y., Zebell, S.G., Anderson, L.K., Wang, W., Mohan, R., and Dong, X. (2014). A noncanonical role for the CKI-RB-E2F cell-cycle signaling pathway in plant effector-triggered immunity. Cell Host Microbe *16*, 787–794. 10.1016/j.chom.2014.10.005.

121. Gu, Y., Zebell, S.G., Liang, Z., Wang, S., Kang, B.-H., and Dong, X. (2016). Nuclear Pore Permeabilization Is a Convergent Signaling Event in Effector-Triggered Immunity. Cell *166*, 1526-1538.e11. 10.1016/j.cell.2016.07.042.

122. Peng, S., Guo, D., Guo, Y., Zhao, H., Mei, J., Han, Y., Guan, R., Wang, T., Song, T., Sun, K., et al. (2022). CONSTITUTIVE EXPRESSER OF PATHOGENESIS-RELATED GENES 5 is an RNA-binding protein controlling plant immunity via an RNA processing complex. Plant Cell. 10.1093/plcell/koac037.

123. Xu, F., Jia, M., Li, X., Tang, Y., Jiang, K., Bao, J., and Gu, Y. (2021). Exportin-4 coordinates nuclear shuttling of TOPLESS family transcription corepressors to regulate plant immunity. Plant Cell *33*, 697–713. 10.1093/plcell/koaa047.

124. Thines, B., Katsir, L., Melotto, M., Niu, Y., Mandaokar, A., Liu, G., Nomura, K., He, S.Y., Howe, G.A., and Browse, J. (2007). JAZ repressor proteins are targets of the SCF^{COI1} complex during jasmonate signalling. Nature *448*, 661–665. 10.1038/nature05960.

125. Chini, A., Fonseca, S., Fernández, G., Adie, B., Chico, J.M., Lorenzo, O., García-Casado, G., López-Vidriero, I., Lozano, F.M., Ponce, M.R., et al. (2007). The JAZ family of repressors is the missing link in jasmonate signalling. Nature *448*, 666–671. 10.1038/nature06006.

126. Wu, F., Deng, L., Zhai, Q., Zhao, J., Chen, Q., and Li, C. (2020). Mediator Subunit MED25 Couples Alternative Splicing of JAZ Genes with Fine-Tuning of Jasmonate Signaling. Plant Cell *32*, 429–448. 10.1105/tpc.19.00583.

127. Chung, H.S., and Howe, G.A. (2009). A critical role for the TIFY motif in repression of jasmonate signaling by a stabilized splice variant of the JASMONATE ZIM-domain protein JAZ10 in Arabidopsis. Plant Cell *21*, 131–145. 10.1105/tpc.108.064097.

128. Niedojadło, J., Dełeńko, K., and Niedojadło, K. (2016). Regulation of poly(A) RNA retention in the nucleus as a survival strategy of plants during hypoxia. RNA Biol. *13*, 531–543. 10.1080/15476286.2016.1166331.

129. Decker, C.J., and Parker, R. (2012). P-bodies and stress granules: possible roles in the control of translation and mRNA degradation. Cold Spring Harb. Perspect. Biol. *4*, a012286. 10.1101/cshperspect.a012286.

130. Mitchell, S.F., and Parker, R. (2014). Principles and properties of eukaryotic mRNPs. Mol. Cell *54*, 547–558. 10.1016/j.molcel.2014.04.033.

131. Yu, X., Li, B., Jang, G.-J., Jiang, S., Jiang, D., Jang, J.-C., Wu, S.-H., Shan, L., and He, P. (2019). Orchestration of Processing Body Dynamics and mRNA Decay in Arabidopsis Immunity. Cell Rep. *28*, 2194-2205.e6. 10.1016/j.celrep.2019.07.054.

132. Souret, F.F., Kastenmayer, J.P., and Green, P.J. (2004). AtXRN4 degrades mRNA in Arabidopsis and its substrates include selected miRNA targets. Mol. Cell *15*, 173–183. 10.1016/j.molcel.2004.06.006.

133. Song, L., Fang, Y., Chen, L., Wang, J., and Chen, X. (2021). Role of non-coding RNAs in plant immunity. Plant Commun. *2*, 100180. 10.1016/j.xplc.2021.100180.

134. Rambani, A., Hu, Y., Piya, S., Long, M., Rice, J.H., Pantalone, V., and Hewezi, T. (2020). Identification of Differentially Methylated miRNA Genes During Compatible and Incompatible Interactions Between Soybean and Soybean Cyst Nematode. Mol. Plant Microbe Interact. *33*, 1340–1352. 10.1094/MPMI-07-20-0196-R.

135. Seo, J.S., Sun, H.-X., Park, B.S., Huang, C.-H., Yeh, S.-D., Jung, C., and Chua, N.-H. (2017). ELF18-INDUCED LONG-

NONCODING RNA Associates with Mediator to Enhance Expression of Innate Immune Response Genes in Arabidopsis. Plant Cell *29*, 1024–1038. 10.1105/tpc.16.00886.

136. Seo, J.S., Diloknawarit, P., Park, B.S., and Chua, N.-H. (2019). ELF18-INDUCED LONG NONCODING RNA 1 evicts fibrillarin from mediator subunit to enhance PATHOGENESIS-RELATED GENE 1 (PR1) expression. New Phytol. *221*, 2067–2079. 10.1111/nph.15530.

137. Xu, G., Moeder, W., Yoshioka, K., and Shan, L. (2022). A tale of many families: calcium channels in plant immunity. Plant Cell. 10.1093/plcell/koac033.

138. Wang, C., Tang, R.-J., Kou, S., Xu, X., Lu, Y., Rauscher, K., Voelker, A., and Luan, S. (2024). Mechanisms of calcium homeostasis orchestrate plant growth and immunity. Nature. 10.1038/s41586-024-07100-0.

139. Bi, G., Su, M., Li, N., Liang, Y., Dang, S., Xu, J., Hu, M., Wang, J., Zou, M., Deng, Y., et al. (2021). The ZAR1 resistosome is a calcium-permeable channel triggering plant immune signaling. Cell *184*, 3528-3541.e12. 10.1016/j.cell.2021.05.003.

140. Wang, L., Tsuda, K., Truman, W., Sato, M., Nguyen, L.V., Katagiri, F., and Glazebrook, J. (2011). CBP60g and SARD1 play partially redundant critical roles in salicylic acid signaling. Plant J. *67*, 1029–1041. 10.1111/j.1365-313X.2011.04655.x.

141. Kim, Y., Park, S., Gilmour, S.J., and Thomashow, M.F. (2013). Roles of CAMTA transcription factors and salicylic acid in

configuring the low-temperature transcriptome and freezing tolerance of Arabidopsis. Plant J. *75*, 364–376. 10.1111/tpj.12205.

142. Yuan, P., Tanaka, K., and Poovaiah, B.W. (2021). Calmodulin-binding transcription activator AtSR1/CAMTA3 fine-tunes plant immune response by transcriptional regulation of the salicylate receptor NPR1. Plant Cell Environ. *44*, 3140–3154. 10.1111/pce.14123.

143. Lu, Y., Truman, W., Liu, X., Bethke, G., Zhou, M., Myers, C.L., Katagiri, F., and Glazebrook, J. (2018). Different Modes of Negative Regulation of Plant Immunity by Calmodulin-Related Genes. Plant Physiol. *176*, 3046–3061. 10.1104/pp.17.01209.

144. Truman, W., Sreekanta, S., Lu, Y., Bethke, G., Tsuda, K., Katagiri, F., and Glazebrook, J. (2013). The CALMODULIN-BINDING PROTEIN60 family includes both negative and positive regulators of plant immunity. Plant Physiol. *163*, 1741–1751. 10.1104/pp.113.227108.

145. Sun, T., Zhang, Y., Li, Y., Zhang, Q., Ding, Y., and Zhang, Y. (2015). ChIP-seq reveals broad roles of SARD1 and CBP60g in regulating plant immunity. Nat. Commun. *6*, 10159. 10.1038/ncomms10159.

146. Nobori, T., Monell, A., Lee, T.A., Sakata, Y., Shirahama, S., Zhou, J., Nery, J.R., Mine, A., and Ecker, J.R. (2025). A rare PRIMER cell state in plant immunity. Nature *638*, 197–205. 10.1038/s41586-024-08383-z.

147. Hu, Y., Schaefer, R., Rendleman, M., Slattery, A., Cramer, A., Nahiyan, A., Breitweiser, L., Shah, M., Kaehler, E., Yao, C., et al. (2025). Spatial and single-cell transcriptomics capture two distinct cell states in plant immunity. BioRxiv. 10.1101/2025.06.03.657683.

Chapter 2

Modular mechanisms of immune priming and growth inhibition mediated by plant effector-triggered immunity

Himanshu Chhillar[1], Hoang Hung Nguyen[1#], Pei-Min Yeh[1#], Jonathan DG Jones[2], Pingtao Ding[1]

[1] Institute of Biology Leiden, Leiden University, Sylviusweg 72, Leiden 2333 BE, The Netherlands
[2] The Sainsbury Laboratory, University of East Anglia, Norwich Research Park, Norwich NR4 7UH, UK
[#] These authors contributed equally

This chapter is published in: Cell Reports (2025) Mar 25;44(3):115394. doi: 10.1016/j.celrep.2025.115394

Abstract

Excessive activation of effector-triggered immunity (ETI) in plants inhibits plant growth and activates cell death. ETI mediated by intracellular Toll/Interleukin-1 receptor/Resistance protein (TIR) nucleotide-binding leucine-rich-repeat receptors (NLRs) involves two partially redundant signaling nodes in *Arabidopsis*, EDS1-PAD4-ADR1 and EDS1-SAG101-NRG1. Genetic and transcriptomic analyses show that EDS1-PAD4-ADR1 primarily enhances the immune component abundance and is critical for limiting pathogen growth, whereas EDS1-SAG101-NRG1 mainly activates the hypersensitive cell death response (HR) but is dispensable for immune priming. This study enhances our understanding of the distinct contributions of these two signalling modules to ETI and suggests molecular principles and potential strategies for improving disease resistance in crops without compromising yield.

Introduction

Inducible plant defense usually involves the concerted action of responses initiated by cell-surface and intracellular immune receptors. Cell-surface pattern recognition receptors (PRRs) initiate pattern-triggered immunity (PTI) upon detection of relatively conserved apoplastic pathogen molecules such as chitin or flagellin. Effector-triggered immunity (ETI) is activated by intracellular nucleotide-binding, leucine-rich repeat receptors (NLRs) upon recognising specific pathogen effector proteins[1,2]. ETI and PTI together confer a highly effective plant defense against pathogen attack[3–5]. Recent research has significantly expanded our understanding of the signalling pathways downstream of Toll/Interleukin-1 receptor/Resistance protein (TIR)-type NLR (TNL)-triggered ETI, with key roles played by lipase-like proteins ENHANCED DISEASE SUSCEPTIBILITY 1 (EDS1), PHYTOALEXIN DEFICIENT 4 (PAD4), and SENESCENCE-ASSOCIATED GENE 101 (SAG101), and helper NLRs

ADR1 (ACTIVATED DISEASE RESISTANCE 1) family and NRG1 (N REQUIREMENT GENE 1) family proteins, which share RESISTANCE TO POWDERY MILDEW 8 [i](RPW8)-like coiled-coil N-terminal signalling domains[2,6].

EDS1, PAD4, and SAG101 have emerged as central TNL signalling regulators in *Arabidopsis thaliana* (Arabidopsis) and many other plant species[7]. These proteins form distinct heterodimeric complexes regulating cell death and disease resistance[8]. EDS1-PAD4 complexes have been shown to play a crucial role in local and systemic acquired resistance (SAR)[9]. Meanwhile, EDS1-SAG101 complexes are hypothesised to be more critical for local immune responses, such as constraining the spread of plant viruses[10]. PAD4 and SAG101 also influence salicylic acid (SA) accumulation, connecting hormonal signalling pathways with the regulation of cell death and disease resistance[11].

The ADR1 family proteins (ADR1s) in Arabidopsis include ADR1, ADR1-LIKE 1 (ADR-L1), and ADR1-L2, which are also known as helper NLR proteins (hNLRs). They are pivotal in controlling ETI[12]. These proteins act as signal amplifiers, promoting the activation of downstream immune responses upon effector recognition[2,13]. The NRG1 hNLR family proteins (NRG1s), including NRG1A (or NRG1.1) and NRG1B (or NRG1.2), are required by TIR-NLRs to drive hypersensitive response (HR) cell death and contributing to enhanced disease resistance against oomycete pathogens[14]. More recently, it has been shown that *pad4* mutant mimics *adr1s,* while *sag101* mutant mimics *nrg1s* in classical immune responses[15–17]. These genetic results align with the model proposed by several groups that EDS1-PAD4 functions together with ADR1s and contributes more to restricting bacterial growth in TNL-mediated ETI, while EDS1-SAG101 functions with NRG1 and contributes more towards TNL-mediated cell death induced by ETI[15–20]. These results indicate two distinct

immune regulatory nodes associated with EDS1, leading to different downstream signalling.

The growth-defense trade-off, where plants slow growth in response to pests, is a key principle in plant economics affecting both ecosystems and crop breeding[21]. Many constitutive ETI mutants with auto-active NLR have shown severe growth penalties[22], which might act via various hormonal signalling while enabling plants to thwart pathogen attacks[23]. Recently, it has been shown that constitutive induction of ETI in the absence of PTI can also effectively lead to significant growth arrest[24]. Additionally, prior exposure of plants to pathogens or pathogen-derived ligands primes the plants to induce a much more robust immune response to subsequent encounters[25]. For instance, multiple PAMPs have already been shown to prime Arabidopsis plants against virulent *Pseudomonas syringae* pv. *tomato* (*Pst*) DC3000 bacterium[26]. ETI-induced priming has recently shown a similar effect[24]. However, the contribution of crucial immune regulators in governing the phenomenon of ETI-mediated growth-defense trade-off and immune priming remains inadequately understood.

In this study, we unravel the modular signalling pathways downstream of TNL-induced ETI mediated by EDS1-PAD4-ADR1s and EDS1-SAG101-NRG1s, with particular emphasis on their roles in cell death, immune priming, and ETI-induced growth arrest. We have also explored differential transcriptional outcomes between EDS1-PAD4 and EDS1-SAG101 nodes. This work advances our understanding of plant immunity and sheds light on potential strategies for improving disease resistance in crops without impinging on growth and yield.

Results

Differential roles of EDS1-PAD4-ADR1s and EDS1-SAG101-NRG1s in ETI-induced growth arrest

All previous immune phenotypes reported for lipase-like/hNLRs mutants were observed during ETI activation in the presence of PTI. Therefore, it was unknown to what extent prior results are ETI-specific. Here, we used a β-estradiol (E2)-inducible AvrRps4-expressing ('SETI') line, to activate TNL-mediated ETI in the absence of PTI via the two paired TIR-NLRs RPS4 and RRS1, and RPS4B and RRS1B[24]. When growing SETI plants on an E2-containing medium, we observed growth arrest, including a reduction in size and fresh weight (**Figure 1A-C**). This growth arrest was suppressed entirely in the *eds1-2* mutant (SETI_*eds1*) and the *pad4 sag101* double mutant (SETI_*ps*), indicating a critical role for EDS1, PAD4, and SAG101 in modulating ETI-induced growth inhibition mediated by TNLs.

However, the *sag101* single mutant (SETI_*sag101*) exhibited a growth inhibition pattern like SETI_wt (**Figure 1A**), implying that SAG101 does not contribute to ETI-induced growth arrest. Interestingly, the *pad4* single mutant (SETI_*pad4*) appeared to partially suppress the ETI-induced growth arrest in the absence of PTI despite having similar induction in AvrRps4 expression (**Figure S1D**), suggesting PAD4 may play a significant role in mediating ETI-dependent growth arrest independent of SAG101 (**Figure 1A**). Curiously, a severe inhibition in lateral root formation was observed in SETI_wt and SETI_*sag101,* which was partially relieved in SETI_*pad4* plants and completely relieved in SETI_*eds1* and SETI_*ps* suggesting a role for *PAD4* in controlling root growth and development (**Figure 1B**).

In parallel, we observed that the *nrg1a nrg1b* double mutant (SETI_*nrg1s*) mirrored the SETI_*sag101* phenotype (**Figure S1A-C**), implying that the

NRG1 family proteins may not contribute to growth arrest in response to ETI. Finally, the *adr1 adr1-l1 adr1-l2* triple mutant (SETI_*adr1s*) resembled the SETI_*pad4* phenotype, suggesting a functional correlation between PAD4 and ADR1 proteins in the regulation of ETI-mediated growth arrest.

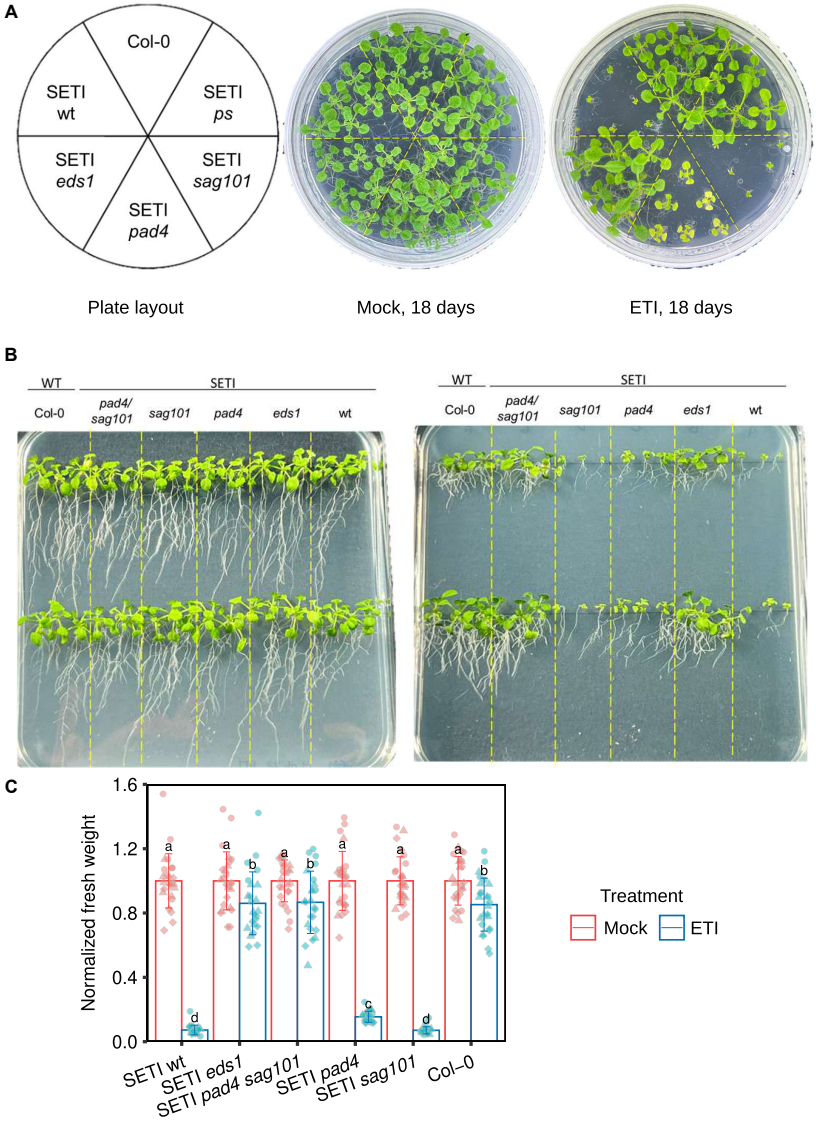

Figure 1. Estradiol induced growth arrest phenotype in lipase-like protein mutants. A. Indicated mutants of lipase-like proteins (SETI_wt, SETI_*sag101*, SETI_*pad4*, SETI_*pad4 sag101*, SETI_*eds1)* were sown on round GM plates with or without E2 (50 µM), and their growth arrest phenotype was recorded 18 days after planting on E2 plates. (Note: We have used the full name of all the mutants

in all the figures for better visualisation). B. Indicated mutants of lipase-like proteins were sown on square GM plates with or without E2 (50 µM), and the plates were grown vertically. Growth arrest and lateral root formation phenotypes were recorded 18 days after sowing on E2 plates. C. Indicated mutant lines were sown vertically on square GM plates with or without E2 (50 µM) and the fresh weight was recorded 18 days after sowing on E2 plates. Fresh weight was normalized to the average fresh weight of the mock controls for the respective lines. The error bars show standard deviation. Letters are highlighting statistical differences (LSD-test, $p \leq 0.05$).

Distinct contributions to ETI-mediated cell death by PAD4-ADR1s and SAG101-NRG1s

SETI_wt shows no macro cell death induced by ETI in the absence of PTI[24]. This hypersensitive response (HR) can be measured by recording ion leakage upon E2 induction, which is easily distinguishable at 4 hours post infiltration (hpi) from the mock treatment and saturates at 22 hpi (**Figure 2A, S2B, S3D**). SETI_*eds1* and SETI_*ps* plants do not show any significant increase in ionic conductivity upon E2 treatment, highlighting the interplay of EDS1, PAD4, and SAG101 in mediating the ETI-mediated cell death.

Interestingly, the increase in ion conductivity in SETI_*pad4* upon E2 induction is similar to SETI_wt, suggesting that PAD4 alone is not sufficient to activate ETI-induced cell death (**Figure 2A**). However, the increase in ion conductivity upon E2 treatment is significantly compromised in SETI_*sag101* plants, showing an independent role of SAG101 from PAD4 in mediating ETI-induced cell death in the absence of PTI (**Figure 2A**). Furthermore, only SETI_*ps* mutant can fully compromise the ETI- induced ion leakage like SETI_*eds1* (**Figure 2A**). This suggests a synergistic contribution of PAD4 and SAG101 to cell death as we only see complete abolishment in ion leakage when both PAD4 and SAG101 are lost. We have also observed similar trends in the hNLR mutants in the

SETI background (SETI_*nrg1s* and SETI_*adr1s*) (**Figure S3A, S3D**). The SETI_*adr1s* mimics SETI_*pad4* while SETI_*nrg1s* mimics SETI_*sag101,* showing that the SAG101-NRG1 node might contribute more to ETI-induced cell death while the PAD4-ADR1 node merely acts as a synergistic module in the presence of the parallel SAG101-NRG1 node.

HR has been shown to have a close association with chlorophyll catabolism[27,28]. Therefore, we sought to test the chlorophyll content as an additional indicator of cell death. A reduction in total chlorophyll content was observed for SETI_wt and SETI_*pad4* upon E2 treatment (**Figure 2B, S2A**), which was intensified significantly upon the 'PTI+ETI' (PTI plus ETI) treatment (50 µM of E2 and *Pst* DC3000 *hrcC*$^-$) which is in line with the previous report[4]. However, in SETI_*sag101*, a significant reduction of the total chlorophyll content is observed after 'PTI+ETI' treatment but not after PTI nor ETI alone (**Figure 2B**). This reduction is not as significant as in SETI_*pad4* and SETI_wt (**Figure 2B**). As expected, there is no reduction in chlorophyll content in SETI_*ps* lines. SETI_*adr1s* also showed a significant reduction in chlorophyll content upon ETI and 'PTI+ETI' treatments (**Figure S3B, S3C**), and this reduction is compromised in SETI_*nrg1s*, which is also in agreement with the ion leakage results that the SAG101-NRG1 node contributes more to ETI-induced cell death.

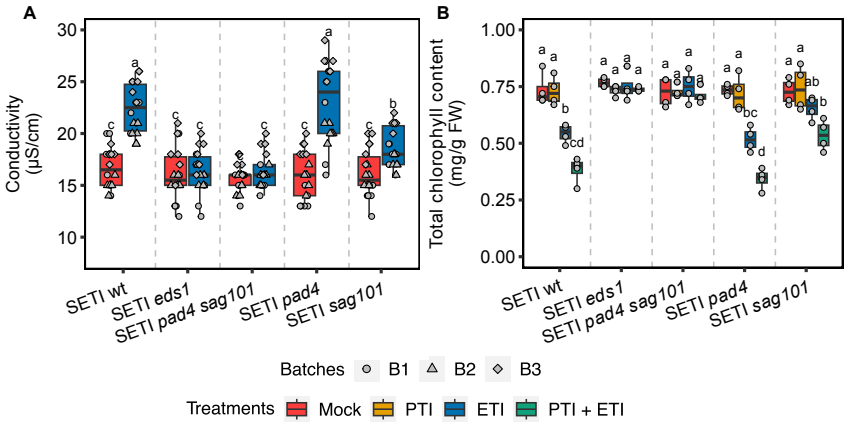

Figure 2. Differential regulation of ETI-induced cell death mediated by lipase-like protein. A. Indicated mutants of lipase-like proteins (SETI_wt, SETI_*sag101*, SETI_*pad4*, SETI_*pad4 sag101*, SETI_*eds1*) were infiltrated with E2 or mock and ion leakage was determined at 24 h time point. Letters showing statistical differences (Tukey-HSD-Test, $p \leq 0.05$). B. Total chlorophyll content was estimated on indicated mutants of lipase-like proteins 3 dpi after E2 infiltration as ETI treatment, *Pst* DC3000 *hrcC*$^-$ as PTI treatment, (E2 + *Pst* DC3000 *hrcC*$^-$) as PTI+ETI treatment and DMSO dissolved in 10 mM $MgCl_2$ as mock. Letters represent statistical differences (Tukey-HSD-Test, $p \leq 0.05$).

ETI-mediated immune priming requires both PAD4-ADR1s and SAG101-NRG1s nodes

Pre-treatment of SETI_wt plants with E2 shows increased disease resistance against subsequent bacterial infection, indicating ETI alone can prime plant immunity[24]. Consistent with this previous report, we also observed a significant reduction in bacterial growth compared to mock control when SETI_wt plants were pre-infiltrated with E2 one day before being inoculated with the virulent bacterial strain, *Pst* DC3000 carrying an empty vector (**Figure 3**). In contrast, E2-pretreated SETI_*eds1* and SETI_*ps* plants show complete loss of priming.

In parallel, we then performed an E2- or ETI-induced disease priming assay with SETI_*pad4* and SETI_*sag101* mutant plants. We found that the E2-pretreated SETI_*sag101* plants show no significant difference from SETI_wt plants in disease resistance priming (**Figure 3**). Similarly, such a priming effect is retained in SETI_*pad4*, though overall bacterial growth in E2-pretreated SETI_*pad4* plants is more than those in SETI_wt and SETI_*sag101* plants (**Figure 3**). It is noteworthy that the *pad4* but not *sag101* mutant was shown to be partially compromised in PTI-primed disease resistance with the elicitor of a 22-amino-acid epitope from bacterial flagellin and fully compromised in nlp20-induced priming[29], indicating that PAD4 may play a more significant role in both ETI- and PTI-primed disease resistance than SAG101 in Arabidopsis, though both PAD4 and SAG101 are required for the disease priming of TNL-mediated ETI.

We further tested ETI-mediated disease priming with SETI_*ngr1s* and SETI_*adr1s* mutants and the higher-order SETI_*helperless* mutant, referring to as a quintuple mutant with the loss-of-function of both *adr1s* and *nrg1s*, *adr1 adr1-l1 adr1-l2 nrg1a nrg1b*[15,17]. E2-pretreated SETI_*nrg1s* show no significant defects in disease priming, which is similar to SETI_wt and SETI_*sag101*, whereas SETI_*adr1s* resembles the phenotype of SETI_*pad4* (**Figure S4**). A complete loss in disease priming is only observed in E2-pretreated SETI_*helperless* plants, and together with the results from SETI_*ps* (**Figure 3**, **S4**), it can be inferred that both PAD4-ADR1 and SAG101-NRG1 nodes are required for TNL-activated ETI-mediated immune priming.

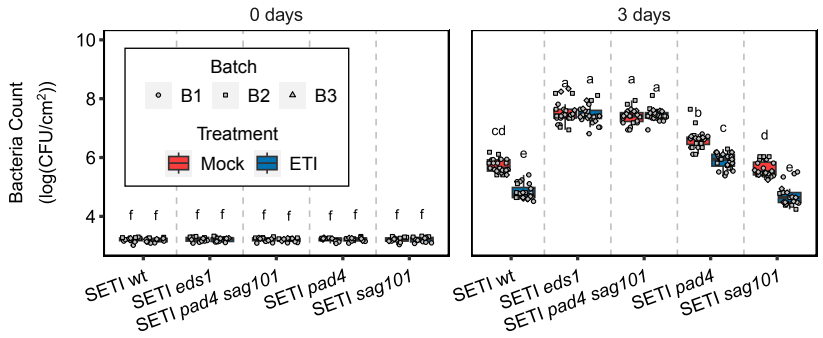

Figure 3. ETI-directed disease priming in SETI lipase-like protein mutants. Indicated mutants of lipase-like proteins were infiltrated with E2 or mock one day before infiltration with *Pst* DC3000 EV. Bacterial CFU were counted at day '0' and day '3' after infiltration with DC3000 EV. Letters showing statistical differences (Tuckey-HSD-Test, $p \leq 0.05$).

ETI-specific defense gene profiling mediated by PAD4-ADR1s and SAG101-NRG1s

We performed genome-wide RNA-seq on SETI mutant lines by specifically inducing ETI through E2 treatment to investigate the differences and similarities of defense gene activation between SAG101-NRG1s and PAD4-ADR1s nodes. We found 5067 differentially expressed genes (DEGs) across all tested genotypes and treatments with *p*-value < 0.01 and |log2[fold change (FC)]| ≥ 1 (**Figure 4**, **Tables S1-S11**). There are 1,902 up-regulated genes in the SETI_wt, 1,707 up-regulated genes in the SETI_*pad4*, and 2,281 up-regulated genes in the SETI_*sag101* E2-treated samples compared to mock-treated samples (**Figure S5B**). The DEGs post E2-treatment, both upregulated and downregulated, are substantially reduced in the SETI_*pad4* mutant compared to the SETI_wt plants (**Figure S5A, S5B**), indicating that PAD4 plays a major role in TNL-mediated ETI-induced transcriptional reprogramming and its loss-of-function could not be compensated by SAG101. Conversely, this reduction in DEGs number is not observed in the SETI_*sag101*. Instead, more

DEGs are found in SETI_*sag101* compared to SETI_wt, which might be due to overcompensation by functional PAD4 or by another unknown mechanism of synergy between PAD4 and SAG101. The persistence of DEGs in the SETI_*sag101* mutant indicates that SAG101 may not be as critical as PAD4 in suppressing or modulating these gene expressions during ETI early activation. This differential impact on gene expression between the two mutants highlights a divergent role of PAD4 and SAG101 in the plant immune response, emphasising the complexity of ETI signalling pathways. These results also highlight the unequal redundancy between PAD4-ADR1s and SAG101-NRG1s, consistent with previous reports that ADR1s can compensate for NRG1s but not *vice versa*[17]. There are no DEGs in SETI_*eds1* and SETI_*pad4 sag101* after E2 treatment compared to mock, demonstrating that *eds1* mutant and *pad4 sag101* double mutant can completely block the TNL-mediated ETI-specific transcriptional reprogramming.

Hierarchical clustering of the DEGs in the heat map revealed 10 clusters using a Euclidean distance and ward.D clustering algorithm (**Figure 4**)[30]. Clusters 3, 5, 6, 7, 8, and 9 show defense-related DEGs according to the gene ontology (GO) analysis from g:Profiler (FDR < 0.05, Benjamini-Hochberg) indicating that these are immune-related clusters (**Figure 4**). The well-known immune-related genes from each cluster and their expression patterns across the SETI mutants were highlighted (**Figure 4**, **Table S1**). Among the immune clusters, cluster 5 comprises genes such as the N-hydroxy pipecolic acid (NHP) biosynthetic genes *FLAVIN-DEPENDENT MONOOXYGENASE* (*FMO1*) and *AGD2-LIKE DEFENSE RESPONSE PROTEIN 1* (*ALD1*)[31], while clusters 5 and 9 contains genes related to cell death. On the other hand, cluster 7 includes genes mainly associated with salicylic acid biosynthesis and signalling, like *ISOCHORISMATE SYNTHASE 1* (*ICS1*), *ENHANCED DISEASE*

SUSCEPTIBILITY 5 (*EDS5*), and *NONEXPRESSOR OF PATHOGENESIS-RELATED GENES 1* (*NPR1*)[32]. Cluster 8 contains genes related to jasmonate signalling. We further extended our analysis on the downregulated DEGs in clusters 1, 2, 4, and 10, predominantly composed of downregulated genes during ETI early activation. GO term analysis of these clusters revealed that most GO terms are related to hormone response, sugar biosynthesis, sugar metabolism, and developmental and photosynthetic pathways (**Figure S5C, S5D, S5E, S5F**). This indicates a significant negative influence of ETI activation on specific plant hormonal, cellular, and metabolic processes, aligning with earlier studies[33]. The constitutive effects of this negative influence might be one of contributing factors to the severe growth retardation of SETI_wt and SETI_*sag101* on E2 plates. We also examined the expression profiles of the genes enriched in selected GO terms (**Figure S6**). Interestingly, the downregulation patterns in SETI_wt and SETI_*sag101* are quite similar, whereas SETI_*pad4* shows a less pronounced downregulation in a majority of genes related to carbohydrate metabolism, plant morphogenesis, and photosynthesis to some extent (**Figure S6**). In addition, similar trends were observed concerning hormone pathway genes, including auxin response genes, which play an integral role in lateral root formation[34]. These findings provide some initial indications that might explain the partial elevation in growth arrest and lateral root formation observed in SETI_*pad4* plants.

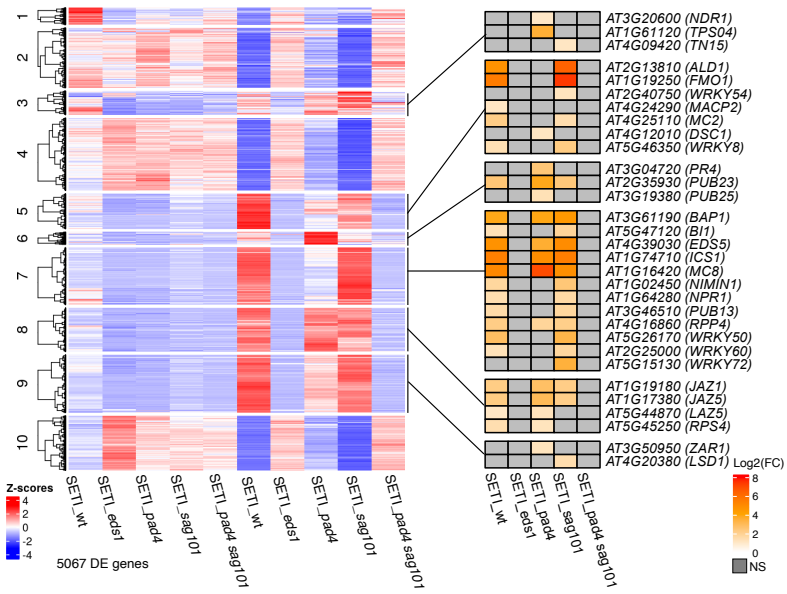

Figure 4. Analysis of TNL-dependent transcriptional changes across SETI lipase-like protein mutants. Five- to six-week-old SETI_wt, SETI_*eds1*, SETI_*pad4*, SETI_*sag101*, and SETI_*pad4 sag101* plants were infiltrated with mock (10 mM $MgCl_2$), and 50 µM E2 (ETI). Samples were collected at 4 h post infiltration (4 hpi) for RNA-seq analysis. The left heatmap shows the normalised expression z-score of all the differently expressed genes with a false discovery rate (FDR) of $p < 0.01$ and a fold change of ≥ 1. No significant gene expression changes in SETI_*eds1* and SETI_*ps* after ETI-treatment induction. SETI_wt, SETI_*pad4*, and SETI_*sag101* show visible expression after ETI-treatment induction. The right heat map represents the expression pattern of key immune genes from each immunity-related cluster among the SETI lipase-like protein mutants i.e. SETI_wt, SETI_*pad4*, and SETI_*sag101*.

Defining the specificity of PAD4 and SAG101-mediated transcriptional reprogramming

The upregulated DEGs were further classified into PAD4- and SAG101-dependent and shared DEGs (**Figure 5A**, **Table S15**). A total of 438 DEGs

were identified as PAD4-dependent, as they were upregulated in both SETI_wt and SETI_*sag101* but downregulated or showed no significant difference in SETI_*pad4*. Similarly, 85 DEGs were classified as SAG101-dependent, being upregulated in SETI_wt and SETI_*pad4* but downregulated or showing no significant difference in SETI_*sag101* (**Figure 5A**). Additionally, 121 DEGs showed shared dependency on both PAD4 and SAG101. Furthermore, 1,258 DEGs were upregulated in SETI_wt, SETI_*pad4*, and SETI_*sag101,* indicating that the transcriptional regulation of these DEGs is ETI-specific but redundantly regulated by PAD4 and SAG101 (**Figure 5A**, **S7A-S7C**). These 1,258 genes were further classified based on partial dependency on PAD4, SAG101, or both (**Table 1**, **Table S16**). GO term analysis of these genes was performed, highlighting those associated with immune-related biological functions (**Figure 5B-5D**, **Table S12-S14**). Interestingly, more DEGs were PAD4-dependent than SAG101-dependent (**Figure 5B**, **5C**). Some genes related to SAR, such as *FMO1* and *ALD1*, were exclusively dependent on PAD4, while other genes showed dependency on both PAD4 and SAG101 (**Figure 4, 5B, 5D**; **Table S12, S14**).

Table 1. Classification of up-regulated genes into partially PAD4-dependent, partially SAG101-dependent, and PAD4/SAG101-dependent categories. *1: DEGs present in SETI_wt, SETI_*pad4*, and SETI_*sag101*. However, in partially PAD4-dependent DEGs the $\log_2$ fold change (FC) difference between SETI and SETI_*pad4* is greater than 1, but there is no $\log_2$ FC difference between SETI_wt and SETI_*sag101*; In partially SAG101-dependent DEGs the $\log_2$ FC difference between SETI_wt and SETI_*sag101* is greater than 1, but no difference between SETI_wt and SETI_*pad4*. *2: DEGs present in SETI_wt, SETI_*pad4* and SETI_*sag101*. The $\log_2$ FC between SETI_wt and SETI_*pad4* and SETI_wt and SETI_*sag101* differ at a magnitude of at least 1.

Categories	DEGs numbers
DEGs partially dependent on *PAD4*[*1]	192
DEGs partially dependent on *SAG101*[*1]	80
DEGs dependent on both *PAD4* and *SAG101*[*2]	64

It is evident from the ion leakage data that SAG101 contributes more to cell death, but PAD4 has synergistic effects in addition to regulating cell death. As expected, cell-death-related genes were found in all categories, including PAD4-specific, SAG101-specific, and PAD4/SAG101-shared. For instance, genes enriched in cell death-related GO terms such as *METACASPASE 2* (*MC2*), *MC8*, *CYSTEINE-RICH RECEPTOR-LIKE KINASE 13* (*CRK13*), *BAX INHIBITOR 1* (*BI1*) are found to be dependent on PAD4 (**Figure 5B**, **Table S12**). On the other hand, genes like *LAZARUS 5* (*LAZ5*) and *CRK4* are dependent on SAG101 (**Figure 5C**, **Table S13**), while *BCL-2 ASSOCIATED ATHANOGENE 6* (*BAG6*) and *MEMBRANE ATTACK COMPLEX/PERFORIN-LIKE 2* (*MACP2*) depend on both PAD4 and SAG101 (**Figure 5C**, **Table S14**). Similar observations were made with the downregulated DEGs, with some DEGs being shared and others exclusively regulated by PAD4 or SAG101 (**Figure S5A**, **Table S18**).

Collectively, these findings highlight the redundant regulation of transcriptional reprogramming by PAD4 and SAG101, demonstrating that while some DEGs are uniquely controlled by one node, a significant portion is co-regulated by both, underscoring their unequal redundant roles in orchestrating the ETI response. In summary, PAD4 seems to play a prominent role in regulating ETI-activated transcriptional reprogramming compared to SAG101, which may explain why PAD4 contributes more to the ETI-induced growth arrest and immune priming, whereas SAG101

plays a more prominent role in cell death. It still needs to be determined how the specificity of transcriptional regulation is achieved by these two unequally redundant nodes downstream of ETI mediated by TNLs.

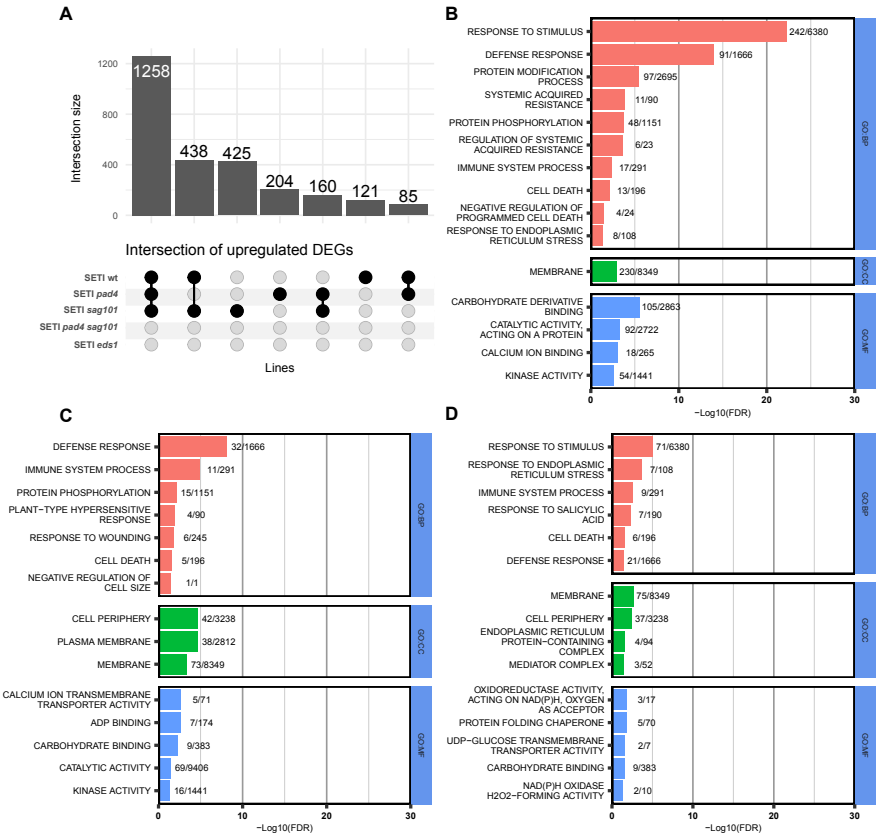

Figure 5. **Comparison of gene up-regulation in ETI treatments across lipase-like protein mutants**. A. Up-Set plot shows 1258 DEGs affected by both PAD4 and SAG101. 438 DEGs are *PAD4*-dependent, and 85 DEGs are SAG101-dependent. B. GO enrichment for PAD4-dependent DEGs. C. GO enrichment for SAG101-dependent DEGs. D. GO enrichment for PAD4/SAG101-shared DEGs. GO analysis is done with g:Profiler, and the GO terms were shown in different enrichment analyses, including biological process (GO:BP), cell components (GO:CC), and molecular function (GO:MF) (FDR ≤ 0.05, Benjamini-Hochberg).

Discussion

EDS1 interacts with either of two other lipase-like proteins, PAD4 and SAG101, to initiate the ETI downstream signalling after sensor TNL activation[8,35,36]. Upon TNL activation, helper NLRs ADR1 or NRG1 interact with the EDS1-PAD4 and EDS1-SAG101 modules, respectively[16]. ETI promotes interaction between NRG1 and EDS1/SAG101 but NRG1/EDS1/SAG101 oligomerization requires PTI[19,37,38]. EDS1-PAD4-ADR1s and EDS1-SAG101-NRG1s have been shown to play unequally redundant roles in plant immune responses[16,17]. EDS1/PAD4/ADR1s contribute more to disease resistance, while EDS1/SAG101/NRG1s, contribute more towards cell death. However, the downstream components and the molecular machinery underlying the unequal roles are still poorly understood.

Here, we focused on investigating ETI-specific roles of the PAD4 and SAG101 nodes. We use the mutants of EDS1 family proteins and helper NLRs in an inducible ETI genetic background to determine the involvement of these proteins in mediating ETI-specific signalling. A partial relief of growth reduction, as well as of inhibition in the lateral root, was observed in SETI_*pad4* compared to SETI_*sag101* on E2 plates, indicating that PAD4 plays an important role in coordinating the balance between growth, development, and defense[23]. SAG101 also synergises with PAD4 in the growth-defense trade-off, as only the SETI_*ps* double mutant shows no growth inhibition. As the detailed mechanisms of growth-defense trade-off remain unexplored, our report regarding the differential roles of PAD4 and SAG101 in mediating ETI-specific growth inhibition provides additional information to help decipher the underlying molecular mechanisms.

We define immune priming as being the strengthening of plant disease resistance after subjecting plants to a priming treatment. Here, we show

that SETI_*pad4* (similarly SETI_*adr1s*) and SETI_*sag101* (similarly SETI_*nrg1s*) both show some immune priming upon ETI activation, though both *pad4* (or *adr1s* triple mutant) and *sag101* (or *nrg1s* double mutant) plants are more disease susceptible[14,16]. These indicate that plants with partially compromised immunity still retain priming capacity for disease resistance. This insight could support improved agricultural practices. For instance, for emerging or remerging pathogens that can partially escape from the immune surveillance system or dampen the immune activation process, one can test whether ETI-mediated immune priming can enhance crop disease resistance. Here, we have only explored the short-term priming capacity in such mutants, and priming could provide longer-term protection. Therefore, it will be interesting to investigate the persistence of this immune memory and how this priming effect has been 'memorised' or 'imprinted' inside plant cells.

Previous studies have elucidated that HR and disease resistance mechanisms can operate independently[39]. Extending this understanding, our analysis shows that the SAG101-NRG1s module predominantly facilitates ETI-activated cell death, while the PAD4-ADR1s module is more critical for initiating disease resistance. Despite this specificity, both modules have overlapped functions in regulating HR and resistance, though in partially redundant roles. Specifically, NRG1s are required for TNL-mediated disease resistance to obligate biotrophic oomycete pathogens, including the downy mildew agent *Hyaloperonospora arabidopsidis* (*Hpa*) and the white rust causative *Albugo candida*[14]. ADR1s are also required for TNL-mediated resistance against *Hpa*[12]. While the *sag101* single mutant exhibits only isolated single-cell HR cell death, which appears to confer a less severe susceptibility than the *nrg1a nrg1b* double mutant, both SAG101 and NRG1s are consistently implicated as part of the same downstream signalling pathway mediated

by EDS1 in multiple instances[14–16,40]. The *pad4* single mutant can produce conidiospores accompanied by single-cell trailing necrosis, which aligns with that observed in the *adr1s* triple mutant[40,41]. More intriguingly, SAG101 and NRG1s appear dispensable for conferring resistance against the hemibiotrophic bacterial pathogen *P. syringae*, where the PAD4-ADR1s node assumes a more important role. Therefore, it is imperative for future studies to comprehensively evaluate disease resistance across a range of mutants, including those carrying mutations in lipase-like protein-encoding genes (*pad4*, *sag101*, and their double mutant), as well as those affecting hNLR-encoding genes (*nrg1s*, *adr1s*, and their quintuple *helperless* mutant). It is also crucial to expand testing their responses to more different types of plant pathogens. Furthermore, it is key to investigate further how each node modulates the functional preference towards HR and resistance and how these are linked to the differential phenotypes of ETI-induced growth inhibition and disease priming. In addition, it will provide valuable insights into NLR-mediated immune effectiveness to explore how the synergistic effects of SAG101-NRG1s and PAD4-ADR1s nodes are achieved.

Importantly, ETI is always preceded by PTI in authentic interactions with microbes, making it challenging to study ETI-specific responses. For instance, in the heat map that encompasses all the treatments (PTI, ETI, 'PTI+ETI'), gene expression patterns in 'PTI+ETI' are much less distinguishable across different lipase-like mutants compared to those in the ETI-only treatment (**Figure S8**). We suspect that PTI can potentially mask the overall ETI transcriptome by pre-emptively activating a set of defense-related pathways that overlap with those induced during ETI. Specifically, PTI-induced genes may saturate the cellular response machinery, thereby attenuating or obscuring the subsequent activation of ETI-specific genes. This is supported by the observation that, in SETI_wt,

ETI activates a distinct set of genes that are not revealed in combined PTI+ETI treatment, via the analysis of DEGs across all conditions (PTI, ETI, and PTI+ETI) (**Figure S9**, **Table S17**). This observation reinforces the value of examining ETI in isolation to identify its unique contributions to gene regulation. In addition, a considerable reduction in the number of upregulated genes in PTI+ETI treatment is observed compared to ETI treatment alone. This suggests that PTI treatment may lead to the expression of specific genes reaching a threshold that renders subsequent responses to ETI less pronounced. This masking effect might explain why the PTI and PTI+ETI profiles appear similar in our heatmap (**Figure S8**). Moreover, the choice of using the 4 hours post infiltration (hpi) time point might have contributed to this observation. This time point is relatively late for capturing early PTI responses[42] but still within the window where downstream ETI effects could manifest. It's plausible that at this stage, some responses typically associated with ETI could be acting synergistically with PTI, especially since the bacteria utilised have a functional Type III Secretion System. We also found similar effects in several recent reports[17,43]. TNLs or TIR-only proteins possess enzymatic activities to produce small molecules that associate with different EDS1 complexes with either PAD4-ADR1s or SAG101-NRG1s[44]. Our transcriptome profiling results for either PAD4-ADR1s or SAG101-NRG1s modules specific to ETI might provide additional insights. It has been shown that EDS1-SAG101-NRG1s hNLR resistosome formation requires the cell-surface immune receptor-mediated PTI; it would be interesting to compare the gene expression patterns between PTI, ETI, and 'PTI+ETI' in SETI_*pad4*. A few other important unresolved questions remain: How do the resistosomes formed by NRG1s and ADR1s activate ETI downstream responses? Are the cation channel activities of NRG1s and ADR1s sufficient to activate the observed transcriptional reprogramming?

More broadly, it has been reported that PAD4 and SAG101 from different plant species may have various functions during TNL-mediated ETI activation. For instance, the Solanaceae genome mainly encodes two SAG101 isoforms (SAG101a, SAG101b), and EDS1-SAG101b has been shown to play a crucial and sufficient role in nearly all TNL-mediated ETI immune responses in *Nicotiana benthamiana* (*Nb*). In contrast, *Nb*PAD4 did not show any significant roles[36]. However, similar to *Nb*SAG101s, *Nb*NRG1 is important in regulating ETI downstream of EDS1 in *Nb*[37,45]. Conceivably, the EDS1-SAG101-NRG1 node plays a crucial role in regulating both disease resistance and cell death in *Nb*, while in contrast, EDS1-SAG101-NRG1 in Arabidopsis is more specialised to HR. It will be interesting in the future to generate ETI-inducible lines in *Nb* that are similar to SETI in Arabidopsis, to study ETI-specific responses mediated by *Nb*PAD4 and *Nb*SAG101 to dissect the ETI-specific downstream signalling in comparison to those in Arabidopsis, which may provide more insights in ETI-mediated growth-defense trade-off and immune priming. In summary, our studies have provided valuable datasets to dissect modular mechanisms of immune priming and growth inhibition mediated by ETI, which could underpin more innovative plant breeding for disease resistance.

Acknowledgements

We thank Marc Gebauer for their technical assistance with the genotyping of mutants and Ewout van Diepen for their invaluable help during the more labour-intensive aspects of our experimentation. Their contributions were instrumental to the successful completion of this work. HC, HHN, PY and PD acknowledge a European Research Council Starting Grant 'R-ELEVATION' (grant agreement: 101039824). JDGJ was supported by the Gatsby Foundation (United Kingdom).

We sincerely thank the readers of our initial preprint for their valuable feedback and for pointing out errors. We have incorporated these corrections into this second version. We welcome any further suggestions or comments that can help us improve our manuscript.

Competing interests

The authors declare no competing interests.

Author contributions

PD conceptualised and oversaw the inception of the research project. The experimental work was collaboratively conducted by PD, HC, and PY. Data analysis and figure generation were performed by HC, HHN, PY and PD. JDGJ was involved throughout the project, providing valuable discussions that significantly shaped the research. HC and PD wrote the initial manuscript draft. All co-authors contributed to subsequent revisions and editorial processes. The final manuscript was prepared by HC and PD and was approved for submission by all authors.

Data and code availability

- The RNA-seq data for this study have been deposited in the European Nucleotide Archive (ENA) at EMBL-EBI under accession number: PRJEB62154.
- All codes are available via GitHub: https://github.com/dinglab-plants/ETI_Project and deposited in Zenodo under https://doi.org/10.5281/zenodo.14673399.

Material and Methods

Plant material and growth conditions

Arabidopsis thaliana accessions Col-0 and a β-estradiol (E2) inducible Super-ETI line (SETI_wt), were used as the wild-type controls in this study. The lipase-like mutants SETI *eds1-2* (SETI_*eds1*), SETI *pad4-1* (SETI_*pad4*), SETI *sag101-1* (SETI_*sag101*), and SETI *pad4-1 sag101-*

1 (SETI_*ps*) and helper NLR mutants, including SETI *adr1-1 adr1-L1 adr1-L2 nrg1a nrg1b* (SETI_*helplerless*), SETI *nrg1a nrg1b* (SETI_*nrg1s*), and SETI *adr1-1 adr1-L1 adr1-L2* (SETI_*adr1s*) are generated by crossing all the previously reported mutants with SETI plants[12,14,40].

For square and round plate assay, seeds were processed by liquid sterilization (70% ethanol 5 minutes, bleach solution 5 minutes, 100% ethanol 5 minutes, washed three times with sterilized water, and soaked into 0.5% agarose in 4 °C dark condition for one day). Seeds were sown on a 9 cm petri dish or square petri dish (120 mm x 120 mm), GM (Germination media) plate, or GM plate with 50 μM of E2. For square plates 1.2% agarose was used while for circular plates 0.8% agarose was used. Plants were grown at 21 °C under long-day conditions (16 h light, 8 h dark), and at 50% humidity. Photos were taken 14 and 18 days after sowing. Col-0 was used as the negative and SETI as the positive control.

Bacterial strains and growth conditions

The various bacteria strains used in this study were described in the Key Resources Table. *Pseudomonas syringae* pv. tomato (*Pst*) DC3000 EV (carrying empty vector) grown on the King's B medium plates 25 μg mL^{-1} rifampicin, and 50 μg mL^{-1} kanamycin and *Pst* DC3000 *hrcC*$^{-}$ were grown on the King's B medium plates 25 μg mL^{-1} rifampicin. *Pseudomonas fluorescens* engineered with a Type III secretion system (Pf0-1 'EtHAn' strains) expressing empty vector was grown on the King's B medium plates with. All the Pseudomonas strains were grown on plates at 28°C for 2 days for further inoculum preparation.

Fresh weight measurement

The seeds were processed by liquid sterilization and sown on a square petri dish, GM plate, or GM plate with 50 μM of E2 for 18 days. Six seedlings were pooled together to measure the fresh weight. All statistics

and figures are generated in R version 4.3.1. ANOVA (p- value ≤ 0.05) was used for identifying significant factors. A least significant difference (LSD) test (p-value ≤ 0.05) was used to identify differences between treatment and lines. A detailed statistical summary is available on GitHub: https://github.com/dinglab-plants/ETI_Project.

RNA-seq raw data processing, alignment, quantification of expression, and data visualization

DMSO in 10 mM $MgCl_2$, 50 µM E2 in 10 mM $MgCl_2$, *Pseudomonas fluorescens* (Pf0-1)[46] in 10 mM $MgCl_2$, or Pf0-1 and 50 µM E2 in 10 mM $MgCl_2$ was infiltrated in 5 to 6-week-old Arabidopsis leaves with 1 mL needleless syringe for RNA-seq sample collection. Two leaves per sample were collected at 0 and 4 hpi as 1 biological replicate. RNA was extracted with the Zymo RNA extraction kit[47].

The RNA sample was sequenced by Novogene. Raw reads were trimmed into 390 bp clean reads by the Novogene bioinformatics service. At least 12 million paired-end clean reads for each sample were provided by Novogene for RNA-seq analysis. All reads passed FastQC before the following analyses[48]. All clean reads were mapped either to the TAIR10 Arabidopsis genome/transcriptome via TopHat2 or to a comprehensive Reference Transcript Dataset for Arabidopsis Quantification of Alternatively Spliced Isoforms (AtRTD2_QUASI) containing 82,190 non-redundant transcripts from 34,212 genes via Galaxy and Salmon tools[49,50]. The estimated gene transcript counts were used for differential gene expression analysis and statistical analysis with the 3D RNA-seq software[51]. The low-expressed transcripts were filtered if they did not meet the criteria of ≥3 samples with ≥1 count per million reads. The batch effects between three biological replicates were removed to reduce artificial variance with the RUVSeq method[52]. The expression data were normalised across samples with the TMM (weighted trimmed mean of M-

values)[53]. The significance of expression changes in the contrasting groups 'SETI_wt_ETI vs SETI_wt_mock', groups 'SETI_*eds1*_ETI vs SETI_wt_mock', 'SETI_*pad4*_ETI vs SETI_wt_mock', 'SETI_*sag101*_ETI vs SETI_wt_mock' and 'SETI_*ps*_ETI vs SETI_wt_mock' were determined by the limma-voom method[54,55]. A gene was defined as a significant differentially expressed gene (DEG) if it had a Benjamini–Hochberg adjusted *p*-value < 0.01 and log2[fold change (FC)] ≥ 1 (upregulated) or log2[fold change (FC)] ≤ -1 (downregulated). The GO term analysis was analysed with g:Profiler[56].

Electrolyte leakage assay

Two leaves of 5-week-old Arabidopsis plants were hand infiltrated using a 1 mL needleless syringe with 50 µM E2 dissolved in Mili-Q water or DMSO in Mili-Q water as mock. Leaf discs were collected with a 7-mm diameter cork borer from infiltrated leaves on paper towels. Leaf discs were dried and transferred into 2 mL of deionised water in 12-well plates (2 leaf disks per well. The plate was incubated for 30 minutes in a growth chamber with controlled conditions at 21 °C under long-day conditions (16-h light/8-h dark) with a light intensity of 120-150 µmol m^{-2}. The water was replaced after incubation with 2 mL of deionised water. Electrolyte leakage was measured with Pocket Water Quality Meters (LAQUAtwin-EC-33; Horiba) calibrated at 1.41 mS/cm. Around 100 µL of the sample was used to measure conductivity at the indicated time points. ANOVA (*p*-value ≤ 0.05) was used for identifying significant factors. Tukey-HSD-Test (*p*- value ≤ 0.05) was used to determine differences between treatment and lines. A detailed statistical summary is available on GitHub: https://github.com/dinglab-plants/ETI_Project.

Semi-quantitative real time-PCR

Complementary DNAs (cDNAs) were synthesised from the RNA extracted for RNA-seq from SETI_wt and all lipase mutants in SETI background

using a first-strand cDNA synthesis kit (Thermo Scientific) according to the manufacturer's instructions. 1 µL of cDNA was combined in a 15 µL reaction with 3mM dNTP, 2µM of each primer, 10xPCR buffer and Milli Q water. Semi-quantitative real-time-PCR (RT-PCR) analysis was performed using *AvrRps4* specific primers (*AvrRps4_F*: 5'-TCCAGCTTCAGTTACTCGGC-3'; *AvrRps4*_R: 5'-TTGGCTATTTCGGCTGGGTT-3'). The elongation factor 1α (*EF1α*) primers (*EF1α*_F: 5'-CAGGCTGATTGTGCTGTTCTTA-3'; *EF1α*_R: 5'GTTGTATCCGACCTTCTTCAGG-3') were used as an internal control. The semi-quantitative RT-PCR reaction was performed as follows: pre-denaturation at 94°C (2 minutes), then 35 cycles at 94°C (15 s); 55°C (30 s) and 68°C (1 minute), and a final extension at 68°C for 5 min. The RT-PCR products were electrophoresed and compared on 1.5% TAE agarose gel.

Bacterial growth assay

Pst DC3000 EV (carrying empty vector)[57] was grown on selective King's B (KB) medium plates containing 15% (w/v) agar, 25 µg mL^{-1} rifampicin, and 50 µg mL^{-1} kanamycin for 48 h at 28 °C. Bacteria were harvested and resuspended in 10 mM $MgCl_2$. The concentration of the suspension was adjusted to an optical density of 0.001 at 600 nm [OD_{600}=0.001, representing ~5×10^5 colony-forming units (CFU) mL^{-1}]. Two 5-week-old Arabidopsis leaves were hand infiltrated with 50 µM E2 dissolved in 10 mM $MgCl_2$ or DMSO in 10 mM $MgCl_2$ with a needleless syringe. The following day, the same leaves were infiltrated with bacteria. For quantification, leaf samples were harvested with a 7-mm diameter cork borer, resulting in leaf discs with an area of 0.38 cm^2. Two leaf discs per leaf were collected as a single sample. For each genotype and condition, four samples were collected immediately after infiltration as 'day 0' samples, and eight samples were collected at 3 dpi as 'day 3' samples to

compare the bacterial titres between different genotypes, conditions, and treatments. For 'day 0', samples were ground in 200 µL of 10 mM $MgCl_2$ and spotted (10 µL per spot) on selective KB medium agar plates to grow for 48 h at 28 °C. For 'day 3', samples were ground in 200 µL of infiltration buffer, serially diluted (5, 50, $5x10^2$, $5x10^3$, $5x10^4$, $5x10^5$ times), and spotted (6 µL per spot) on selective King's B medium agar plates to grow for 48 h at 28 °C. The number of colonies (CFU per drop) was counted, and bacterial growth was represented as CFU cm^{-2} of leaf tissue. ANOVA (*p*-value ≤ 0.05) was used for identifying significant factors. Tukey-HSD-Test (*p*-value ≤ 0.05) was used to identify differences between treatment and lines. A detailed statistical summary is available on GitHub: https://github.com/dinglab-plants/ETI_Project.

Chlorophyll content estimation

Two leaves of 5-week-old Arabidopsis plants (SETI_wt, SETI_*eds1*, SETI_*pad4*, SETI_*sag101*, SETI_*ps*, SETI_*adr1s*, SETI_*nrg1s*, and SETI_*helperless*) were hand infiltrated using a 1 mL needleless syringe with 50 µM E2 dissolved in 10 mM $MgCl_2$ as ETI treatment, *Pst* DC3000 *hrcC*$^-$ (0.2 OD)[58] dissolved in 10 mM $MgCl_2$ as PTI treatment, E2+*Pst* DC3000 *hrcC*$^-$ with same concentration as 'PTI+ETI' treatment and DMSO dissolved in 10 mM $MgCl_2$ as mock. Leaf disks were collected using a 7-mm diameter cork borer from 3 individual plants as 1 sample for each treatment. Samples were ground and resuspended in 1 mL of 80% acetone. The samples were then centrifuged at 10,000 g for 5 mins. The absorbance of the supernatant was measured at 645 nm and 633 nm using UV–VIS spectrophotometer (UV-6300PC, VWR). Total and chlorophyll a, b content were calculated according to the following equations[59]:

Chl-a = 12.72A663-2.59A645/1000 mg per g FW (mg g^{-1})

Chl-b = 22.9A645 -4.67A663/1000 mg per g FW (mg g^{-1})

Chl-t= 20.31 A645 +8.05 A663/1000 mg per g FW (mg g^{-1})

ANOVA (p-value ≤ 0.05) was used for identifying significant factors. Tukey-HSD-Test (p-value ≤ 0.05) was used to identify differences between treatment and lines. A detailed statistical summary is available on GitHub: https://github.com/dinglab-plants/ETI_Project.

Quantification and statistical analysis

R version 4.3.1 was used for data analysis. Boxplots and bar plots were generated using ggplot2. The heatmap on the right side in **figure 4** was generated with the R package 'ComplexHeatmap'[60]. The upset plot and the volcano plot were generated with the R packages 'ComplexUpset'[61] and 'EnhancedVolcano'[62]. **Figure S6** was done with 'gt'[63] and 'gtExtras'[64]. The following packages were used for data formatting and statistics: 'Tidyverse'[65], 'multcompView'[66], 'agricolae'[67], 'ggpubr'[68], 'stringr'[69], 'r2r'[70] and 'circlize'[71]. RNA-seq analysis was done as described above.

Supplementary information

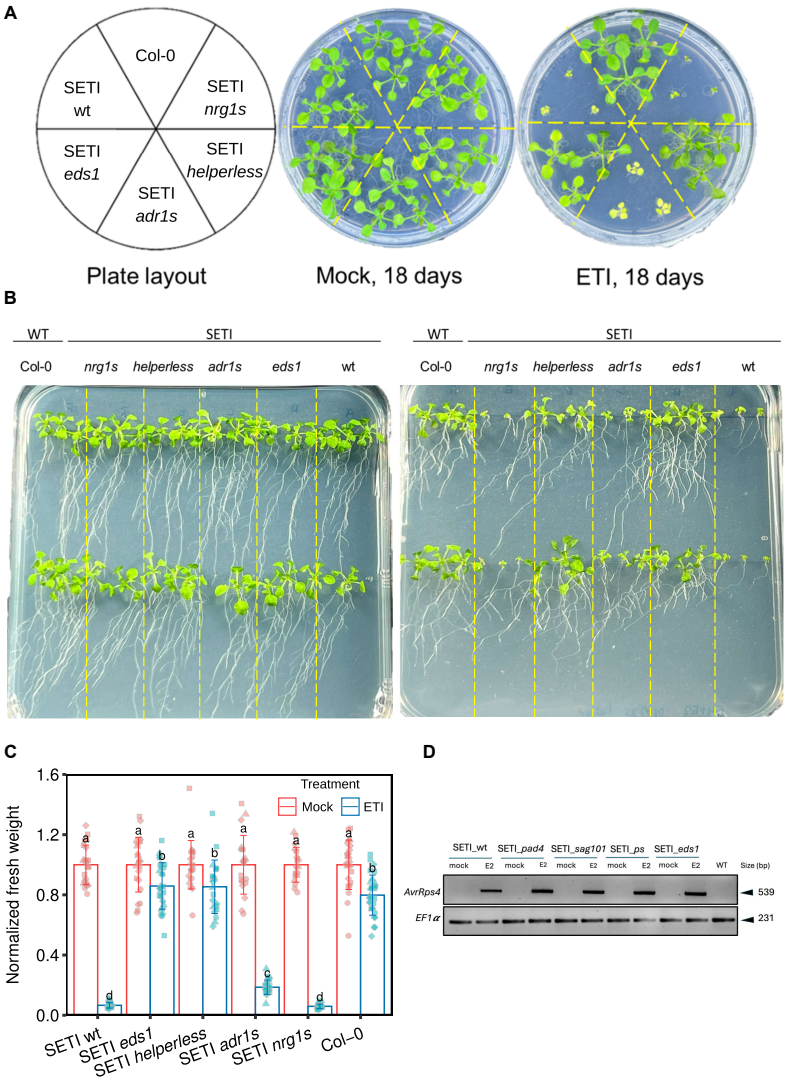

Figure S1. Estradiol induced growth arrest phenotype in helper NLR mutants. Related to Figure 1. A. Indicated mutants of helper-NLRs (SETI_wt, SETI_*nrg1s*, SETI_*adr1s* and SETI_*helperless*, SETI_*eds1*) were sown on round plates with or without E2 (50 µM), and their growth

arrest phenotypes were observed 18 days after planting on E2 plates. B. Indicated helper-NLR mutants were sown on square plates with or without E2 (50 µM) and were grown vertically. Growth arrest and lateral root formation phenotypes were recorded 18 days after planting on E2 plates. C. Indicated mutant lines were grown on vertical GM plates with or without E2 (50 µM), and the fresh weight was recorded 18 days after sowing on E2 plates. Fresh weight was normalized to the average fresh weight of the mock controls for the respective lines. The error bars indicate the standard deviation. Letters showing statistical differences (LSD-test, $p \leq 0.05$). D. Semi-quantitative RT-PCR analysis of *AvrRps4* expression in wild-type (SETI_wt) and indicated lipase-like protein mutants (SETI_*sag101*, SETI_*pad4*, SETI_*pad4 sag101*, SETI_*eds1*) compared to Col-0. The upper panel shows PCR amplification of *AvrRps4*, while the lower panel displays PCR products for the *EF1α* housekeeping gene in the same samples, ensuring consistent expression levels across the conditions.

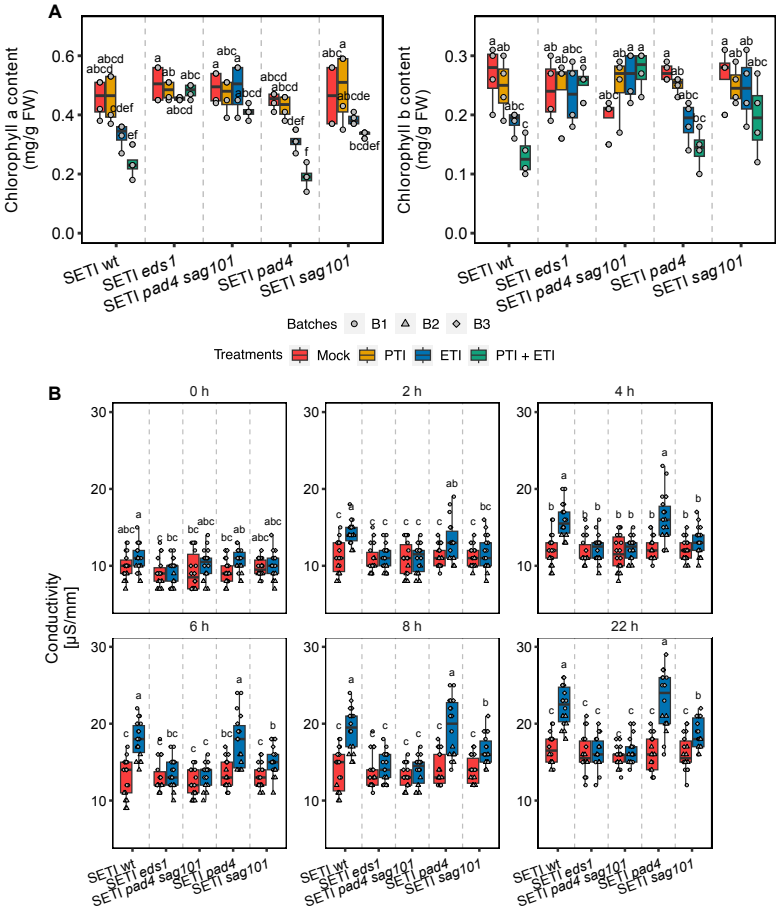

Figure S2. Varying responses of PAD4 and SAG101 modules in ETI-induced cell death. A. SETI lipase-like protein mutants were hand infiltrated with mock, E2 (ETI), E2 + *Pst* DC3000 *hrcC*$^{-}$ (PTI+ETI) and chlorophyll a and b content were recorded 3 dpi. Letters showing statistical differences (Tukey-HSD-Test, *p*-value ≤ 0.05). B. Indicated mutants of lipase-like proteins (SETI_wt, SETI_*sag101*, SETI_*pad4*, SETI_*pad4 sag101*, SETI_*eds1*) were infiltrated with E2 or mock and ion leakage was determined at several timepoints including 0, 2, 4, 6, 8 and 22h. Letters showing statistical differences (Tukey-HSD-Test, $p \leq 0.05$).

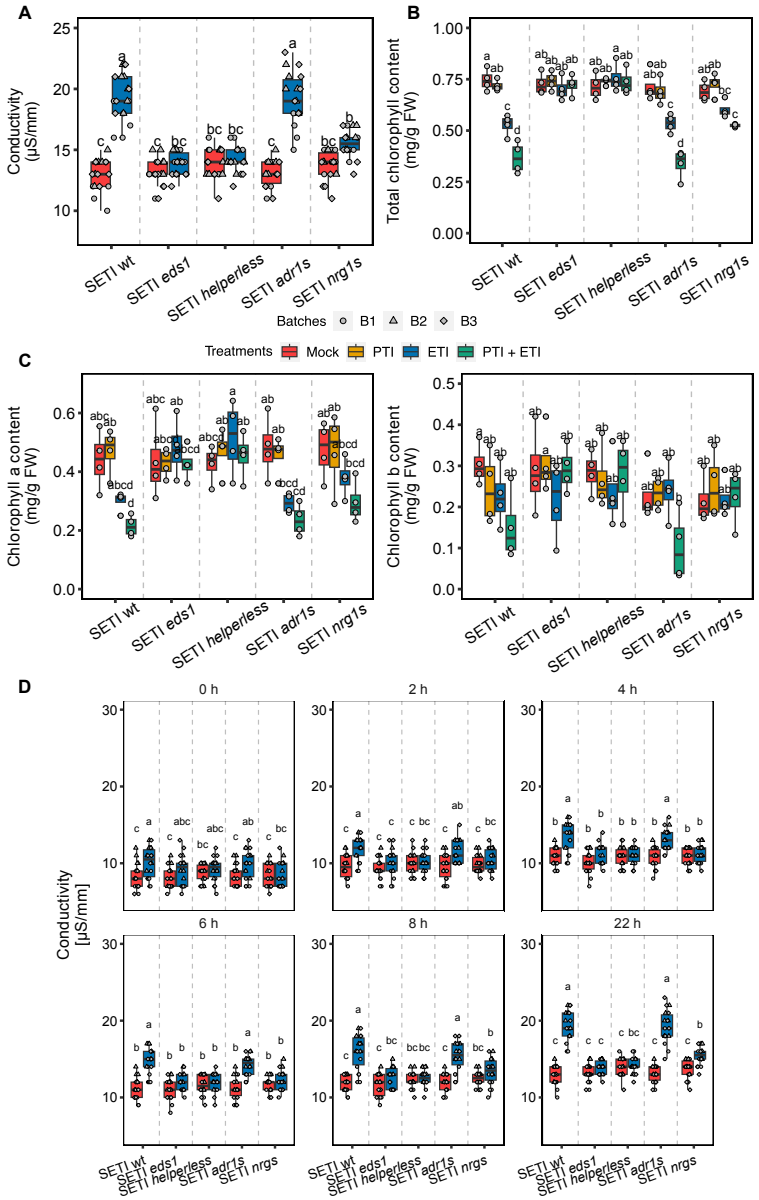

Figure S3. Varying responses of NRG1s and ADR1s modules in ETI-induced cell death. Related to Figure 2. A. Indicated mutant lines of helper-NLRs (SETI_wt, SETI_*nrg1s*, SETI_*adr1s*, SETI_*helperless*,

SETI_*eds1*) in SETI background were infiltrated with E2 or mock and ion leakage was determined at 24 h time point. Letters showing statistical differences (Tukey-HSD-Test, $p \leq 0.05$). B. Total chlorophyll content was estimated on indicated mutants of helper NLRs 3 dpi after E2 infiltration as ETI treatment, *Pst* DC3000 *hrcC*$^-$ as PTI treatment, (E2 + *Pst* DC3000 *hrcC*$^-$) as PTI+ETI treatment and DMSO dissolved in 10 mM $MgCl_2$ as mock. Letters showing statistical differences (Tukey-HSD- Test, $p \leq 0.05$). C. SETI helper-NLR mutants were hand infiltrated with mock, E2 (ETI), E2 + *Pst* DC3000 *hrcC*$^-$ (PTI+ETI) and chlorophyll a and b content were recorded 3 dpi. Letters showing statistical differences (Tukey-HSD-Test, $p \leq 0.05$). D. Indicated mutant lines of helper NLRs (SETI_wt, SETI_*nrg1s*, SETI_*adr1s*, SETI_helperless, SETI_*eds1-2*) in SETI background were infiltrated with E2 or mock and ion leakage was determined at several time points including 0, 2, 4, 6, 8 and 22h. Letters showing statistical differences (Tukey-HSD-Test, $p \leq 0.05$).

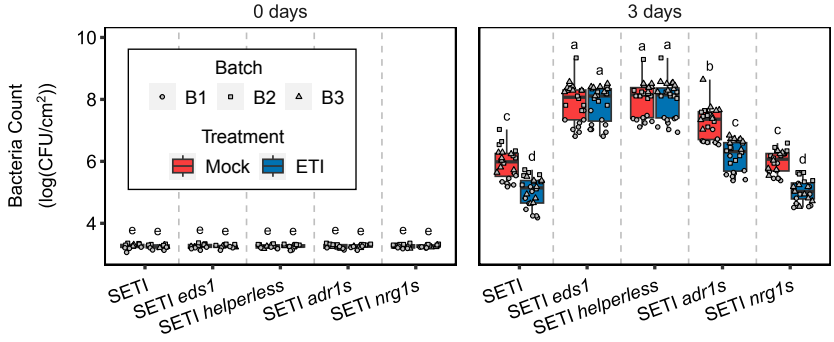

Figure S4. ETI-directed disease priming in SETI helper-NLR mutants. Related to Figure 3. Indicated mutants of helper NLRs were infiltrated with E2 or mock one day before infiltration with Pst DC3000 EV. Bacterial CFU were counted at day '0' and day '3' after infiltration with DC3000 EV. Letters showing statistical differences (Tuckey-HSD-Test, $p \leq 0.05$).

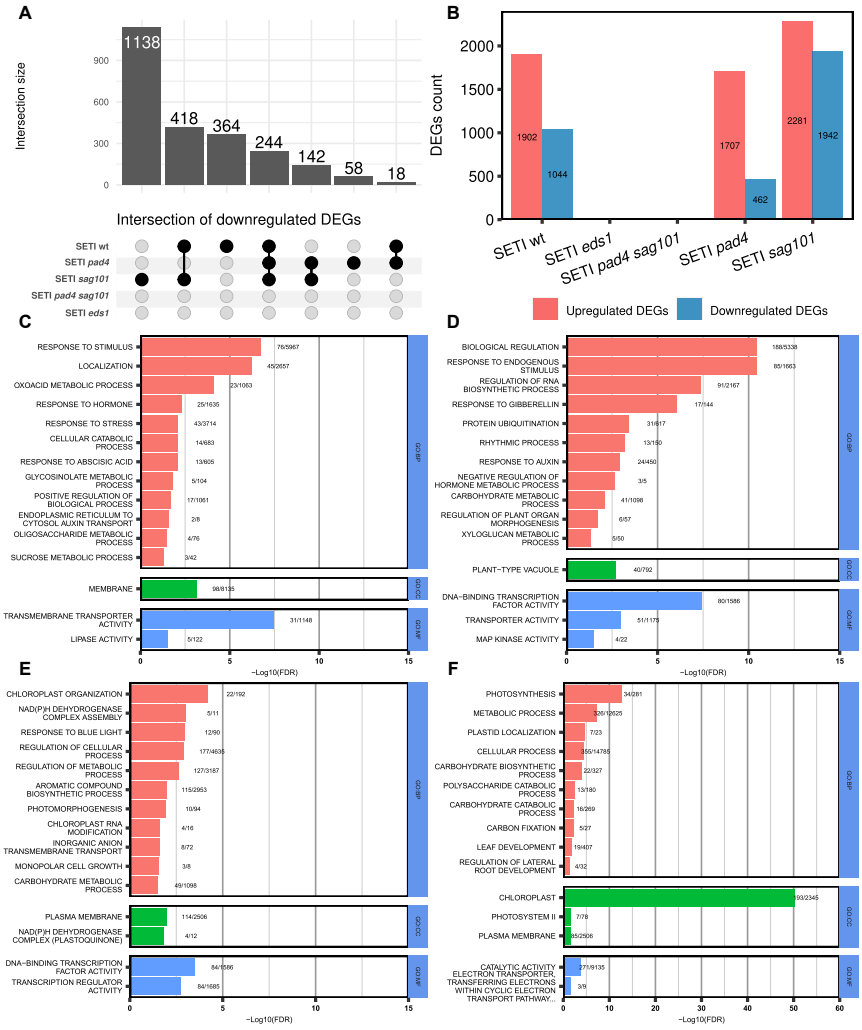

Figure S5. Comparison of gene down-regulation in ETI treatments across lipase-like protein mutants. Related to Figure 4. A. UpSet plot illustrating the intersection sizes of downregulated differentially expressed genes (DEGs) in SETI_wt and SETI lipase-like protein mutants. B. Total number of upregulated and downregulated DEGs across lipase-like protein upon ETI treatment. C. GO enrichment for DEGs in cluster 1 from heatmap in Figure 4, D cluster 2, E cluster 4 and F Cluster 10.

Gene ID	SETI	SETI *pad4*	SETI *sag101*	SETI *pad4 sag101*
Regulation of lateral root development				
AT3G48430	-0.599	-0.398	-1.019	0.234
Photomorphogenesis				
AT4G32980	-1.238	-1.018	-2.641	0.212
AT2G20180	-1.282	-0.924	-1.889	-0.329
AT3G48590	-1.076	-0.867	-1.106	-0.205
AT2G31380	-1.518	-0.852	-1.368	0.051
AT4G08920	-1.096	-0.720	-1.466	-0.178
AT2G36910	-0.701	-0.483	-1.079	-0.047
AT1G69935	-0.498	-0.468	-1.096	0.017
AT2G18790	-0.792	-0.455	-1.006	0.017
AT1G53090	-0.739	-0.425	-1.124	0.231
Leaf development				
AT1G31770	-1.817	-1.607	-2.306	0.336
AT4G25420	-1.106	-0.976	-2.795	-0.099
AT5G04810	-1.049	-0.868	-1.711	0.106
AT1G15690	-0.857	-0.651	-1.756	0.208
AT1G55350	-0.369	-0.330	-1.108	0.108
AT5G55540	-0.434	-0.329	-1.311	0.164
AT3G52910	-2.315	0.176	-2.188	0.310
Photosynthesis				
AT4G25910	-1.078	-0.934	-1.688	0.173
AT3G15095	-1.224	-0.898	-1.772	-0.041
AT5G21930	-0.664	-0.510	-1.517	-0.049
AT1G68890	-0.549	-0.495	-1.566	0.129
AT5G38420	-0.482	-0.479	-1.288	0.096
AT5G01920	-0.479	-0.396	-1.134	0.035
AT4G31390	-0.567	-0.383	-1.209	0.194
AT5G44660	-0.527	-0.309	-1.008	-0.020
Response to gibberellin				
AT2G04240	-1.349	-1.208	-1.547	0.127
AT2G01570	-1.368	-0.876	-1.583	0.062
AT5G67480	-2.336	-0.872	-1.765	-0.024
AT3G47620	-1.623	-0.848	-1.975	0.110
AT3G19100	-1.234	-0.822	-0.991	0.398
AT1G50420	-1.048	-0.627	-1.053	-0.254
AT1G12240	-1.274	-0.580	-1.474	0.158
AT1G66350	-1.563	-0.512	-0.814	0.063
AT4G23060	-1.237	-0.268	-0.944	0.361

Gene ID	SETI	SETI *pad4*	SETI *sag101*	SETI *pad4 sag101*
Regulation of plant organ morphogenesis				
AT5G10150	-1.865	-1.510	-2.318	-0.268
AT2G43010	-1.268	-0.909	-1.328	-0.096
AT1G01030	-1.747	-0.314	-0.387	-0.541
AT3G61460	-1.190	0.206	-0.762	-0.082
Carbohydrate metabolic process				
AT4G36870	-1.337	-0.896	-1.690	0.036
AT2G25450	-1.853	-0.871	-1.504	0.108
AT1G68020	-1.106	-0.756	-0.805	-0.005
AT4G02130	-1.345	-0.728	-1.406	-0.251
AT1G70230	-1.544	-0.689	-1.357	-0.037
AT4G32190	-1.145	-0.683	-1.227	0.290
AT4G17090	-1.438	-0.654	-1.345	0.102
AT2G23760	-1.029	-0.547	-1.437	0.074
AT2G01850	-2.105	-0.521	-1.326	0.026
AT3G62660	-1.205	-0.364	-0.811	0.016
AT1G50460	-1.317	-0.281	-0.596	-0.362
AT1G55850	-1.492	-0.196	-1.494	-0.235
Response to auxin				
AT5G18020	-1.823	-1.543	-3.308	0.089
AT4G34750	-1.293	-0.995	-1.581	-0.351
AT5G67480	-2.336	-0.872	-1.765	-0.024
AT1G12110	-1.418	-0.837	-1.487	-0.226
AT2G28350	-1.685	-0.776	-1.365	-0.115
AT1G12820	-0.983	-0.694	-1.105	-0.064
AT5G47370	-1.735	-0.490	-1.933	0.557
AT2G42580	-1.045	-0.487	-0.497	-0.392
AT2G42620	-0.929	-0.415	-1.168	0.116
AT4G14560	-1.198	-0.401	-1.570	0.399
AT1G75500	-0.890	-0.335	-1.130	-0.177
AT1G22530	-1.498	-0.325	-0.873	-0.066
AT1G19220	-0.940	-0.270	-1.047	0.214
AT1G30330	-1.245	-0.115	-0.583	0.009
AT5G12050	-0.073	0.082	-1.655	-0.291
AT1G19850	-1.193	0.274	-0.091	0.359
AT1G69160	-1.622	0.445	-0.806	0.600
AT1G73590	-0.190	0.487	-1.388	-0.057
Response to abscisic acid				
AT2G35940	-1.528	-0.097	-1.207	0.151

Log$_2$FC

2 to 5
1.5 to 2
1 to 1.5
0.9 to 1
0.8 to 0.9
0.7 to 0.8
0.6 to 0.7
0.5 to 0.6
0.4 to 0.5
0.3 to 0.4
0.2 to 0.3
−0.2 to 0.2
−0.3 to −0.2
−0.4 to −0.3
−0.5 to −0.4
−0.6 to −0.5
−0.7 to −0.6
−0.8 to −0.7
−0.9 to −0.8
−1 to −0.9
−1.5 to −1
−2 to −1.5
−5 to −2

Fig. S6

Figure S6. ETI-induced expression changes in downregulated gene clusters. Related to Figure 4. A Go-term analysis of downregulated DEG cluster 1, 2, 4 and 10 from Figure 4 was conducted and representative GO-terms for each cluster were selected. The log2FC of each DEG from

the selected GO-term categories are listed in the table. Colours are showing the magnitude of the expression change in SETI (SETI_wt), SETI *pad4* (SETI_*pad4*), SETI *sag101* (SETI_*sag101*), and SETI *pad4 sag101* (SETI_*ps*) plants. DEGs and significant Go-terms were defined in the same manner as in Figure 4 and 5.

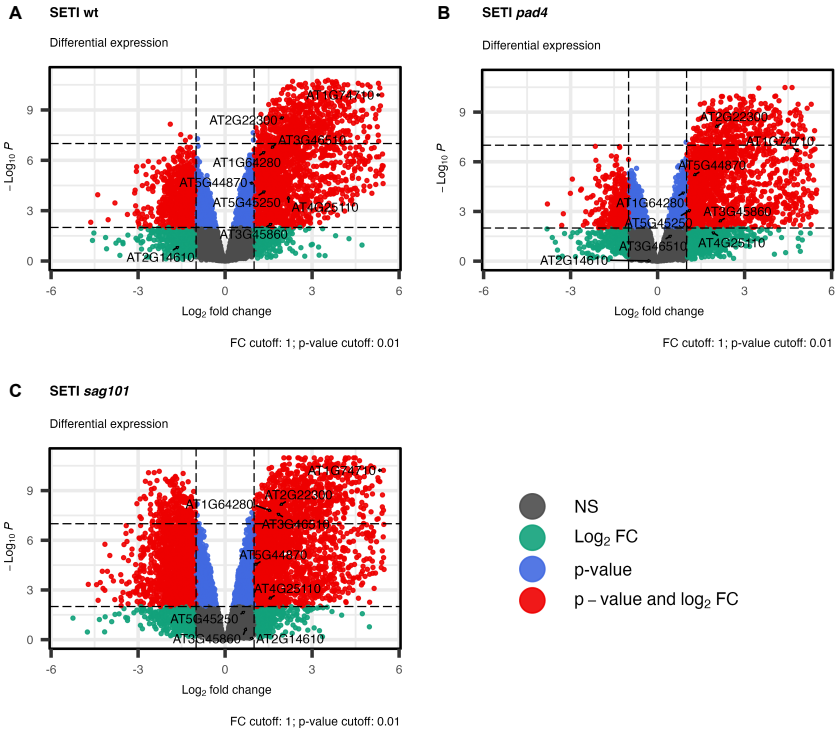

Figure S7. Volcano plot for SETI lipase-like protein mutants. Related to Figure 4. Volcano plot showing expression changes between E2- vs mock-treated samples of SETI_wt plants (A). The gene names of three immune marker genes, three PAD4-dependent genes (B) and three SAG101-dependent genes (C) are highlighted here. Different colours highlighting different thresholds: red ($p \leq 0.01$, $|\log2(FC)| \geq 1$), blue ($p \leq 0.01$, $|\log 2(FC)| < 1$), green ($p > 0.01$, $|\log2(FC)| \geq 1$), and grey ($p > 0.01$, $|\log 2(FC)| < 1$).

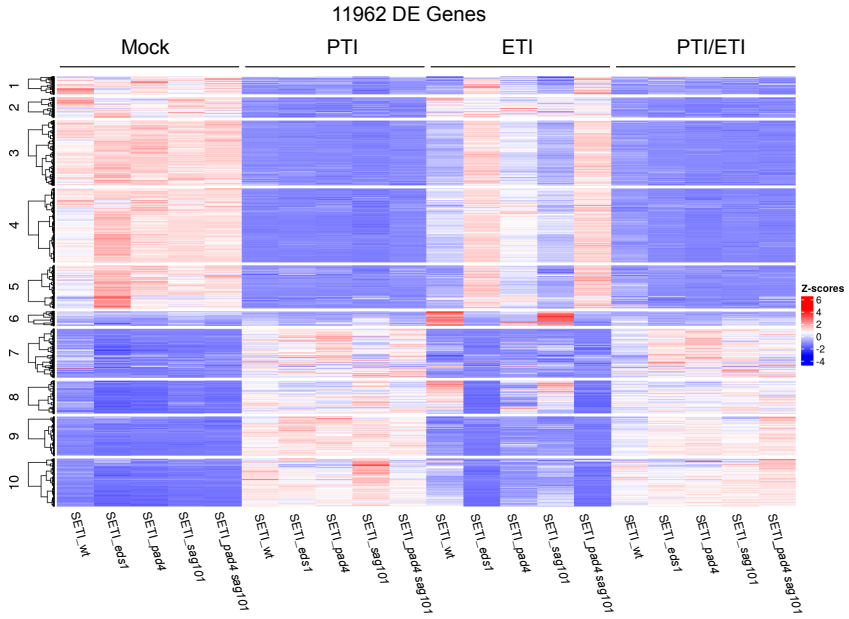

Figure S8. Differential expression profiles of lipase-like protein mutants during immune activation. Related to Figure 4. Five- to six-week-old SETI_wt, SETI_*eds1*, SETI_*pad4*, SETI_*sag101*, and SETI_*pad4 sag101* plants were infiltrated with mock (10 mM $MgCl_2$), PTI (*Pseudomonas fluorescens* (Pf0-1) in 10 mM $MgCl_2$), ETI (50 µM E2 in 10 mM $MgCl_2$), and PTI + ETI respectively. Samples were collected at 4 hours post infiltration (4 hpi) for RNA-seq analysis. The heat map displays the normalized expression (z- scores) of 11,962 differentially expressed genes (DEGs) identified under these conditions across all genotypes. DEGs were filtered based on a false discovery rate (FDR) of $p \leq 0.01$ and a fold change of ≥1.

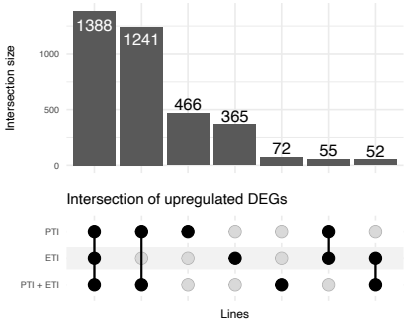

Figure S9. Comparison of gene up-regulation in SETI_wt across PTI, ETI and PTI+ETI treatment. Related to Figure 4-5. The Up-Set plot illustrating the intersection sizes of upregulated differentially expressed genes (DEGs) in SETI_wt across the indicated treatments.

Supplemental tables can be accessed online at (https://doi.org/10.1016/j.celrep.2025.115394)

References

1. Dodds, P.N., and Rathjen, J.P. (2010). Plant immunity: towards an integrated view of plant-pathogen interactions. Nat. Rev. Genet. *11*, 539–548. 10.1038/nrg2812.

2. Duxbury, Z., Wu, C.-H., and Ding, P. (2021). A comparative overview of the intracellular guardians of plants and animals: nlrs in innate immunity and beyond. Annu. Rev. Plant Biol. *72*, 155–184. 10.1146/annurev-arplant-080620-104948.

3. Jones, J.D.G., and Dangl, J.L. (2006). The plant immune system. Nature *444*, 323–329. 10.1038/nature05286.

4. Ngou, B.P.M., Ahn, H.-K., Ding, P., and Jones, J.D.G. (2021). Mutual potentiation of plant immunity by cell-surface and intracellular receptors. Nature *592*, 110–115. 10.1038/s41586-021-03315-7.

5. Yuan, M., Ngou, B.P.M., Ding, P., and Xin, X.-F. (2021). PTI-ETI crosstalk: an integrative view of plant immunity. Curr. Opin. Plant Biol. *62*, 102030. 10.1016/j.pbi.2021.102030.

6. Parker, J.E., Hessler, G., and Cui, H. (2022). A new biochemistry connecting pathogen detection to induced defense in plants. New Phytol. *234*, 819–826. 10.1111/nph.17924.

7. Wiermer, M., Feys, B.J., and Parker, J.E. (2005). Plant immunity: the EDS1 regulatory node. Curr. Opin. Plant Biol. *8*, 383–389. 10.1016/j.pbi.2005.05.010.

8. Wagner, S., Stuttmann, J., Rietz, S., Guerois, R., Brunstein, E., Bautor, J., Niefind, K., and Parker, J.E. (2013). Structural basis for signaling by exclusive EDS1 heteromeric complexes with SAG101 or PAD4 in plant innate immunity. Cell Host Microbe *14*, 619–630. 10.1016/j.chom.2013.11.006.

9. Bhattacharjee, S., Halane, M.K., Kim, S.H., and Gassmann, W. (2011). Pathogen effectors target Arabidopsis EDS1 and alter its interactions with immune regulators. Science *334*, 1405–1408. 10.1126/science.1211592.

10. Zhu, S., Jeong, R.-D., Venugopal, S.C., Lapchyk, L., Navarre, D., Kachroo, A., and Kachroo, P. (2011). SAG101 forms a ternary complex with EDS1 and PAD4 and is required for resistance signaling against turnip crinkle virus. PLoS Pathog. *7*, e1002318. 10.1371/journal.ppat.1002318.

11. Vlot, A.C., Dempsey, D.A., and Klessig, D.F. (2009). Salicylic Acid, a multifaceted hormone to combat disease. Annu. Rev. Phytopathol. *47*, 177–206. 10.1146/annurev.phyto.050908.135202.

12. Bonardi, V., Tang, S., Stallmann, A., Roberts, M., Cherkis, K., and Dangl, J.L. (2011). Expanded functions for a family of plant intracellular immune receptors beyond specific recognition of pathogen effectors. Proc Natl Acad Sci USA *108*, 16463–16468. 10.1073/pnas.1113726108.

13. Dong, O.X., Tong, M., Bonardi, V., El Kasmi, F., Woloshen, V., Wünsch, L.K., Dangl, J.L., and Li, X. (2016). TNL-mediated immunity in Arabidopsis requires complex regulation of the

redundant ADR1 gene family. New Phytol. *210*, 960–973. 10.1111/nph.13821.

14. Castel, B., Ngou, P.-M., Cevik, V., Redkar, A., Kim, D.-S., Yang, Y., Ding, P., and Jones, J.D.G. (2019). Diverse NLR immune receptors activate defence via the RPW8-NLR NRG1. New Phytol. *222*, 966–980. 10.1111/nph.15659.

15. Wu, Z., Li, M., Dong, O.X., Xia, S., Liang, W., Bao, Y., Wasteneys, G., and Li, X. (2019). Differential regulation of TNL-mediated immune signaling by redundant helper CNLs. New Phytol. *222*, 938–953. 10.1111/nph.15665.

16. Lapin, D., Kovacova, V., Sun, X., Dongus, J.A., Bhandari, D., von Born, P., Bautor, J., Guarneri, N., Rzemieniewski, J., Stuttmann, J., et al. (2019). A Coevolved EDS1-SAG101-NRG1 Module Mediates Cell Death Signaling by TIR-Domain Immune Receptors. Plant Cell *31*, 2430–2455. 10.1105/tpc.19.00118.

17. Saile, S.C., Jacob, P., Castel, B., Jubic, L.M., Salas-Gonzáles, I., Bäcker, M., Jones, J.D.G., Dangl, J.L., and El Kasmi, F. (2020). Two unequally redundant "helper" immune receptor families mediate Arabidopsis thaliana intracellular "sensor" immune receptor functions. PLoS Biol. *18*, e3000783. 10.1371/journal.pbio.3000783.

18. Collier, S.M., Hamel, L.-P., and Moffett, P. (2011). Cell death mediated by the N-terminal domains of a unique and highly conserved class of NB-LRR protein. Mol. Plant Microbe Interact. *24*, 918–931. 10.1094/MPMI-03-11-0050.

19. Sun, X., Lapin, D., Feehan, J.M., Stolze, S.C., Kramer, K., Dongus, J.A., Rzemieniewski, J., Blanvillain-Baufumé, S., Harzen, A., Bautor, J., et al. (2021). Pathogen effector recognition-dependent association of NRG1 with EDS1 and SAG101 in TNL receptor immunity. Nat. Commun. *12*, 3335. 10.1038/s41467-021-23614-x.

20. Wu, Z., Tian, L., Liu, X., Zhang, Y., and Li, X. (2021). TIR signal promotes interactions between lipase-like proteins and ADR1-L1 receptor and ADR1-L1 oligomerization. Plant Physiol. *187*, 681–686. 10.1093/plphys/kiab305.

21. He, Z., Webster, S., and He, S.Y. (2022). Growth-defense trade-offs in plants. Curr. Biol. *32*, R634–R639. 10.1016/j.cub.2022.04.070.

22. van Wersch, R., Li, X., and Zhang, Y. (2016). Mighty dwarfs: arabidopsis autoimmune mutants and their usages in genetic dissection of plant immunity. Front. Plant Sci. *7*, 1717. 10.3389/fpls.2016.01717.

23. Denancé, N., Sánchez-Vallet, A., Goffner, D., and Molina, A. (2013). Disease resistance or growth: the role of plant hormones in balancing immune responses and fitness costs. Front. Plant Sci. *4*, 155. 10.3389/fpls.2013.00155.

24. Ngou, B.P.M., Ahn, H.-K., Ding, P., Redkar, A., Brown, H., Ma, Y., Youles, M., Tomlinson, L., and Jones, J.D.G. (2020). Estradiol-inducible AvrRps4 expression reveals distinct properties of TIR-NLR-mediated effector-triggered immunity. J. Exp. Bot. *71*, 2186–2197. 10.1093/jxb/erz571.

25. Cooper, A., and Ton, J. (2022). Immune priming in plants: from the onset to transgenerational maintenance. Essays Biochem. *66*, 635–646. 10.1042/EBC20210082.

26. Liu, J., Ding, P., Sun, T., Nitta, Y., Dong, O., Huang, X., Yang, W., Li, X., Botella, J.R., and Zhang, Y. (2013). Heterotrimeric G proteins serve as a converging point in plant defense signaling activated by multiple receptor-like kinases. Plant Physiol. *161*, 2146–2158. 10.1104/pp.112.212431.

27. Mur, L.A.J., Aubry, S., Mondhe, M., Kingston-Smith, A., Gallagher, J., Timms-Taravella, E., James, C., Papp, I., Hörtensteiner, S., Thomas, H., et al. (2010). Accumulation of chlorophyll catabolites photosensitizes the hypersensitive response elicited by Pseudomonas syringae in Arabidopsis. New Phytol. *188*, 161–174. 10.1111/j.1469-8137.2010.03377.x.

28. Mur, L.A.J., Kenton, P., Lloyd, A.J., Ougham, H., and Prats, E. (2008). The hypersensitive response; the centenary is upon us but how much do we know? J. Exp. Bot. *59*, 501–520. 10.1093/jxb/erm239.

29. Pruitt, R.N., Locci, F., Wanke, F., Zhang, L., Saile, S.C., Joe, A., Karelina, D., Hua, C., Fröhlich, K., Wan, W.-L., et al. (2021). The EDS1-PAD4-ADR1 node mediates Arabidopsis pattern-triggered immunity. Nature *598*, 495–499. 10.1038/s41586-021-03829-0.

30. Saraçli, S., Doğan, N., and Doğan, İ. (2013). Comparison of hierarchical cluster analysis methods by cophenetic correlation. J. Inequal. Appl. *2013*, 203. 10.1186/1029-242X-2013-203.

31. Ding, P., Rekhter, D., Ding, Y., Feussner, K., Busta, L., Haroth, S., Xu, S., Li, X., Jetter, R., Feussner, I., et al. (2016). Characterization of a pipecolic acid biosynthesis pathway required for systemic acquired resistance. Plant Cell *28*, 2603–2615. 10.1105/tpc.16.00486.

32. Ding, P., and Ding, Y. (2020). Stories of salicylic acid: A plant defense hormone. Trends Plant Sci. *25*, 549–565. 10.1016/j.tplants.2020.01.004.

33. Rojas, C.M., Senthil-Kumar, M., Tzin, V., and Mysore, K.S. (2014). Regulation of primary plant metabolism during plant-pathogen interactions and its contribution to plant defense. Front. Plant Sci. *5*, 17. 10.3389/fpls.2014.00017.

34. Du, Y., and Scheres, B. (2018). Lateral root formation and the multiple roles of auxin. J. Exp. Bot. *69*, 155–167. 10.1093/jxb/erx223.

35. Rietz, S., Stamm, A., Malonek, S., Wagner, S., Becker, D., Medina-Escobar, N., Corina Vlot, A., Feys, B.J., Niefind, K., and Parker, J.E. (2011). Different roles of Enhanced Disease Susceptibility1 (EDS1) bound to and dissociated from Phytoalexin Deficient4 (PAD4) in Arabidopsis immunity. New Phytol. *191*, 107–119. 10.1111/j.1469-8137.2011.03675.x.

36. Gantner, J., Ordon, J., Kretschmer, C., Guerois, R., and Stuttmann, J. (2019). An EDS1-SAG101 Complex Is Essential for TNL-Mediated Immunity in Nicotiana benthamiana. Plant Cell *31*, 2456–2474. 10.1105/tpc.19.00099.

37. Qi, T., Seong, K., Thomazella, D.P.T., Kim, J.R., Pham, J., Seo, E., Cho, M.-J., Schultink, A., and Staskawicz, B.J. (2018). NRG1 functions downstream of EDS1 to regulate TIR-NLR-mediated plant immunity in Nicotiana benthamiana. Proc Natl Acad Sci USA *115*, E10979–E10987. 10.1073/pnas.1814856115.

38. Feehan, J.M., Wang, J., Sun, X., Choi, J., Ahn, H.-K., Ngou, B.P.M., Parker, J.E., and Jones, J.D.G. (2023). Oligomerization of a plant helper NLR requires cell-surface and intracellular immune receptor activation. Proc Natl Acad Sci USA *120*, e2210406120. 10.1073/pnas.2210406120.

39. de Ronde, D., Butterbach, P., and Kormelink, R. (2014). Dominant resistance against plant viruses. Front. Plant Sci. *5*, 307. 10.3389/fpls.2014.00307.

40. Feys, B.J., Wiermer, M., Bhat, R.A., Moisan, L.J., Medina-Escobar, N., Neu, C., Cabral, A., and Parker, J.E. (2005). Arabidopsis SENESCENCE-ASSOCIATED GENE101 stabilizes and signals within an ENHANCED DISEASE SUSCEPTIBILITY1 complex in plant innate immunity. Plant Cell *17*, 2601–2613. 10.1105/tpc.105.033910.

41. Bonardi, V., Cherkis, K., Nishimura, M.T., and Dangl, J.L. (2012). A new eye on NLR proteins: focused on clarity or diffused by complexity? Curr. Opin. Immunol. *24*, 41–50. 10.1016/j.coi.2011.12.006.

42. Bjornson, M., Pimprikar, P., Nürnberger, T., and Zipfel, C. (2021). The transcriptional landscape of Arabidopsis thaliana pattern-

triggered immunity. Nat. Plants *7*, 579–586. 10.1038/s41477-021-00874-5.

43. Ding, P., Sakai, T., Krishna Shrestha, R., Manosalva Perez, N., Guo, W., Ngou, B.P.M., He, S., Liu, C., Feng, X., Zhang, R., et al. (2021). Chromatin accessibility landscapes activated by cell-surface and intracellular immune receptors. J. Exp. Bot. *72*, 7927–7941. 10.1093/jxb/erab373.

44. Locci, F., Wang, J., and Parker, J.E. (2023). TIR-domain enzymatic activities at the heart of plant immunity. Curr. Opin. Plant Biol. *74*, 102373. 10.1016/j.pbi.2023.102373.

45. Peart, J.R., Mestre, P., Lu, R., Malcuit, I., and Baulcombe, D.C. (2005). NRG1, a CC-NB-LRR protein, together with N, a TIR-NB-LRR protein, mediates resistance against tobacco mosaic virus. Curr. Biol. *15*, 968–973. 10.1016/j.cub.2005.04.053.

46. Thomas, W.J., Thireault, C.A., Kimbrel, J.A., and Chang, J.H. (2009). Recombineering and stable integration of the Pseudomonas syringae pv. syringae 61 hrp/hrc cluster into the genome of the soil bacterium Pseudomonas fluorescens Pf0-1. Plant J. *60*, 919–928. 10.1111/j.1365-313X.2009.03998.x.

47. Bjornson, M., Kajala, K., Zipfel, C., and Ding, P. (2020). Low-cost and High-throughput RNA-seq Library Preparation for Illumina Sequencing from Plant Tissue. Bio Protoc *10*, e3799. 10.21769/BioProtoc.3799.

48. Andrews, S. (2023). FastQC.

49. Zhang, R., Kuo, R., Coulter, M., Calixto, C.P.G., Entizne, J.C., Guo, W., Marquez, Y., Milne, L., Riegler, S., Matsui, A., et al. (2022). A high-resolution single-molecule sequencing-based Arabidopsis transcriptome using novel methods of Iso-seq analysis. Genome Biol. *23*, 149. 10.1186/s13059-022-02711-0.

50. Bray, N.L., Pimentel, H., Melsted, P., and Pachter, L. (2016). Near-optimal probabilistic RNA-seq quantification. Nat. Biotechnol. *34*, 525–527. 10.1038/nbt.3519.

51. Guo, W., Tzioutziou, N.A., Stephen, G., Milne, I., Calixto, C.P., Waugh, R., Brown, J.W.S., and Zhang, R. (2021). 3D RNA-seq: a powerful and flexible tool for rapid and accurate differential expression and alternative splicing analysis of RNA-seq data for biologists. RNA Biol. *18*, 1574–1587. 10.1080/15476286.2020.1858253.

52. Risso, D., Ngai, J., Speed, T.P., and Dudoit, S. (2014). Normalization of RNA-seq data using factor analysis of control genes or samples. Nat. Biotechnol. *32*, 896–902. 10.1038/nbt.2931.

53. Robinson, M.D., and Oshlack, A. (2010). A scaling normalization method for differential expression analysis of RNA-seq data. Genome Biol. *11*, R25. 10.1186/gb-2010-11-3-r25.

54. Law, C.W., Chen, Y., Shi, W., and Smyth, G.K. (2014). voom: Precision weights unlock linear model analysis tools for RNA-seq read counts. Genome Biol. *15*, R29. 10.1186/gb-2014-15-2-r29.

55. Ritchie, M.E., Phipson, B., Wu, D., Hu, Y., Law, C.W., Shi, W., and Smyth, G.K. (2015). limma powers differential expression analyses for RNA-sequencing and microarray studies. Nucleic Acids Res. *43*, e47. 10.1093/nar/gkv007.

56. Kolberg, L., Raudvere, U., Kuzmin, I., Adler, P., Vilo, J., and Peterson, H. (2023). g:Profiler-interoperable web service for functional enrichment analysis and gene identifier mapping (2023 update). Nucleic Acids Res. *51*, W207–W212. 10.1093/nar/gkad347.

57. Sohn, K.H., Zhang, Y., and Jones, J.D.G. (2009). The Pseudomonas syringae effector protein, AvrRPS4, requires in planta processing and the KRVY domain to function. Plant J. *57*, 1079–1091. 10.1111/j.1365-313X.2008.03751.x.

58. Petnicki-Ocwieja, T., van Dijk, K., and Alfano, J.R. (2005). The hrpK operon of Pseudomonas syringae pv. tomato DC3000 encodes two proteins secreted by the type III (Hrp) protein secretion system: HopB1 and HrpK, a putative type III translocator. J. Bacteriol. *187*, 649–663. 10.1128/JB.187.2.649-663.2005.

59. Chazaux, M., Schiphorst, C., Lazzari, G., and Caffarri, S. (2022). Precise estimation of chlorophyll a, b and carotenoid content by deconvolution of the absorption spectrum and new simultaneous equations for Chl determination. Plant J. *109*, 1630–1648. 10.1111/tpj.15643.

60. Gu, Z. (2022). Complex heatmap visualization. iMeta *1*, e43. 10.1002/imt2.43.

61. Lex, A., Gehlenborg, N., Strobelt, H., Vuillemot, R., and Pfister, H. (2014). Upset: visualization of intersecting sets. IEEE Trans. Vis. Comput. Graph. *20*, 1983–1992. 10.1109/TVCG.2014.2346248.

62. Blighe, K., Rana, S., and Lewis, M. (2018). EnhancedVolcano: Publication-ready volcano plots with enhanced colouring and labeling. Bioconductor. 10.18129/b9.bioc.enhancedvolcano.

63. Iannone, R., Cheng, J., Schloerke, B., Hughes, E., Lauer, A., Seo, J., Brevoort, K., and Roy, O. (2024). gt: Easily Create Presentation-Ready Display Tables.

64. Mock, T. (2023). gtExtras: Extending “gt” for Beautiful HTML Tables.

65. Wickham, H., Averick, M., Bryan, J., Chang, W., McGowan, L., François, R., Grolemund, G., Hayes, A., Henry, L., Hester, J., et al. (2019). Welcome to the tidyverse. JOSS *4*, 1686. 10.21105/joss.01686.

66. Graves, S., Piepho, H.-P., and Luciano Selzer with help from Sundar Dorai-Raj (2023). multcompView: Visualizations of Paired Comparisons.

67. de Mendiburu, F. (2023). agricolae: Statistical Procedures for Agricultural Research.

68. Kassambara, A. (2023). ggpubr: “ggplot2” Based Publication Ready Plots.

69. Wickham, H. (2023). stringr: Simple, Consistent Wrappers for Common String Operations.

70. Gherardi, V. (2021). r2r: R-Object to R-Object Hash Maps.

71. Gu, Z., Gu, L., Eils, R., Schlesner, M., and Brors, B. (2014). circlize Implements and enhances circular visualization in R. Bioinformatics *30*, 2811–2812. 10.1093/bioinformatics/btu393.

Chapter 3
Cell-type-specific execution of effector-triggered immunity

Himanshu Chhillar[1,#], Leonardo Jo[2,3,#], Amey Redkar[4,5], Kaisa Kajala[2], Jonathan DG Jones[4], Pingtao Ding[1*]

[1]Institute of Biology Leiden, Leiden University, 2333 BE Leiden, The Netherlands
[2]Experimental & Computational Plant Development, Institute of Environmental Biology, Utrecht University, 3584 CH Utrecht, The Netherlands
[3]Current address: Laboratory of Molecular Biology, Wageningen University & Research, 6708PB Wageningen, The Netherlands
[4]The Sainsbury Laboratory, University of East Anglia, NR4 7UH Norwich, United Kingdom
[5]Current address: National Centre for Biological Sciences, Tata Institute of Fundamental Research, GKVK Campus, 560065 Bangalore, India
#equal contribution

This chapter is published in: bioRxiv (2025) July. doi: https://doi.org/10.1101/2025.06.28.662111 and is currently under revision.

Abstract

Effector-triggered immunity (ETI) is a central component of host defense, but whether all cell types execute ETI similarly remains unknown. We combined chemically imposed immune activation with single-cell transcriptomics to profile ETI responses across all leaf cell types in Arabidopsis. Despite uniform ETI perception, we find striking divergence between transcriptional outputs: a core set of defense genes is broadly induced, while distinct cell types activate specialized immune modules. We infer that downstream immune execution is shaped not only by immune receptor activation, but also by cell identity and its associated transcriptional regulatory context, including local transcription factor availability and chromatin accessibility. We further demonstrate that transcriptional regulators preferentially induced in epidermal cells are required to restrict invasion by non-adapted pathogens. Their absence permits pathogen entry into deeper tissues despite intact recognition, revealing a spatial division of immune functions. Our findings uncover a layered immune architecture in plants, challenges the assumption of uniform immune execution, and provides a framework for exploring cell-type-specific resistance logic in multicellular hosts.

Key words

Effector-triggered immunity (ETI), cell-autonomous immunity, cell-type-specific immunity, single-cell RNA sequencing, transcriptional regulation

Introduction

In multicellular organisms lacking adaptive immunity, such as plants, immune responses are largely cell-autonomous: each cell must independently perceive and counter pathogenic threats in the absence of mobile immune cells[1]. While this principle has long shaped our understanding of plant defense, recent studies highlight the importance of intercellular communication in modulating local responses and

coordinating systemic immunity[2–4]. Nevertheless, how immune execution at the resolution of individual cell types remains poorly understood. Specifically, it is unknown whether all plant cell types engage immune programs equivalently, or whether transcriptional responses are modulated by cell identity, developmental state, or physiological role.

Effector-triggered immunity (ETI), mediated by intracellular nucleotide-binding leucine-rich repeat (NB-LRR) receptors (NLRs), is a core component of plant innate immunity. Upon recognizing pathogen-derived effectors, ETI activates a robust transcriptional response that drives defense gene expression, cell wall fortification, immune metabolite production, and often culminates in a localized cell death[5]. While ETI is widely regarded as a canonical and system-wide immune program, most insights to date stem from bulk tissue measurements or natural infections, where immune activation is spatially heterogeneous and confounded by pathogen distribution and pattern-triggered immunity (PTI), mediated by cell-surface immune receptors. These limitations have obscured a fundamental question: Do all plant cell types execute ETI similarly when immune activation is synchronized?

Recent studies have begun to explore immune responses at single-cell resolution. For example, single-cell profiling of *Pseudomonas syringae*-infected *Arabidopsis thaliana* (Arabidopsis) leaves revealed transcriptional shifts linked to pathogen proximity[6], and fungal infection studies have identified cell-type-specific defense signatures under biotic stress[7]. Most recently, the concept of a primary immune responder (PRIMER) cell state was proposed, based on single-cell RNA-seq analysis of ETI-inducing bacterial infections during which host cells experience PTI, ETI and also defense suppression via pathogen effectors[8]. While these studies have uncovered valuable spatial features

of plant immunity, they are inherently confounded by pathogen load, PTI co-activation, and the spatial unpredictability of natural infections.

To overcome these limitations, we established a synthetic system for uniform and pathogen-free ETI induction using estradiol-triggered NLR activation in Arabidopsis[9]. Combining this with single-cell RNA sequencing, we constructed a high-resolution atlas of ETI-responsive transcriptional states across major leaf cell types. Our analysis uncovered a layered immune architecture: despite of a shared core transcriptional response activated across all cell types, ETI responses were shaped by local gene regulatory networks in cell-type-specific transcriptional modules, demonstrating a complementary mechanism between both. This suggests that immune execution is not merely a product of perception but is also intrinsically constrained by cell identity and chromatin context.

To directly test whether cell-type-specific transcriptional modules are functionally required for immune execution, we focused on CAMODULIN-BINDING PROTEIN 60 G (CBP60g) and SYSTEMIC ACQUIRED RESISTANCE DEFICIENT 1 (SARD1), two closely related transcription factors known to act downstream of NLR signaling. Both have been established as central regulators of salicylic acid biosynthesis and systemic acquired resistance during ETI [10–13]. Strikingly, our single-cell data revealed their preferential induction in pavement cells, the epidermal layer that interfaces directly with the external environment. This was particularly intriguing in the context of enabling a non-adapted *Albugo candida*, isolate to invade Arabidopsis through stomata that would normally be resisted. While guard cells form the stomatal pore, it is the surrounding pavement cells that must constrain early pathogen entry. We hypothesized that CBP60g and SARD1 may act as key mediators of spatial immune execution in this vulnerable layer. Supporting this, we found that *cbp60g sard1* mutants permitted haustoria formation by *A.*

candida specifically in the epidermal and sub-epidermal cells, despite intact immunity in internal tissues. This provides direct evidence that cell-type-specific transcriptional activation, rather than receptor activation alone, is required to restrict nonhost pathogen ingress.

Together, our findings redefine our understanding of immune coordination in plants, not as a uniform switch, but as a mosaic of modular, spatially distributed programs embedded within tissues. By decoupling immune activation from pathogen-associated variables and resolving transcriptional responses at cellular scale, this work has broad implications for how multicellular hosts orchestrate defense and opens avenues for engineering more precise and spatially tuned immune activation in multicellular systems, including crops.

Results

ETI activation defines distinct immune-responsive cell clusters

To profile the transcriptional landscape of effector-triggered immunity (ETI) at single-cell resolution, we developed a synthetic ETI activation system in Arabidopsis leaves using estradiol (E2)-inducible expression of *AvrRps4*, a bacterial effector recognized by the nucleotide-binding leucine-rich repeat (NB-LRR) receptor (NLR) pairs, RESISTANT TO RALSTONIA SOLANACEARUM 1 (RRS1)/RESISTANT TO PSEUDOMONAS SYRINGAE 4 (RPS4) and RRS1B/RPS4B, referred to as the SUPER ETI (SETI) line[9,14]. Leaves of the SETI plants were infiltrated with mock or E2 solution, and protoplasts were isolated 4 hours post infiltration (hpi) for single-cell analysis (**Figure 1A**). Real-time quantitative PCR confirmed robust induction of one of the ETI early responsive marker genes, *ISOCHORISMATE SYNTHASE 1* (*ICS1*) (**Figure 1B**)[15,16], validating effective immune activation.

We performed single-cell RNA sequencing (scRNA-seq) on protoplasts from mock and E2 treated samples using the 10X Genomics Chromium X platform and obtained approximately 300 million reads. After quality control, we recovered 7932 and 5739 high-quality cells in the mock- and E2-treated samples, respectively, with a median of 527 and 1134 genes and 776 and 2153 unique transcripts per cell, recovering approximately 70% of annotated protein-coding genes in the Arabidopsis genome. ETI activation led to notable changes in the relative abundance of specific cell types (**Figure S2A**), possibly reflecting global transcriptional reprogramming.

Unsupervised graph-based clustering identified 16 major cell clusters after integration of mock and E2 treated samples, visualized using uniform manifold approximation and projection (UMAP) (**Figure 1C-1D**). Cells from both mock and E2 conditions were represented across clusters (**Figure S1A-B**). To assign cell identities, we leveraged a recently published single-cell atlas of Arabidopsis leaf tissue and the well-known canonical marker genes[17]. A violin plot of selected cell-type-specific genes (**Figure S1C**) confirmed robust classification of 16 clusters corresponding to nine distinct cell types, with a predominant mesophyll identity (clusters M1–M8) along with pavement cells (epidermal cells), bundle sheath, hydathode, phloem, and other known leaf cell types (**Figure 1D**).

Together, these data establish a comprehensive single-cell atlas of early ETI activation across Arabidopsis leaf tissue, in the absence of PTI, providing a foundation for dissecting immune responses at cellular resolution without confounding pathogen-derived heterogeneity or defense suppression.

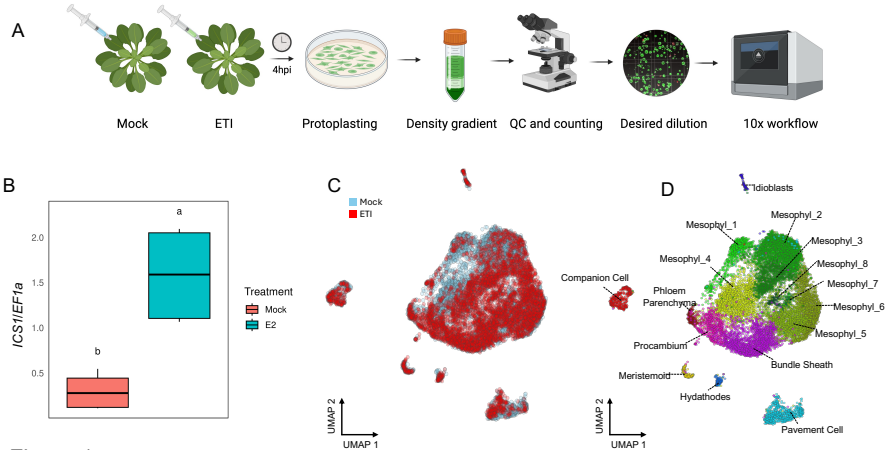

Figure 1. Single-cell transcriptomic landscape of immune activation in Arabidopsis leaf tissue. A. Experimental workflow. Arabidopsis leaves were treated with mock or estradiol (E2) to induce effector-triggered immunity (ETI), followed by protoplast isolation at 4 h post infiltration (hpi) and single-cell RNA sequencing (scRNA-seq). B. qPCR analysis of the immune marker gene *ISOCHORISMATE SYNTHASE 1* (*ICS1*). This confirms effective ETI induction in treated samples, validating immune activation prior to scRNA-seq library preparation. C. UMAP projection of integrated single-cell transcriptomes from mock and ETI-treated samples, colored by condition. D. UMAP showing unsupervised clustering of major Arabidopsis leaf cell types including pavement cells, mesophyll subtypes (Mesophyl_1 to Mesophyl_8), phloem parenchyma, companion cells, hydathodes, idioblasts, meristemoids, procambium, and bundle sheath cells.

Uniform immune activation elicits heterogeneous transcriptional responses

To dissect the spatial pattern of immune execution, we examined the expression of canonical immune and susceptibility genes across annotated cell types. Core components of the Toll/Interleukin-1 receptor/Resistance protein (TIR) NLR immune signaling cascades including *ENHANCED DISEASE SUSCEPTIBILITY 1* (*EDS1*),

PHYTOALEXIN DEFICIENT 4 (*PAD4*) and *SENESCENCE ASSOCIATED GENE 101* (*SAG101*) were broadly expressed, along with downstream helper NLR encoding genes, *ACTIVATED DISEASE RESISTANCE 1* (*ADR1*), *ADR1-L1, ADR1-L2*, *N REQUIREMENT GENE 1.1* (*NRG1.1*) and *NRG1.2* (**Figure 2A**)[18], with *ADR1* and *NRG1.2* exhibiting relatively sparse expression. This widespread expression suggests that the EDS1-dependent module is transcriptionally accessible across the entire leaf tissue, equipping most cell types to mount ETI responses upon intracellular effector recognition.

Consistently, the phytohormone salicylic acid (SA) biosynthesis pathway[19], downstream of EDS1 signaling, was also globally activated. Genes including *ICS1*, *ENHANCED DISEASE SUSCEPTIBILITY 5* (*EDS5*) and *AVRPPHB SUSCEPTIBLE 3* (*PBS3*) were robustly expressed across nearly all cell clusters (**Figures 2A**, **S2B-S2C**)[19], in line with broad SA pathway activation previously observed in ETI[16,20]. The widespread induction of *ETHYLENE INSENSITIVE 2* (*EIN2*) further supports the notion of a tissue-wide immune readiness (**Figure 2A**). Notably, negative immune regulators such as Nudix hydrolase encoding genes*, NUDTs*, and *CALMODULIN-BINDING TRANSCRIPTION ACTIVATORs* (*CAMTAs*) were also broadly induced (**Figure 2A**), indicating that immune repression mechanisms are similarly embedded across the tissue.

Moreover, key signaling components that mediate the mutual potentiation between PTI and ETI, including shared protein kinases and transcriptional regulators[14], were also ubiquitously expressed (**Figure S3A**). This suggests that all cells in Arabidopsis leaves harbour an immunity-supporting infrastructure that is transcriptionally primed to interpret and integrate diverse immune cues.

In contrast to these broadly distributed immune modules, we identified marked spatial restriction in the expression of N-hydroxy pipecolic acid (NHP) biosynthesis genes. Specifically, *AGD2-LIKE DEFENSE RESPONSE PROTEIN 1* (*ALD1*) and *FLAVIN-CONTAINING MONOOXYGENASE 1* (*FMO1*), which encodes enzymes catalyzing the first and last steps in NHP production[21–23], were almost exclusively expressed in companion cells (**Figure 2A**, **S2D-S2E**), consistent with recent findings[8]. Surprisingly, *SYSTEMIC ACQUIRED RESISTENCE DEFICIENT 4* (*SARD4*), which encodes the oxidoreductase catalyzing the intermediate step of NHP biosynthesis[21,24], exhibited widespread expression (**Figure S2F**), suggesting a division of labor wherein companion cells complete NHP biosynthesis to support systemic signal propagation. These findings indicate a spatial configuration of NHP biosynthesis and reinforce the role of companion cells as specialized immune hubs for systemic acquired resistance (SAR)-related metabolites.

We also observed cell-type-restricted expression for genes in the jasmonic acid (JA) signaling pathway and members of the E2F transcription factor family (**Figure 2A**), previously implicated in cell cycle control and immune regulation[15,25,26]. These results suggest that hormone signaling, and proliferation-linked regulators may modulate ETI output in a spatially restricted and context-dependent manner. For instance, loss-of-function of *E2Fa/b/c* compromises ETI responses mediated by both TIR and coiled-coil (CC) NLRs[26].

Importantly, because our system triggers ETI uniformly and in a pathogen-free manner[9], it offers a unique opportunity to examine whether immune-enhanced cell states, such as primary immune responder (PRIMER) and bystander cell states[8], can arise independently of pathogen spatial distribution. We observed broad induction of the trihelix transcription factor encoding gene, *GT-MOTIF BINDING FACTOR-3A* (*GT-3A*)[27], a canonical

marker of the PRIMER cell state[8], across all ETI-activated cell types (**Figure 2A**), consistent with its role as a general ETI-responsive gene. This confirms that *GT-3A* expression reflects the proximity to pathogens that can induce robust cell-autonomous ETI. In contrast, its close homologues *GT-3B* and *GT-4* were preferentially induced in hydathodes (**Figure 2A**), indicating cell-type-specific modulation of the transcriptional responses mediated by putatively redundant components. These findings refine the PRIMER cell state concept by suggesting that its transcriptional hallmarks can be broadly accessible to almost all plant cells but differentially tuned by cell identity. Rather than being exclusively driven by pathogen contact, PRIMER-like transcriptional cell states may emerge from intrinsic regulatory programs that govern immune execution across tissues.

Taken together, these results reveal that while the capacity to initiate immune signaling is broadly encoded in all leaf cells, the execution of immune programs is highly modular and spatially patterned. Even under synchronized and pathogen-free ETI activation, immune outputs such as NHP biosynthesis and PRIMER-like transcriptional states remain confined to specific cell types. This indicates that plant tissues harbor intrinsic immune compartmentalization, likely reflecting functional specializations that balance defense intensity, metabolic cost, and coordination of systemic immunity. These insights offer a new framework to explore how spatial immune signaling is uncoded in development and potentially exploited during natural infections.

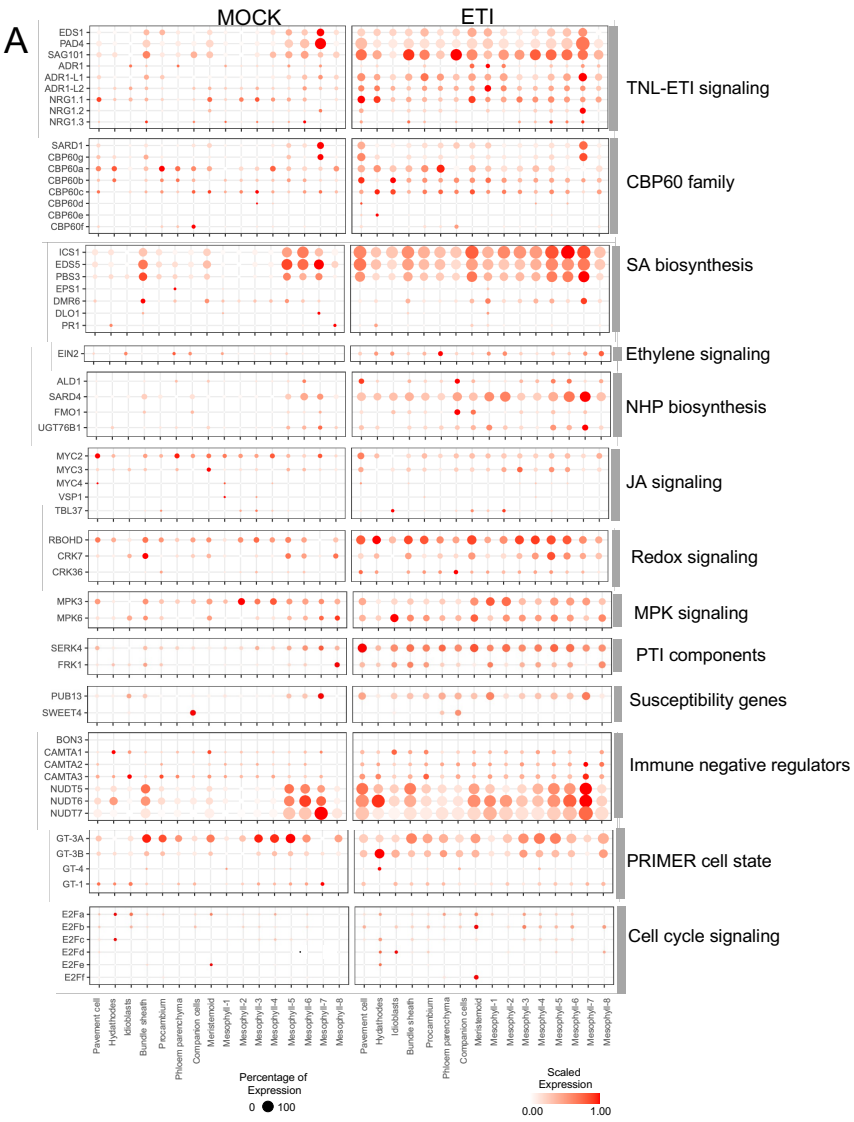
A
MOCK
ETI
EDS1
PAD4
SAG101
ADR1
ADR1-L1
ADR1-L2
NRG1.1
NRG1.2
NRG1.3
TNL-ETI signaling
SARD1
CBP60g
CBP60a
CBP60b
CBP60c
CBP60d
CBP60e
CBP60f
CBP60 family
ICS1
EDS5
PBS3
EPS1
DMR6
DLO1
PR1
SA biosynthesis
EIN2
Ethylene signaling
ALD1
SARD4
FMO1
UGT76B1
NHP biosynthesis
MYC2
MYC3
MYC4
VSP1
TBL37
JA signaling
RBOHD
CRK7
CRK36
Redox signaling
MPK3
MPK6
MPK signaling
SERK4
FRK1
PTI components
PUB13
SWEET4
Susceptibility genes
BON3
CAMTA1
CAMTA2
CAMTA3
NUDT5
NUDT6
NUDT7
Immune negative regulators
GT-3A
GT-3B
GT-4
GT-1
PRIMER cell state
E2Fa
E2Fb
E2Fc
E2Fd
E2Fe
E2Ff
Cell cycle signaling
Pavement cell
Hydathodes
Idioblasts
Bundle sheath
Procambium
Phloem parenchyma
Companion cells
Meristemoid
Mesophyll-1
Mesophyll-2
Mesophyll-3
Mesophyll-4
Mesophyll-5
Mesophyll-6
Mesophyll-7
Mesophyll-8
Percentage of Expression
0
100
Scaled Expression
0.00
1.00

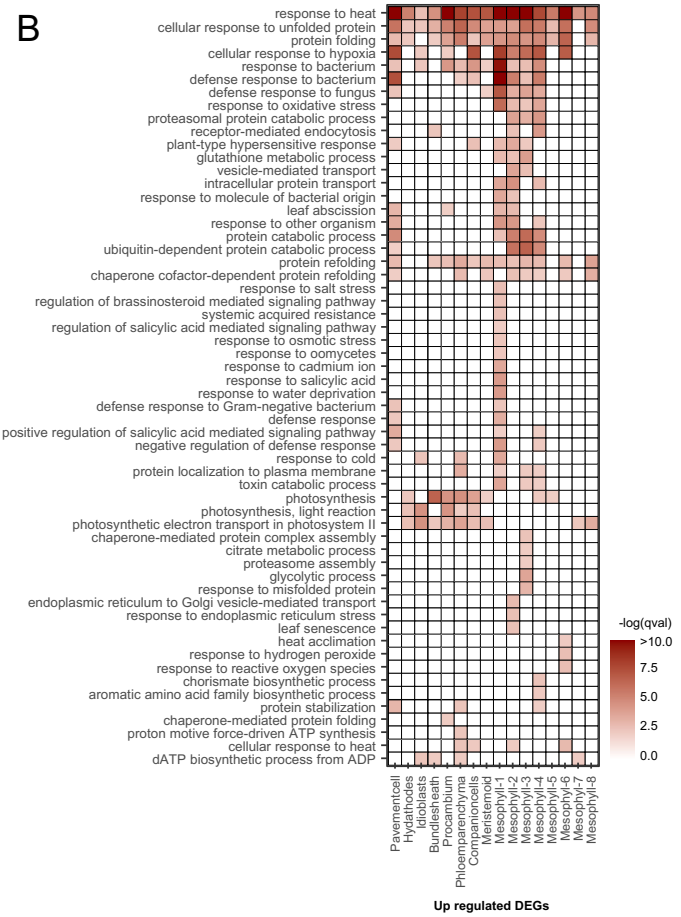

Figure 2. Cell-type-specific transcriptional responses to ETI in Arabidopsis leaf tissue. A. Bubble plot showing expression of representative immune-related genes across annotated cell types under mock and E2 conditions. Categories include TNL-ETI signaling components, CBP60 family members, salicylic acid (SA), jasmonic acid (JA), ethylene, and NHP signaling, redox and MAP kinase pathways, PTI components, susceptibility factors, and immune repressors. B. Gene Ontology (GO) enrichment of upregulated DEGs in ETI-treated cells. Functional categories include defense responses, hormone signaling, oxidative stress, protein folding, photosynthesis, and vesicle-mediated transport. Enrichment significance is shown as –log10(q-value), illustrating spatially resolved immune reprogramming during ETI.

To map the cellular architecture of immune execution, we performed differential gene expression (DEG) analysis across all annotated cell clusters (**Figure S3B**), followed by gene ontology (GO) term enrichment. As anticipated, defense-related GO terms were predominantly enriched in epidermal and mesophyll cells (**Figure 2B**, **Table S2**), consistent with prior bulk RNA-seq findings[16]. Interestingly, GO terms related to photosynthesis, especially photosystem I components, were significantly enriched among downregulated genes in several mesophyll clusters (**Figure S4A**), indicating that ETI alone can suppress core metabolic programs in addition to activating defense.

To evaluate how cell-resolved responses relate to canonical ETI programs, we compared upregulated DEGs in each cluster with a previously defined list of EDS1-dependent immune-responsive genes (**Table S3**)[16]. Most clusters showed significant overlap, with pavement cells and mesophyll cells exhibiting the highest concordance (**Figure 3A, S4B**). This supports the presence of a broadly conserved core immune program across major cell types.

However, beyond this shared module, many cell clusters displayed distinct expression of immune-activation indicators or regulators, such as *CBP60g*, *SARD1*, *ALD1*, *FMO1*, *SWEET4* and *E2F* family transcription factors etc., which may mediate cell-autonomous immune amplification, niche-specific defense execution, or immune signal propagation contributing to pathogen restriction and distal immune priming signal propagation.

To delineate these features systematically, we classified DEGs as shared (included in more than 2 different clusters; **Table S7**) or cluster-specific (uniquely induced; **Table S8**). Many cluster-specific genes still overlapped with bulk-identified ETI targets, suggesting these are not artifacts of

cellular noise but reflect specialized, cell type-enriched immune indicators and putative regulators. Additionally, these genes overlapped with known EDS1-dependent ETI-responsive genes from bulk RNA-seq, supporting their role as specialized, cell type-enriched immune markers or execution components. Together, these results define a layered transcriptional framework for ETI in Arabidopsis: a core set of conserved immune genes is broadly deployed, while modular, cell-specific programs likely tailor immune outputs in a spatially precise manner. This modular immune architecture likely enables plants to coordinate tissue-scale defense while optimizing energy use and in parallel restrict pathogen invasion.

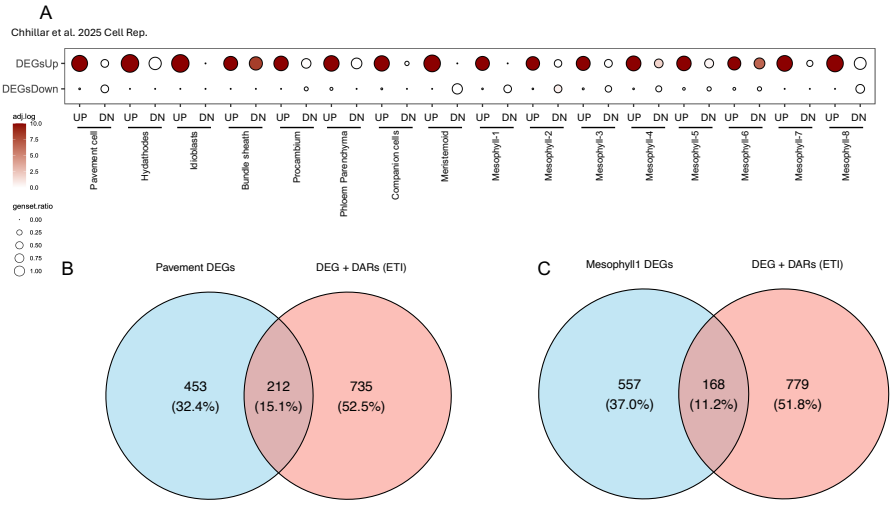

Figure 3. Integration of bulk RNA-seq and chromatin accessibility data with cell-type-specific ETI responses. A. Hypergeometric test showing the significance of overlap between bulk ETI-responsive genes (Chhillar et al. 2025, *Cell Rep.*) and DEGs identified in individual cell clusters from single cell RNA-seq. B-C. Venn diagrams showing overlap between DEGs and genes associated with differentially accessible regions (DARs) during ETI (from Ding et al. 2021, *JXB*) in pavement cells (B) and mesophyll-1 cells (C). A majority of cell-type-

specific DEGs are also associated with DARs, suggesting coordinated transcriptional and chromatin-level regulation. Percentages reflect the proportion of DEGs overlapping with DARs in each cell type.

Gene regulatory networks orchestrate cell-type-specific immune outputs

To elucidate how a uniform ETI activation translates into spatially heterogeneous immune execution, we examined the underlying regulatory mechanisms at the transcriptional level. We intersected upregulated DEGs from pavement and mesophyll 1 clusters with genes previously shown to be both ETI-induced (bulk RNA-seq) and exhibit ETI-enhanced chromatin accessibility (**Table S4**)[20]. This revealed a core set of chromatin-licensed immune genes (**Figure 3B-3C**; **Table S5-S6**), likely under transcriptional control during early ETI, and broadly conserved across both pavement and mesophyll 1 cell types.

To further dissect upstream regulatory control, we mapped cell-type specific DEGs to the Arabidopsis transcription factor (TF) *cistrome* and *epicistrome* database[28]. The *cistrome* defines the genome-wide landscape of transcription factor binding, while the *epicistrome* extends this by incorporating epigenetic features, such as DNA methylation, that modulate TF-DNA interactions, thereby shaping functional access to regulatory DNA. Together, they provide a comprehensive view of how gene regulatory networks are both encoded and epigenetically tuned[28]. WRKY, NAC, ERFs, MYB and bZIP TFs were prominently enriched in our analysis, consistent with established roles in plant immunity and suggesting that shared TF modules are deployed in distinct configurations across cell types to shape local defense outputs (**Figure 4A**)[29].

Notably, the enriched TFs exhibited varied responses across cell types, reflecting diverse regulatory roles in immune activation. Pavement and mesophyll cells showed the highest number of DEGs and the strongest

GO enrichment for immune-related processes. We therefore compared these two cell types to investigate transcriptional regulators underlying spatial specificity. Strikingly, *WRKY8* and *SARD1* were both exclusively expressed in the epidermis (**Figure 4A-4B**). Mapping to the *cistrome* and *epicitrome* database, WRKY8 was enriched at the promoters of a large fraction of pavement-specific ETI-induced DEGs (**Figure 4C**), consistent with its proposed role as an epidermal immune amplifier (**Figure 4B**)[8]. SARD1, a master regulator known to act redundantly with CBP60g to regulate plant immunity[10,11], was similarly epidermis-specific and targeted more than 80% of upregulated DEGs in this cell type (**Figure 4C**). Together, these TFs accounted for the majority of regulatory activity in the epidermal immune network, underscoring their importance in orchestrating cell type–specific defense programs. Similar modular patterns were observed for other TFs with respect to other cell-types (**Figure 4A**), reinforcing idea that different TF families contribute to spatially specialized transcriptional circuits.

Collectively, these findings support a model in which ETI activation is interpreted through a preconfigured, cell-intrinsic transcriptional framework, governed by chromatin accessibility and transcription factor availability. This spatially modular regulatory architecture allows for the diversification of immune outputs despite a common upstream signal, enabling plants to finely tune defense intensity, coordinate intercellular signaling, and maintain metabolic balance under immune stress or during pathogen attack.

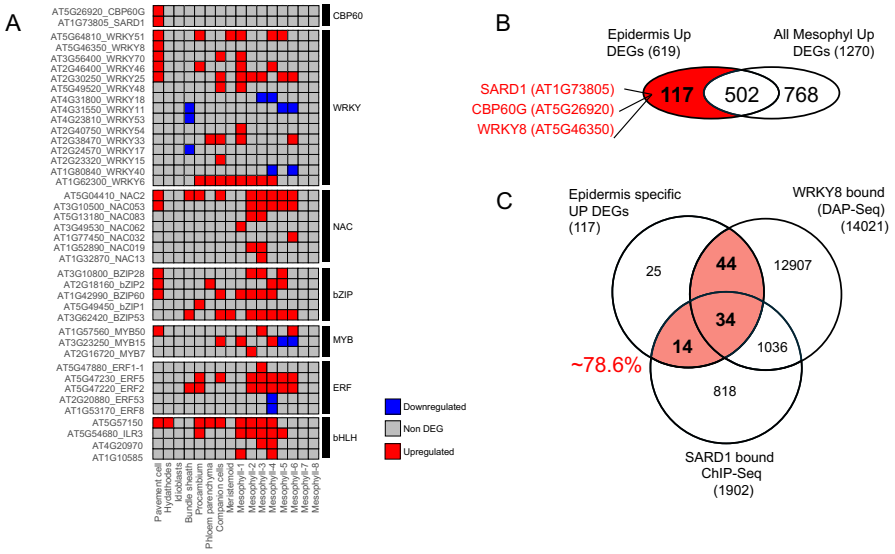

Figure 4. Cell-type-specific transcription factor activity underlies spatial immune regulation. A. Heatmap showing differential expression patterns of selected transcription factors (TFs) across annotated Arabidopsis leaf cell types. TFs are grouped by family (WRKY, NAC, bZIP, MYB, ERF, and bHLH). Red and blue indicate up- and downregulated expression, respectively, under ETI. Each column represents an individual cell type. B. Venn diagram comparing upregulated DEGs in pavement versus mesophyll cells. A subset of 82 genes is uniquely upregulated in pavement cells, including *SARD1* (*AT1g73805*) and *WRKY8* (*AT5g46350*). C. Overlap between pavement-specific upregulated DEGs and genomic targets of WRKY8 (DAP-seq) and SARD1 (ChIP-seq). Approximately 83% of pavement-specific DEGs are putative direct targets of WRKY8 and/or SARD1, indicating coordinated transcriptional control of epidermal immune programs.

Epidermis-specific immune regulators restrict non-host pathogen entry at the leaf surface

While many immune-related genes were broadly expressed across all leaf cell types upon ETI induction, certain transcriptional regulator exhibited strikingly cell-type-specific induction patterns, suggesting functional

compartmentalization in immune execution. Among these, *CBP60g* and *SARD1*, two well-established, partially redundant immune activators[10,11,13], were preferentially more upregulated in pavement cells (**Figure 2A**). SARD1 is a DEG specific to only pavement cells (**Figure 4A**), indicating a potential role in epidermis-localized defense mediated by ETI.

To assess whether this spatial enrichment reflects a functional requirement for immunity, we challenged *cbp60g sard1* double mutants and wild-type (WT) Col-0 with *Albugo candida* isolate AcEm2, a non-adapted oomycete pathogen that exhibits an incompatible interaction with Col-0 due to the NLR WHITE RUST RESISTANCE 4 (WRR4)-mediated recognition[30–32]. In contrast to WT plants, *cbp60g sard1* mutants permitted haustorial formation specifically in the epidermal and sub-epidermal cell layers, by not in deeper mesophyll tissues (**Figure 5A-B**). This indicates that while CBP60g and SARD1 are not globally required for ETI, they play a cell-type-specific role in restricting early pathogen entry at the leaf surface.

Despite their loss, ETI signaling in mesophyll cells appears intact, likely due to broad expression of core components such as EDS1, PAD4, and other transcriptional regulators like WRKY33 or E2Fs that may independently sustain immune competence in internal tissues. This reinforces the concept that cell-type-specific TF modules mediate immune execution in distinct spatial zones, with CBP60g and SARD1 acting as epidermis-enriched executors to enforce localized resistance against non-adapted pathogens. While we did not perform pathogen-infected single-cell profiling, our data provides a transcriptional reference framework for immune potential across cell types and highlights testable hypotheses for future spatial challenge assays.

Furthermore, testing additional pathogens with alternative invasion routes, such as *Blumeria graminis*, which penetrates directly through the epidermis[33], may clarify whether CBP60g- and SARD1-dependent immunity represents a generalizable outer-layer defense strategy. Such studies will further refine our understanding of how immune competence and execution are partitioned across tissue layers to collectively enforce nonhost resistance.

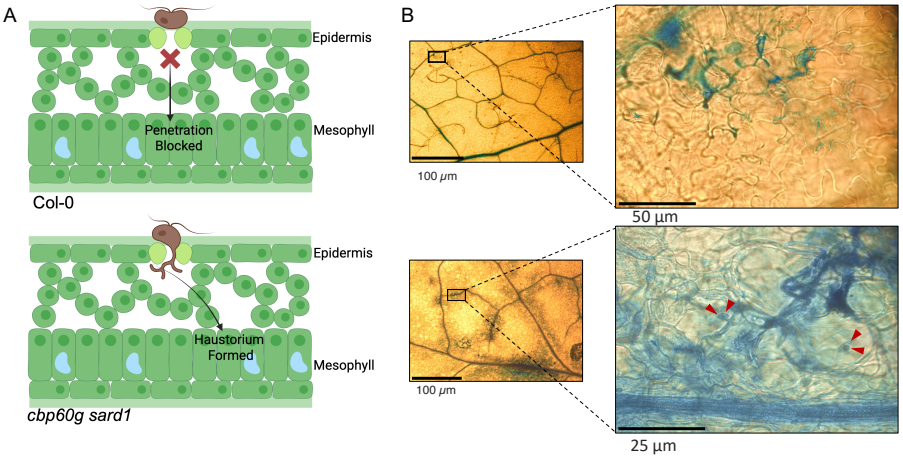

Figure 5. CBP60g and SARD1 mediate epidermis-specific immunity that *Albugo candida* entry. A. Schematic representation of infection outcomes in *Arabidopsis thaliana* Col-0 and the *cbp60g sard1* double mutant following inoculation with *Albugo candida* isolate AcEm2. In Col-0, pathogen entry is blocked at the epidermal layer, whereas *cbp60g sard1* mutants permit haustorium formation in underlying mesophyll cells, indicating compromised epidermal defense. B. Microscopic images of trypan blue-stained leaves infected with *A. candida* AcEm2. In Col-0, infection is restricted to the epidermis with no visible haustoria. In contrast, *cbp60g sard1* leaves show extensive hyphal growth and haustoria (red arrowheads) penetrating into mesophyll tissues, consistent with the model shown in (A).

Discussion

Our study presents a single-cell transcriptional atlas of ETI in Arabidopsis leaves, enabled by the SETI system[9], which uncouples immune activation by pathogen-derived cues (*e.g.* Mechanical perturbations, cell-wall integrity and apoplastic chemical matrix alternations, and cell-surface receptor-mediated signaling upon elicitor recognition, etc.) from the effects of pathogen effectors. This approach reveals how intracellular ETI is broadly perceived yet executed in a spatially heterogeneous manner across different cell types, offering new insights into the modular logic of plant immunity.

ETI activation via TIR-NLRs induces a widespread transcriptional competence across leaf cell types. Genes encoding core components such as EDS1, PAD4, SAG101 and enzymes involved in salicylic acid (SA) biosynthesis are broadly expressed, indicating that immune signal transduction is not restricted to a specialized subset of cells within the leaf, but is accessible to diverse cell types. Nonetheless, specific immune outputs, including the NHP and JA pathways, are spatially restricted, suggesting compartmentalization of defense metabolism. These results imply that metabolic branches of ETI may follow cell-type-specific coordination, raising the need for future integration of single-cell metabolomics to map the immune metabolome with cellular precision.

At the gene regulatory level, our data support a layered and modular tissue architecture of immune control. While certain transcriptional modules are shared across cell types, others are distinctly partitioned. WRKY25 and WRKY70 exhibit broad deployment, whereas WRKY8 appears to function almost exclusively in pavement cells, regulating the majority of immune-induced genes in that cellular layer. Such spatial exclusivity is consistent with proposed role of WRKY8 in the PRIMER cell state. However, our results challenge the notion of the PRIMER state as

a rare phenomenon. Instead, we propose that it represents a manifestation of differential ETI execution programs across cell types, embedded in their intrinsic components such as chromatin landscapes and transcription factor availability. The observed spatial heterogeneity reflects not a stochastic occurrence, but a structured immune regulatory mechanism encoded in tissue architecture. Other TFs, including WRKY17, WRKY33, E2Fs, and trihelix factors, further reinforce the diversity of transcriptional programs orchestrating immune output across spatial domains. This emphasizes that transcriptional immune competence is not synonymous with uniform immune execution. Despite shared upstream signaling through TIR-NLRs and EDS1, each cell type interprets immune signals through its own transcriptional lens, shaped by chromatin accessibility, TF availability, and cellular identity. This modular state likely allows plants to fine-tune defense intensity, optimize resource allocation, and coordinate systemic signaling in a spatially controlled manner.

Conventionally, nonhost resistance (NHR) represents a durable and broad-spectrum form of plant immunity, in which an entire plant species is resistant to all strains of a non-adapted pathogen[34]. While traditionally attributed to preformed barriers and pattern-triggered immunity (PTI), recent studies suggest that intracellular nucleotide-binding leucine-rich repeat (NLR) receptors can also contribute to nonhost restriction, particularly through effector recognition and ETI-like responses in specific pathosystems[35]. For instance, Arabidopsis NLR WRR4A mediates resistance to multiple isolates of *Brassica*-infecting isolates of *Albugo candida* [36], by recognizing lineage-specific effectors and triggering localized immune activation[30–32]. Our results extend this model by demonstrating that spatially restricted transcriptional regulators such as CBP60g and SARD1 are essential for enforcing cell-type-specific

resistance against non-adapted *Albugo* isolates, preventing pathogen ingress at the epidermal layer. In *cbp60g sard1* double mutants, *A. candida* haustoria are formed in cell types at the outer layer of the leaf tissue, despite intact immunity in underlying tissues. This provides direct evidence that immune competence alone is insufficient without proper transcriptional execution at vulnerable interfaces. It also underscores a broader principle: spatially localized immune regulators enforce layered defense barriers that guard vulnerable tissue interfaces, a robust framework that could likely be conserved across diverse plant-pathogen interactions. Building on this, future studies could extend similar analyses, combined with spatial omics approaches, to identify additional spatially enriched immune components and evaluate their cell type–specific functional relevance.

The hydathode, a specialized structure at the leaf margin that connects to the vasculature, exemplifies this principle. Unlike the epidermis, which confronts external pathogens, hydathodes represent potential internal entry points. Prior work has shown that hydathode immunity is mediated by EDS1-PAD4-ADR1 signaling[37,38], and our findings extend this by identifying GT-family transcription factors and GT-3A paralogs, GT-3B and GT-4, as selectively induced in hydathodes during ETI. While GT-3A is expressed in almost all cell types during ETI activation, the restricted expression pattern of GT-3B and GT-4 suggests that these TFs constitute a hydathode immune regulatory module. This underscores how even uniformly activated ETI is interpreted through distinct local transcriptional regulation, shaped by structural vulnerability and functional necessity.

Our findings deliver several conceptual advances. First, we provide direct transcriptional evidence that innate immune competence is broadly encoded in all major cell types of the Arabidopsis leaf, supporting a model of fully distributed, cell-autonomous immunity. Second, we show that even

under uniform activation of intracellular immunity, cell identity exerts a major constraint on the spectrum and strength of transcriptional output. This introduces the concept of cell-type-specific immune execution, highlighting new questions about how chromatin features, TF availability, and metabolic state shape these responses. Our dataset offers a valuable resource for future mechanistic studies into these layers of regulation. Third, our functional validation of the epidermis-enriched transcriptional regulators CBP60g and SARD1 establishes that NHR mediated by NLR-triggered ETI is not uniform across tissues but depends on precise execution in specific cell types. In *cbp60g sard1* double mutants, haustoria of resisted races of oomycete *A. candida* formed specifically in the epidermal and sub-epidermal cells, despite intact immunity in inner layers. This demonstrates that immune competence alone is insufficient without proper transcriptional execution at vulnerable tissue interfaces. These findings provide, to our knowledge, the first direct evidence that NLR-driven NHR displays cell-type specificity, with functional consequences for pathogen entry.

Altogether, our results define a spatially modular model of ETI, where uniformly initiated immune signaling is filtered through localized transcriptional programs. This allows for precise deployment of immunity, which is stronger in vulnerable cell types in Arabidopsis leaf tissue like the epidermis and hydathodes than elsewhere. These insights raise compelling research questions: What molecular features prime certain cells for heightened immune execution? Can spatial chromatin states predict immunocompetence? How do localized defenses coordinate with systemic signaling? Is infection spatially random, or shaped by host–pathogen combinations at the single-cell level? How do highly responsive cells compensate for neighbouring cells with limited immune potential to maintain tissue-wide resilience?

In summary, this work provides a foundational framework for understanding cell-type-resolved immunity in plants. By demonstrating how immune signaling is broadly competent yet differentially executed, we reveal the principles of spatial immune execution. These insights offer a roadmap for engineering durable, precision immune responses in crops, tailored to the distinct roles and vulnerabilities of each cell type.

Acknowledgements

HC and PD acknowledge a European Research Council Starting Grant 'RELEVATION' (grant agreement: 101039824). AR acknowledges support by EMBO LTF (ALTF-842-2015). LJ and KK were supported by the Netherlands Organization for Scientific Research (NWO) VIDI grant number VI.Vidi.193.104. JDGJ was supported by the Gatsby Foundation (United Kingdom).

Competing interests

The authors declare no competing interests.

Author contributions

PD conceptualized and oversaw the inception of the research project. The experimental work was collaboratively conducted by HC, AR, and PD, and. Data analysis and figure generation were performed by LJ, HC, AR, KK, and PD. JDGJ provides valuable discussions that significantly shaped the research during this project. The initial manuscript draft was written by HC, LJ, and PD. All co-authors contributed to subsequent revisions and editorial processes. The final manuscript was prepared by HC and PD and was approved for submission by all authors.

Data and code availability

- All sequencing datasets generated in this study have been deposited in the European Nucleotide Archive (ENA) under the accession number PRJEB91113.

- All custom scripts and analysis code are publicly available at our GitHub repository: https://github.com/dinglab-plants/scETI.

Material and Methods

Plant material and growth conditions

Arabidopsis thaliana Col-0 ecotype was used as the wild-type background. The β-estradiol (E2)–inducible SUPER-ETI line (*SETI_WT)* and the *cbp60g sard1* double mutant used in this study have been previously described[9,10]**.** Plants were grown at 21°C under long-day conditions (16 h light, 8 h dark), and at 50% humidity.

Protoplast isolation

Four-week-old leaves from *SETI_WT* plants were infiltrated with 50 μM estradiol (E2), and protoplasts were isolated 4 hours post infiltration (hpi) using the Tape-Arabidopsis Sandwich method[39]. Peeled leaf tissue was incubated in enzyme digestion solution containing 0.4 M D-sorbitol, 20 mM KCl, 20 mM MES, 10 mM $CaCl_2$, 0.1% (w/v) BSA, 1.5% (w/v) Cellulase R10 (Duchefa), 0.5% (w/v) Macerozyme R10 (Duchefa), 5% (v/v) Viscozyme® L (Sigma), and 3.56 mM 2-mercaptoethanol. The digestion was carried out for 2 hours at 40 rpm. The resulting protoplast suspension was filtered through a 40 μm mesh and centrifuged at 200 × g for 5 minutes at 4°C using a swinging bucket rotor with minimal deceleration.

Protoplasts were resuspended in 2 mL of washing buffer composed of 0.4 M D-mannitol, 20 mM KCl, 20 mM MES, 1 mM $CaCl_2$, 0.1% (w/v) BSA, and 3.56 mM 2-mercaptoethanol. Purification of intact protoplasts was achieved using a three-phase density gradient centrifugation with OptiPrep™ (Stemcell Technologies). The OptiPrep working solution (WS) was prepared by dissolving 0.06 g of KCl in 10 mL of OptiPrep. For the gradient, 2 mL of protoplast suspension was mixed with 500 μL of OptiPrep WS (final density: 1.064 g mL^{-1}) and layered at the bottom of a

5 mL centrifuge tube. The middle layer consisted of 1 mL of a 2:0.4 (v/v) mix of resuspension buffer and OptiPrep WS (final density: 1.053 g mL^{-1}), gently added atop the bottom layer. The top layer comprised 200 µL of resuspension buffer carefully pipetted over the middle layer.

The gradient was centrifuged at 200 × g for 5 minutes at 4°C using a swinging bucket rotor. Protoplasts were recovered from the topmost layer, resuspended in washing buffer, visualized under microscope and adjusted to a final concentration of ~1,000 cells/µL. The purified protoplast suspension was loaded into the 10x Genomics Chromium Controller for microfluidic droplet generation. Single-cell libraries were prepared using the Chromium Single Cell 3' Reagent Kit v3.1 (10x Genomics), following the manufacturer's protocol. Libraries were sequenced on an Illumina NovaSeq X Plus platform (paired-end 150 bp reads).

Single cell data analysis

Cellranger (10X Genomics) was used to map the reads to the Arabidopsis reference genome (Araport11). Upon alignment, the 'force-cells' option was used to detect the top 10,000 cells based on UMI counts. For each sample, low-quality cells were removed based on mitochondrial and chloroplast read counts (5% mitochondrial and 20% chloroplast counts), which resulted in the identification of 7932 and 5739 high-quality cells in the mock and induced samples, respectively. The Seurat R package (reference) was used for integration, dimensionality reduction, scaling, clustering and DEG analysis. We used the canonical correlation analysis (CCA) integration option for the integration of both datasets. Uniform manifold approximation and projection (UMAP) were calculated using 32 principal component dimensions and cell-clusters were identified using the Seurat 'FindClusters' function with the resolution parameter set to 0.8, which resulted in the identification of 16 cell clusters. For each cluster, gene markers were identified using the 'FindAllMarkers' function with a

threshold of adjusted *p*-value < 0.01, log2FC > 0.25, percentage of cells within the cluster that expresses the gene greater than 10% and percentage difference to other clusters greater than 20%. The identities of each cell cluster were determined based on the expression of putative leaf cell-markers [17]. For the DEG analysis we first aggregate the expression values of both datasets using the 'AggregateExpression' function followed by a pair-wise comparison between from mock and treated sample in each individual cluster using the function 'FindMarkers', with a threshold of adjusted *p*-value <= 0.01, log2FC >= 0.58496250072 for genes that are expressed in at least 20% of the cells.

Reverse transcription-quantitative PCR (RT-qPCR)

For gene expression analysis, RNA was isolated from protoplast isolated from 4-week-old Arabidopsis leaves 4 hpi after E2 infiltration and used for subsequent RT–qPCR analysis. RNA was extracted with a Quick-RNA Plant Kit (R2024; Zymo Research) and treated with RNase-free DNase (4716728001; Merck-Roche). Reverse transcription was carried out using SuperScript IV Reverse Transcriptase (18090050; ThermoFisher Scientific). qPCR was performed using a CFX96 Touch™ Real-Time PCR Detection System. Primers for qPCR analysis of *ISOCHORISMATE SYNTHASE1* (*ICS1*), *ELONGATION FACTOR 1 ALPHA* (*EF1α*) are as follows: *ICS1* primers (*ICS1*_F: 5′-CAATTGGCAGGGAGACTTACG-3'; *ICS1*_R: 5′-GAGCTGATCTGATCCCGACTG-3′). *EF1α* primers (*EF1α*_F: 5′-CAGGCTGATTGTGCTGTTCTTA-3'; *EF1α*_R: 5′GTTGTATCCGACCTTCTTCAGG-3′) and Data were analysed using the double delta Ct method[40]. All results are plotted using ggplot2 in R[41], and a detailed statistical summary can be found in Table S1.

***Albugo candida* propagation and infection assay**

For testing the susceptibility in the A. thaliana genotypes in this study, an incompatible isolate of A. candida AcEm2 was used[42]. Infection assays

were performed as previously described[32]. Pre-infected leaves with pustules bearing sporangiophores were suspended in water (c. 10^5 spores mL^{-1}). This suspension was incubated on ice for 30 min for release of the zoospores. The inoculum of spore suspension was filtered through a double layered muslin cloth and then sprayed on plants using a Humbrol® (Hornby Hobbies Ltd, Sandwich, UK) spray gun (c. 700 µL per plant). Post spraying, plants were incubated at 4°C overnight in the dark, for promoting zoospore germination. Infected plants were kept under 10 h light (20°C) and 14 h dark (16°C) cycles. Susceptibility on the infected plants with an incompatible strain was scored at 6 days post infection (dpi) by trypan blue imaging of the AcEm2 colonization and its establishment in the host.

Trypan blue staining

Infected leaves were boiled for 1 min in stain solution (10 mL lactic acid, 10 mL glycerol, 10 g phenol, 10 mg trypan blue and water in a final volume of 10 mL, mixed in a 1 : 1 ratio with ethanol) and then decolorized in chloral hydrate (2.5 gm chloral hydrate in water in a final volume of 1 mL). The leaves were mounted in 60% glycerol and examined using a Leica M165 FC stereomicroscope.

Supplementary Information

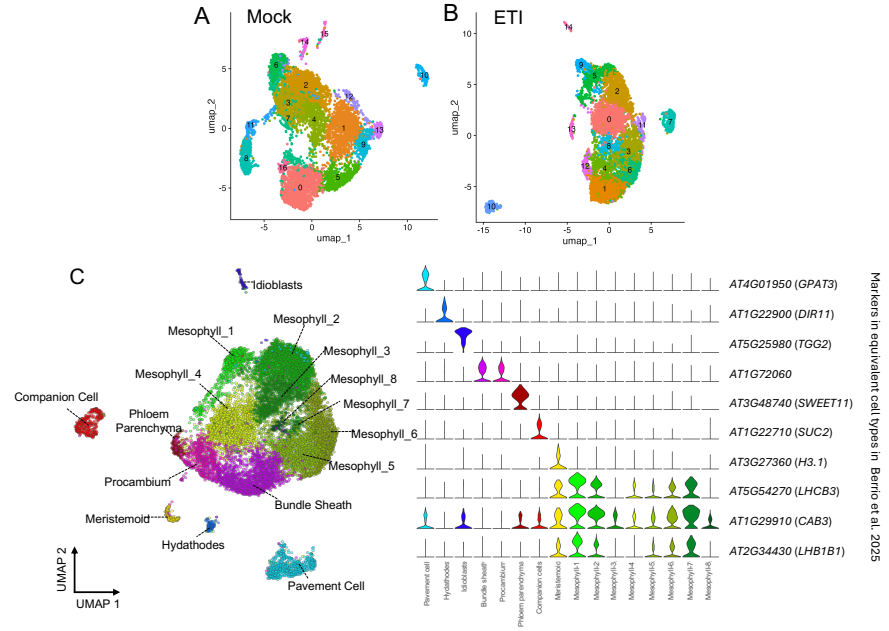

Figure S1. UMAP-based clustering and cell-type annotation of Arabidopsis leaf single-cell transcriptomes. A-B. UMAP projections of single-cell transcriptomes from mock-treated (A) and effector-triggered immunity (ETI)-induced (B) Arabidopsis leaf tissues. Cells are colored by unsupervised clusters, corresponding to major and minor leaf cell types. Overall cluster architecture remains conserved upon ETI induction. C. Cell-type assignment based on the expression of canonical marker genes. Violin plots display representative marker expression across annotated clusters, supporting the identification of pavement, hydathode, idioblast, vascular, mesophyll, and meristem-like cell types. Marker gene identities are cross-referenced with equivalent annotations from Barrio et al., 2025.

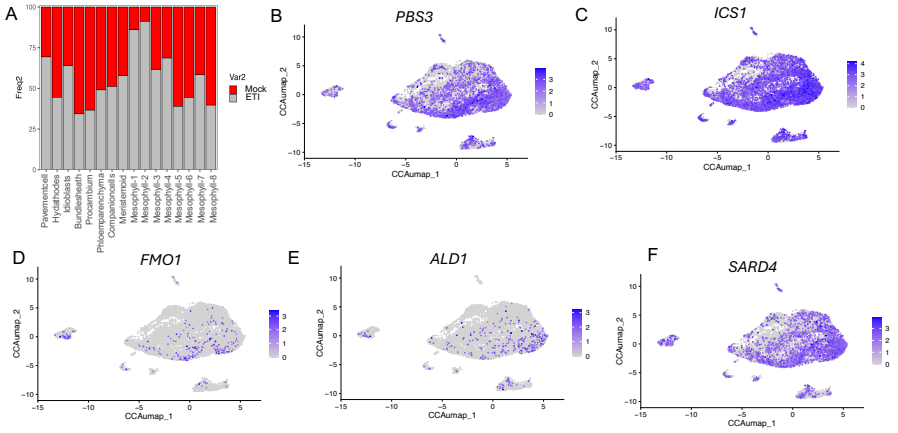

Figure S2. Cell-type compositional changes and activation of salicylic acid and NHP biosynthetic pathways during ETI. A. Stacked bar plot showing the relative abundance of annotated cell types under mock (gray) and ETI-induced (red) conditions. Increased representation of epidermal and multiple mesophyll subtypes is observed under ETI, indicating shifts in cellular transcriptional states. B-F. Single-cell feature plots depicting expression of genes involved in salicylic acid (SA) biosynthesis (*ISOCHORISMATE SYNTHASE 1* (*ICS1*), *AVRPPHB SUSCEPTIBLE 3* **(***PBS3*) and *N-HYDROXY PIPECOLIC ACID* (NHP) biosynthesis (*AGD2-LIKE DEFENSE RESPONSE PROTEIN 1* (*ALD1*), *SYSTEMIC ACQUIRED RESISTANCE DEFICIENT 4* (*SARD4*), *FLAVIN-DEPENDENT MONOOXYGENASE 1* (*FMO1*)). Expression of *ICS1* and *SARD4* is broadly distributed across mesophyll and vascular cells, whereas *FMO1* and *ALD1* show more spatially restricted activation.

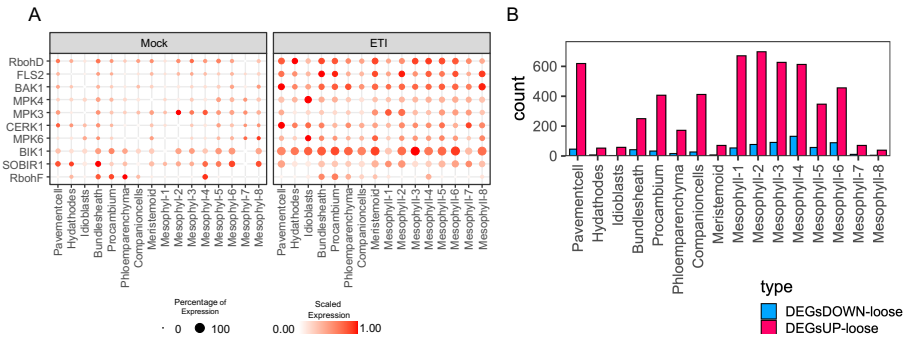

Figure S3. Cell-type-specific expression and transcriptional activation of immune signaling components during ETI. A. Dot plot illustrates the expression of key pattern-triggered immunity (PTI) and effector-triggered immunity (ETI) signaling genes across annotated leaf cell types under mock and ETI conditions. Dot size indicates the proportion of cells expressing each gene, and colour intensity reflects scaled average expression. Genes include receptor kinases (FLAGELLIN SENSING 2 (*FLS2*), BRI1-ASSOCIATED KINASE 1 (*BAK1*), *CHITIN ELICITOR RECEPTOR KINASE 1* (*CERK1*)), MAP kinases (*MPK3, MPK4, MPK6*), and signaling intermediates (*BOTRYTIS-INDUCED KINASE 1* (*BIK1*), *SUPPRESSOR OF BIR1-1* (*SOBIR1*), *RESPIRATORY BURST OXIDASE HOMOLOG D* (*RbohD)*, *RbohF*). B. Bar graph showing the number of upregulated (pink) and downregulated (blue) differentially expressed genes (DEGs) across each cell type upon ETI induction. Strong transcriptional activation is observed in mesophyll and pavement cells, consistent with their central role in immune responses.

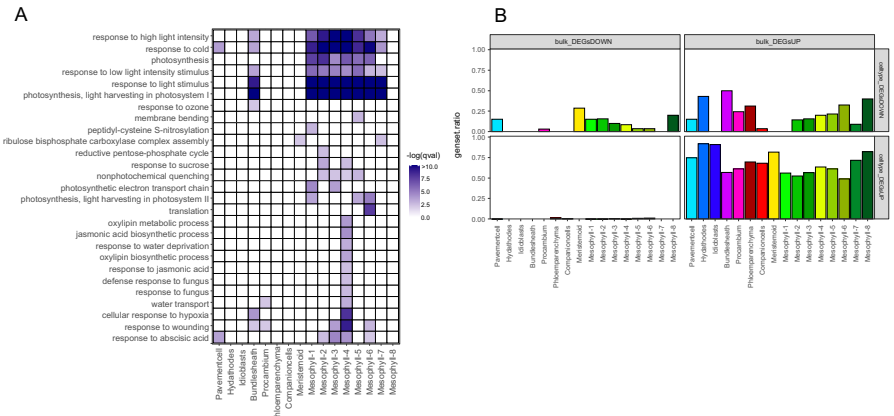

Figure S4. Functional enrichment analysis of bulk ETI-regulated genes across leaf cell types. A. Heatmap showing Gene Ontology (GO) biological process terms enriched among downregulated genes (DEGsDOWN) mapped to specific cell types using single-cell deconvolution. Colour scale indicates statistical significance (log_{10}-transformed adjusted *q*-value). Suppressed photosynthetic and light-responsive pathways are predominantly enriched in mesophyll cluster. B. Bar plots showing the cell-type distribution of upregulated (DEGsUP, bottom) and downregulated (DEGsDOWN, top) bulk DEGs, inferred by scRNA-seq expression patterns. ETI-upregulated genes are broadly represented across epidermal and mesophyll cells, while downregulated genes are more restricted to photosynthetically active mesophyll populations.

Supplemental tables can be accessed online at (https://doi.org/10.1101/2025.06.28.662111)

References

1. Pradeu, T., Thomma, B.P.H.J., Girardin, S.E., and Lemaitre, B. (2024). The conceptual foundations of innate immunity: Taking stock 30 years later. Immunity *57*, 613–631. 10.1016/j.immuni.2024.03.007.

2. Sun, T., and Zhang, Y. (2021). Short- and long-distance signaling in plant defense. Plant J. *105*, 505–517. 10.1111/tpj.15068.

3. Tabassum, N., and Blilou, I. (2022). Cell-to-Cell Communication During Plant-Pathogen Interaction. Mol. Plant Microbe Interact. *35*, 98–108. 10.1094/MPMI-09-21-0221-CR.

4. Jones, J.D.G., Staskawicz, B.J., and Dangl, J.L. (2024). The plant immune system: From discovery to deployment. Cell *187*, 2095–2116. 10.1016/j.cell.2024.03.045.

5. Ngou, B.P.M., Jones, J.D.G., and Ding, P. (2022). Plant immune networks. Trends Plant Sci. *27*, 255–273. 10.1016/j.tplants.2021.08.012.

6. Zhu, J., Lolle, S., Tang, A., Guel, B., Kvitko, B., Cole, B., and Coaker, G. (2023). Single-cell profiling of Arabidopsis leaves to Pseudomonas syringae infection. Cell Rep. *42*, 112676. 10.1016/j.celrep.2023.112676.

7. Tang, B., Feng, L., Hulin, M.T., Ding, P., and Ma, W. (2023). Cell-type-specific responses to fungal infection in plants revealed by single-cell transcriptomics. Cell Host Microbe *31*, 1732-1747.e5. 10.1016/j.chom.2023.08.019.

8. Nobori, T., Monell, A., Lee, T.A., Sakata, Y., Shirahama, S., Zhou, J., Nery, J.R., Mine, A., and Ecker, J.R. (2025). A rare PRIMER cell state in plant immunity. Nature *638*, 197–205. 10.1038/s41586-024-08383-z.

9. Ngou, B.P.M., Ahn, H.-K., Ding, P., Redkar, A., Brown, H., Ma, Y., Youles, M., Tomlinson, L., and Jones, J.D.G. (2020). Estradiol-inducible AvrRps4 expression reveals distinct properties of TIR-NLR-mediated effector-triggered immunity. J. Exp. Bot. *71*, 2186–2197. 10.1093/jxb/erz571.

10. Zhang, Y., Xu, S., Ding, P., Wang, D., Cheng, Y.T., He, J., Gao, M., Xu, F., Li, Y., Zhu, Z., et al. (2010). Control of salicylic acid synthesis and systemic acquired resistance by two members of a plant-specific family of transcription factors. Proc Natl Acad Sci USA *107*, 18220–18225. 10.1073/pnas.1005225107.

11. Wang, L., Tsuda, K., Truman, W., Sato, M., Nguyen, L.V., Katagiri, F., and Glazebrook, J. (2011). CBP60g and SARD1 play partially redundant critical roles in salicylic acid signaling. Plant J. *67*, 1029–1041. 10.1111/j.1365-313X.2011.04655.x.

12. Sun, T., Zhang, Y., Li, Y., Zhang, Q., Ding, Y., and Zhang, Y. (2015). ChIP-seq reveals broad roles of SARD1 and CBP60g in regulating plant immunity. Nat. Commun. *6*, 10159. 10.1038/ncomms10159.

13. Sun, T., Liang, W., Zhang, Y., and Li, X. (2018). Negative regulation of resistance protein-mediated immunity by master transcription factors SARD1 and CBP60g. J. Integr. Plant Biol *60*, 1023–1027. 10.1111/jipb.12698.

14. Ngou, B.P.M., Ahn, H.-K., Ding, P., and Jones, J.D.G. (2021). Mutual potentiation of plant immunity by cell-surface and intracellular receptors. Nature *592*, 110–115. 10.1038/s41586-021-03315-7.

15. Ding, P., Ngou, B.P.M., Furzer, O.J., Sakai, T., Shrestha, R.K., MacLean, D., and Jones, J.D.G. (2020). High-resolution expression profiling of selected gene sets during plant immune activation. Plant Biotechnol. J. *18*, 1610–1619. 10.1111/pbi.13327.

16. Chhillar, H., Nguyen, H.H., Yeh, P.-M., Jones, J.D.G., and Ding, P. (2025). Modular mechanisms of immune priming and growth inhibition mediated by plant effector-triggered immunity. Cell Rep. *44*, 115394. 10.1016/j.celrep.2025.115394.

17. Tenorio Berrío, R., Verhelst, E., Eekhout, T., Grones, C., De Veylder, L., De Rybel, B., and Dubois, M. (2025). Dual and spatially resolved drought responses in the Arabidopsis leaf mesophyll revealed by single-cell transcriptomics. New Phytol. *246*, 840–858. 10.1111/nph.20446.

18. Duxbury, Z., Wu, C.-H., and Ding, P. (2021). A comparative overview of the intracellular guardians of plants and animals: nlrs in innate immunity and beyond. Annu. Rev. Plant Biol. *72*, 155–184. 10.1146/annurev-arplant-080620-104948.

19. Ding, P., and Ding, Y. (2020). Stories of salicylic acid: A plant defense hormone. Trends Plant Sci. *25*, 549–565. 10.1016/j.tplants.2020.01.004.

20. Ding, P., Sakai, T., Krishna Shrestha, R., Manosalva Perez, N., Guo, W., Ngou, B.P.M., He, S., Liu, C., Feng, X., Zhang, R., et al. (2021). Chromatin accessibility landscapes activated by cell-surface and intracellular immune receptors. J. Exp. Bot. *72*, 7927–7941. 10.1093/jxb/erab373.

21. Ding, P., Rekhter, D., Ding, Y., Feussner, K., Busta, L., Haroth, S., Xu, S., Li, X., Jetter, R., Feussner, I., et al. (2016). Characterization of a pipecolic acid biosynthesis pathway required for systemic acquired resistance. Plant Cell *28*, 2603–2615. 10.1105/tpc.16.00486.

22. Hartmann, M., Zeier, T., Bernsdorff, F., Reichel-Deland, V., Kim, D., Hohmann, M., Scholten, N., Schuck, S., Bräutigam, A., Hölzel, T., et al. (2018). Flavin Monooxygenase-Generated N-Hydroxypipecolic Acid Is a Critical Element of Plant Systemic Immunity. Cell *173*, 456-469.e16. 10.1016/j.cell.2018.02.049.

23. Chen, Y.-C., Holmes, E.C., Rajniak, J., Kim, J.-G., Tang, S., Fischer, C.R., Mudgett, M.B., and Sattely, E.S. (2018). *N* -hydroxy-pipecolic acid is a mobile metabolite that induces systemic disease resistance in *Arabidopsis*. Proc. Natl. Acad. Sci. USA *115*. 10.1073/pnas.1805291115.

24. Hartmann, M., Kim, D., Bernsdorff, F., Ajami-Rashidi, Z., Scholten, N., Schreiber, S., Zeier, T., Schuck, S., Reichel-Deland, V., and Zeier, J. (2017). Biochemical principles and functional aspects of pipecolic acid biosynthesis in plant immunity. Plant Physiol. *174*, 124–153. 10.1104/pp.17.00222.

25. Ramirez-Parra, E., López-Matas, M.A., Fründt, C., and Gutierrez, C. (2004). Role of an atypical E2F transcription factor in the control of Arabidopsis cell growth and differentiation. Plant Cell *16*, 2350–2363. 10.1105/tpc.104.023978.

26. Wang, S., Gu, Y., Zebell, S.G., Anderson, L.K., Wang, W., Mohan, R., and Dong, X. (2014). A noncanonical role for the CKI-RB-E2F cell-cycle signaling pathway in plant effector-triggered immunity. Cell Host Microbe *16*, 787–794. 10.1016/j.chom.2014.10.005.

27. Ayadi, M., Delaporte, V., Li, Y.-F., and Zhou, D.-X. (2004). Analysis of GT-3a identifies a distinct subgroup of trihelix DNA-binding transcription factors in Arabidopsis. FEBS Lett. *562*, 147–154. 10.1016/S0014-5793(04)00222-4.

28. O'Malley, R.C., Huang, S.-S.C., Song, L., Lewsey, M.G., Bartlett, A., Nery, J.R., Galli, M., Gallavotti, A., and Ecker, J.R. (2016). Cistrome and epicistrome features shape the regulatory DNA landscape. Cell *165*, 1280–1292. 10.1016/j.cell.2016.04.038.

29. Aerts, N., Chhillar, H., Ding, P., and Van Wees, S.C.M. (2022). Transcriptional regulation of plant innate immunity. Essays Biochem. *66*, 607–620. 10.1042/EBC20210100.

30. Borhan, M.H., Gunn, N., Cooper, A., Gulden, S., Tör, M., Rimmer, S.R., and Holub, E.B. (2008). WRR4 encodes a TIR-NB-LRR protein that confers broad-spectrum white rust resistance in *Arabidopsis thaliana* to four physiological races of *Albugo candida*. Mol. Plant Microbe Interact. *21*, 757–768. 10.1094/MPMI-21-6-0757.

31. Borhan, M.H., Holub, E.B., Kindrachuk, C., Omidi, M., Bozorgmanesh-Frad, G., and Rimmer, S.R. (2010). WRR4, a broad-spectrum TIR-NB-LRR gene from Arabidopsis thaliana that confers white rust resistance in transgenic oilseed Brassica crops. Mol. Plant Pathol. *11*, 283–291. 10.1111/j.1364-3703.2009.00599.x.

32. Redkar, A., Cevik, V., Bailey, K., Zhao, H., Kim, D.S., Zou, Z., Furzer, O.J., Fairhead, S., Borhan, M.H., Holub, E.B., et al. (2023). The Arabidopsis WRR4A and WRR4B paralogous NLR proteins both confer recognition of multiple Albugo candida effectors. New Phytol. *237*, 532–547. 10.1111/nph.18378.

33. Zimmerli, L., Stein, M., Lipka, V., Schulze-Lefert, P., and Somerville, S. (2004). Host and non-host pathogens elicit different jasmonate/ethylene responses in Arabidopsis. Plant J. *40*, 633–646. 10.1111/j.1365-313X.2004.02236.x.

34. Mysore, K.S., and Ryu, C.-M. (2004). Nonhost resistance: how much do we know? Trends Plant Sci. *9*, 97–104. 10.1016/j.tplants.2003.12.005.

35. Panstruga, R., and Moscou, M.J. (2020). What is the molecular basis of nonhost resistance? Mol. Plant Microbe Interact. *33*, 1253–1264. 10.1094/MPMI-06-20-0161-CR.

36. Cevik, V., Boutrot, F., Apel, W., Robert-Seilaniantz, A., Furzer, O.J., Redkar, A., Castel, B., Kover, P.X., Prince, D.C., Holub, E.B., et al. (2019). Transgressive segregation reveals mechanisms of Arabidopsis immunity to Brassica-infecting races of white rust

(Albugo candida). Proc Natl Acad Sci USA *116*, 2767–2773. 10.1073/pnas.1812911116.

37. Paauw, M., van Hulten, M., Chatterjee, S., Berg, J.A., Taks, N.W., Giesbers, M., Richard, M.M.S., and van den Burg, H.A. (2023). Hydathode immunity protects the Arabidopsis leaf vasculature against colonization by bacterial pathogens. Curr. Biol. *33*, 697-710.e6. 10.1016/j.cub.2023.01.013.

38. Paauw, M., Schravesande, W.E.W., Taks, N.W., Rep, M., Pfeilmeier, S., and van den Burg, H.A. (2025). Evolution of a vascular plant pathogen is associated with the loss of CRISPR-Cas and an increase in genome plasticity and virulence genes. Curr. Biol. *35*, 954-969.e5. 10.1016/j.cub.2025.01.003.

39. Wu, F.-H., Shen, S.-C., Lee, L.-Y., Lee, S.-H., Chan, M.-T., and Lin, C.-S. (2009). Tape-Arabidopsis Sandwich - a simpler Arabidopsis protoplast isolation method. Plant Methods *5*, 16. 10.1186/1746-4811-5-16.

40. Livak, K.J., and Schmittgen, T.D. (2001). Analysis of relative gene expression data using real-time quantitative PCR and the 2(-Delta Delta C(T)) Method. Methods *25*, 402–408. 10.1006/meth.2001.1262.

41. Wickham, H. (2016). ggplot2: Elegant Graphics for Data Analysis (Use R!) 2nd ed. (Springer).

42. McMullan, M., Gardiner, A., Bailey, K., Kemen, E., Ward, B.J., Cevik, V., Robert-Seilaniantz, A., Schultz-Larsen, T., Balmuth, A., Holub, E., et al. (2015). Evidence for suppression of immunity as a driver

for genomic introgressions and host range expansion in races of Albugo candida, a generalist parasite. eLife *4*. 10.7554/eLife.04550.

Chapter 4
Uncoupling hypersensitive cell death response and disease resistance activated by effector-triggered immunity

Himanshu Chhillar[1], Henk-jan Schoonbeek[2,3], Bruno Pok Man Ngou[3,4,5], Jonathan DG Jones[3,4], Pingtao Ding[1*]

[1]Institute of Biology Leiden, Leiden University, 2333 BE Leiden, The Netherlands
[2]John Innes Centre, Norwich Research Park, Colney Lane, NR4 7UH Norwich, UK
[3] University of East Anglia, Norwich Research Park, NR4 7TJ Norwich, UK
[4] The Sainsbury Laboratory, Norwich Research Park, Colney Lane, NR4 7UH Norwich, UK
[5]Current address: RIKEN Center for Sustainable Resource Science (CSRS), Kanagawa, 230-0045 Yokohama, Japan

This chapter is published in: bioRxiv (2025) October. doi: https://doi.org/10.1101/2025.10.22.683861 and is currently under review.

Abstract

Effector-triggered immunity (ETI) is a major defense strategy in plants and is frequently associated with the hypersensitive response (HR), a localized form of programmed cell death long assumed to be essential for pathogen resistance. However, the causal relationship between HR and effective immunity remains unresolved. We show that the *Arabidopsis cbp60g sard1* double mutant exhibits exaggerated ETI-associated HR but only partial resistance to bacterial and oomycete pathogens, thereby genetically uncoupling cell death from disease resistance without any visible pleiotropic defects. Genome-wide transcriptome profiling reveals that the absence of CBP60g and SARD1 disrupts the balance between immune activators and suppressors, including reduced induction of the Nudix hydrolase NUDT7. Overexpression of *NUDT7* diminishes but does not abolish the heightened HR phenotype in *cbp60g sard1* mutant, indicating that multiple negative regulators act redundantly to restrain immune-associated cell death. These findings demonstrate that HR is not an obligatory determinant of effective resistance against all pathogens and provide mechanistic insight into how plants coordinate transcriptional networks to balance pathogen defense with the containment of host cell death. By refining the relationship between HR and immunity, this work challenges a long-standing paradigm in plant biology and advances our understanding of immune regulation.

Key words

Hypersensitive response (HR), effector-triggered immunity (ETI), master regulators, SA signalling

Introduction

Plants are constantly challenged by diverse pathogens that threaten global crop productivity, causing an estimated 20-40% yield loss annually and over US$220 billion in damages according to the Food and Agriculture

Organization of the United Nations (FAO)[1]. To defend themselves, plants deploy two interconnected layers of innate immunity. Pattern recognition receptors (PRRs) located at the plasma membrane perceive pathogen-associated molecular patterns (PAMPs) to activate pattern-triggered immunity (PTI), while intracellular nucleotide-binding leucine-rich repeat receptors (NLRs) sense pathogen effectors and trigger effector-triggered immunity (ETI)[2]. In *Arabidopsis thaliana* (Arabidopsis), NLRs are classified into coiled-coil (CC)-type (CNLs), Toll/Interleukin-1 receptor/Resistance protein (TIR)-type (TNLs), and RESISTANCE TO POWDERY MILDEW (RPW8)-like CC-type (RNLs) based on their N-terminal domains[3]. Although PTI and ETI share many downstream outputs, including calcium (Ca^{2+}) influx, reactive oxygen species (ROS) production, and large-scale transcriptional reprogramming, ETI responses are typically more robust and sustained[4].

Calcium (Ca^{2+}) signalling is a critical mediator of both PTI and ETI[5]. Ca^{2+} signals are sensed by calcium-binding protein calmodulin (CaM) or/and CaM-like (CML) proteins, which interact with downstream CaM-binding proteins (CBPs) to transduce immune signals[6]. The Arabidopsis CBP60 family is comprised of eight members, seven of which contain canonical Ca^{2+}-dependent CaM-binding domains, whereas SYSTEMIC ACQUIRED RESISTANCE DEFICIENT 1 (SARD1) lacks this domain[7]. Among them, CBP60g and SARD1 are pathogen-inducible transcription factors that promote salicylic acid (SA) biosynthesis by directly activating *ISOCHORISMATE SYNTHASE 1* (*ICS1*) and other defense-associated genes[8–11]. *cbp60g sard1* double mutants lacking both factors CBP60g and SARD1 display reduced SA accumulation, enhanced susceptibility to the bacterial pathogen *Pseudomonas syringae*, and loss of systemic acquired resistance (SAR)[8,12]. Thus, CBP60g and SARD1 have been recognized as central positive regulators of SA-mediated immunity.

A hallmark of ETI is the hypersensitive response (HR), a localized form of programmed cell death that often accompanies disease resistance[13,14]. HR in plants share some morphological features with animal cell death (e.g., cytoplasmic shrinkage, chromatin condensation) but also exhibits plant-specific traits such as vacuolization and chloroplast disruption[15]. While HR and pathogen resistance are often tightly correlated, several genetic studies indicate they can be uncoupled. Early genetic analyses in oat crown rust resistance showed that hypersensitive cell death can be genetically separated from resistance through independent loci, demonstrating that HR is not required for effective disease resistance[16]. Consistent with this principle, analogous uncoupling has been observed in Arabidopsis, where loss of the metacaspase *mc1* drastically reduces HR but does not abolish resistance[17,18], and mutants such as *defense, no death* (*dnd1*), *HR-like lesion mimic 1* (*hlm1*), and *lesion simulating disease resistance 1* (*lsd1*) maintain resistance despite altered or spontaneous cell death[19–21]. However, these Arabidopsis mutants often show pleiotropic effects, complicating interpretation[22].

Here, we identify the *cbp60g sard1* double mutant as a valuable model to dissect the relationship between disease resistance and HR. Unlike other uncoupling mutants, *cbp60g sard1* exhibits enhanced HR in the absence of growth defects, providing a genetically tractable system to separate cell death from resistance. We demonstrate that CBP60g and SARD1 contribute to ETI-mediated resistance mediated by different types of NLRs, while paradoxically restraining ETI-associated HR. In addition, we test their contribution to necrotrophic pathogen interactions to gain a broader understanding of its immune function.

By integrating genome-wide transcriptomic profiling with functional assays, we uncover that CBP60g and SARD1 serve as dual regulators of the immune transcriptome: they promote defense-related gene activation

while simultaneously maintaining negative regulatory circuits, including members of the Nudix hydrolase family (NUDT). Functional analysis of *NUDT7* demonstrates its role in buffering ETI-associated cell death but also reveals that its overexpression cannot fully rescue the enhanced HR of *cbp60g sard1* double mutant. Together, our findings establish CBP60g and SARD1 as master integrators of positive and negative immune regulation and provide mechanistic insight into how plants fine-tune immune output, while decoupling HR from disease resistance.

Results

The *cbp60g sard1* mutant partially compromises ETI-mediated bacterial resistance but does not impair PTI

To assess the role of CBP60g and SARD1 in effector-triggered immunity (ETI), we challenged the *cbp60g sard1* (*gh* thereafter) double mutant with *Pseudomonas syringae* pv. *tomato* DC3000 strains carrying either AvrRps4 or AvrRpt2, alongside the corresponding empty vector (EV) controls. In wild-type (WT) Col-0, both effectors conferred strong resistance compared with EV infections, whereas *gh* plants showed only partial restriction of bacterial growth (**Figure 1A, S1A**), in consistence with previous studies[8,9]. AvrRps4 is recognized by the Toll/Interleukin-1 receptor/Resistance protein (TIR)-type nucleotide-binding leucine-rich-repeat receptors (NLRs) (or TNLs) RESISTANCE TO RASTONIA SOLANACEARUM 1 (RRS1)/RESISTANCE TO PSEUDOMONAS SYRINGAE 4 (RPS4) and RRS1B/RPS4B[23,24], and AvrRpt2 is recognized by the Coiled-coil (CC)-type NLR (or CNL) RPS2[25,26]. Therefore, the observed reduction of immunity in *gh* was comparable across TNL- and CNL-triggered pathways, indicating CBP60g and SARD1 contribute broadly to PTI+ETI-mediated defense. However, resistance was not completely abolished, suggesting residual immune signalling through

salicylic acid (SA), N-hydroxy pipecolic acid (NHP), or additional regulatory modules[27].

In contrast, when infected with the non-pathogenic strain DC3000 hrcC$^-$, which activated pattern-triggered immunity (PTI) but lacks a type-III secretion system, *gh* mutant supported bacterial growth at levels similar to WT Col-0 (**Figure 1B**). Consistently, *gh* plants displayed WT-like flg22-induced reactive oxygen species (ROS) bursts (**Figure S1B, S1C**). These results indicate that the absence of CBP60g and SARD1 are not sufficient to compromise canonical PTI signalling outputs but instead play a more specific and central role in PTI+ETI.

Together, these findings establish that CBP60g and SARD1 are broadly required for full ETI-mediated resistance across distinct NLR classes, while their absence leaves PTI early signaling intact. The partial loss of ETI in *gh* mutants highlights both the robustness of immune signalling and the presence of compensatory pathways that operate in parallel to CBP60g and SARD1.

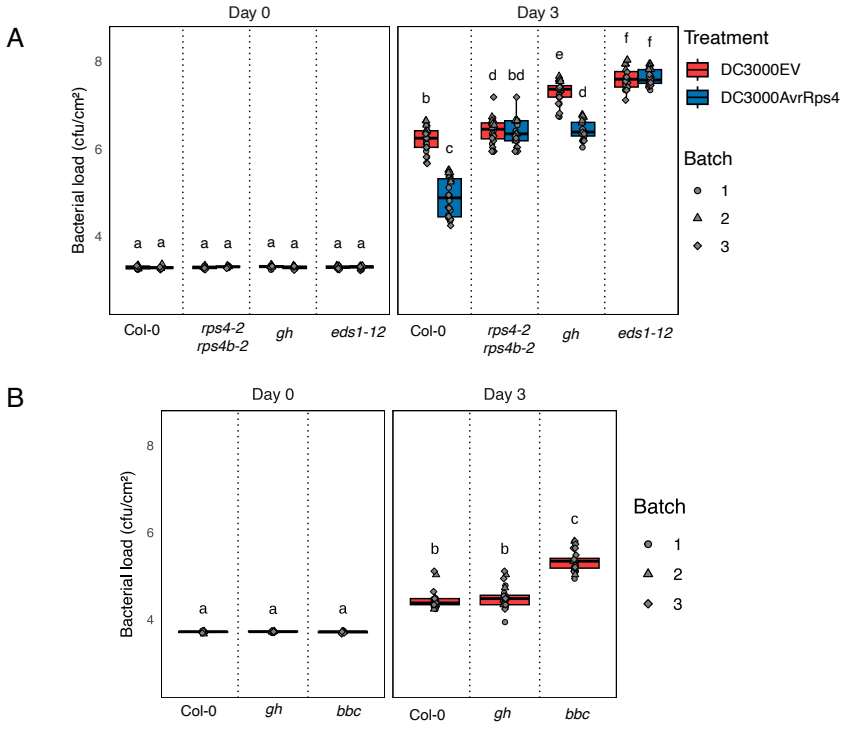

Figure 1. Contribution of CBP60g and SARD1 in PTI and ETI. A. Leaves of Col-0, *resistant to p. syringae* (*rps4-2 rps4b-2*), *enhanced disease susceptibility 1* (*eds1-12*) and *cbp60g sard1* (*gh*) were infiltrated with *Pseudomonas syringae* pv. *tomato* DC3000 carrying either an empty vector (EV) or AvrRps4. Bacterial growth was quantified as colony-forming units (CFU) at 0- and 3-days post-inoculation (dpi). Statistical differences are indicated by different letters (Tukey's honestly significant difference [HSD] test, $p \leq 0.05$). B. Col-0, *gh* (*cbp60g sard1*), and *bbc* (*bak1-5, bkk1-1, and cerk1*) plants were infiltrated with DC3000 *hrcC*$^{-}$, and bacterial titres were measured at 0 and 3 dpi. Statistical differences are denoted by different letters (Tukey's HSD test, $p \leq 0.05$).

The *sard1 cbp60g* mutant enhances ETI-induced hypersensitive cell death

The hypersensitive response (HR) is a hallmark of effector-triggered immunity (ETI), so we examined whether CBP60g and SARD1 contribute

to the regulation of ETI-associated cell death. When infiltrated with *Pseudomonas fluorescence* (Pf0-1 'EtHAn' strains) expressing AvrRps4 or AvrRpt2[28,29], *gh* mutants showed markedly stronger macroscopic HR symptoms compared with WT Col-0 (**Figure 2A**). This phenotype was corroborated by electrolyte leakage assays, which revealed significantly elevated ion leakage in *gh* relative to WT following both TNL- and CNL-mediated (AvrRps4 and AvrRpt2, respectively) recognition (**Figure 2B-D, S2A, S2B**). Enhanced HR in *gh* was evident as early as 4 hours post infiltration (hpi) and was much pronounced at 22 hpi in Col-0 or other control genotypes. These results indicate that CBP60g and SARD1 normally act to limit the amplitude of ETI-associated cell death across distinct NLR classes.

To exclude potential contributions of pattern-triggered immunity (PTI), we analysed HR phenotype in inducible ETI systems[30]. When crossed into estradiol-inducible AvrRps4 (the Super ETI or SETI line) or AvrRpt2 plants[30,31], *gh* mutants exhibited enhanced cell death upon ETI induction but not under mock conditions (**Figure 2C-E, S3A, S3B**). Moreover, when PTI and ETI were activated separately or in combination (PTI+ETI), SETI_*gh* displayed stronger cell death under both ETI and PTI+ETI compared with SETI_WT, while PTI alone induced no such enhancement (**Figure S3C**).

Thus, despite reduced pathogen resistance, *gh* plants paradoxically undergo more severe ETI-associated HR. This genetic separation of cell death from disease resistance highlights the distinct regulatory layers governing immune outputs and positions the *gh* mutant as a powerful model for dissecting how plants balance defense activation with the containment of self-damaging responses.

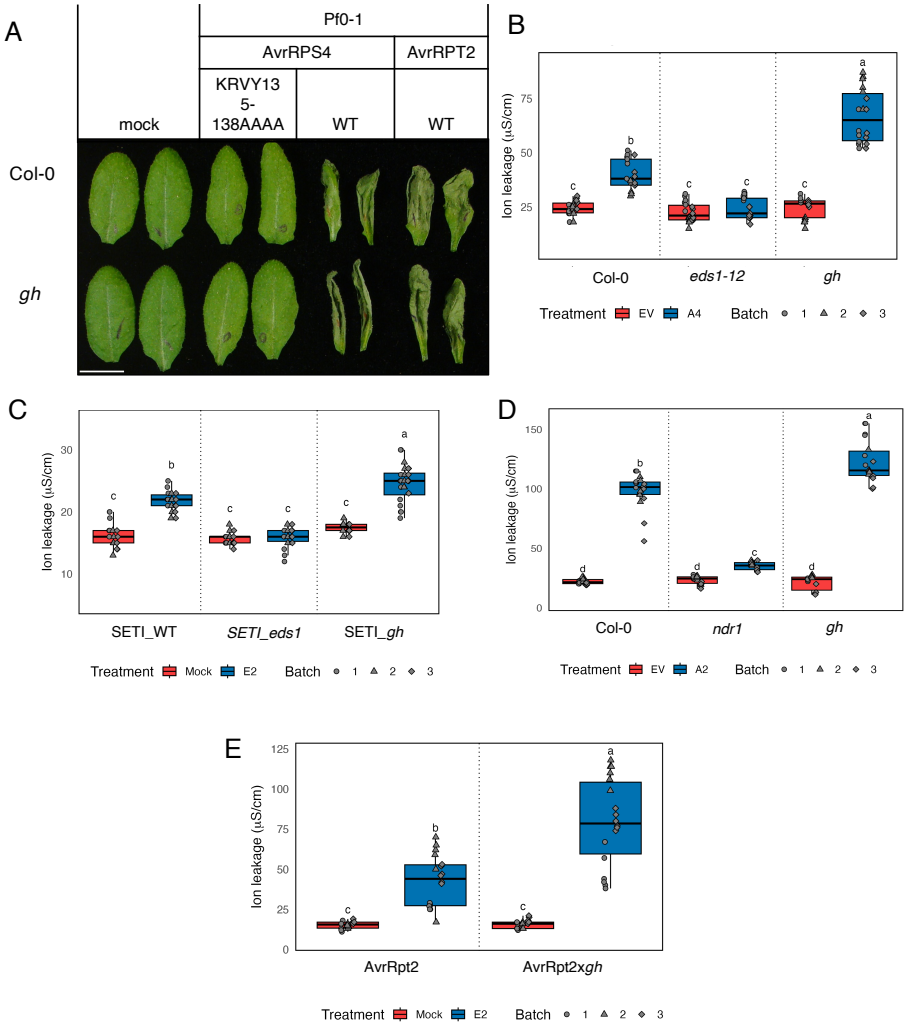

Figure 2. Role of CBP60g and SARD1 in ETI-enhanced HR. A. Leaves of the indicated genotypes were infiltrated with Pf0-1 strains expressing AvrRps4 ^{WT}, AvrRps4 $^{KRVY135–138AAAA}$, or AvrRpt2 and imaged at 1-day post-infiltration (dpi). Scale bar = 1 cm. B, C. Ion leakage assays were performed in Col-0, *enhanced disease susceptibility 1* (*eds1-12*), and *cbp60g sard1* (*gh*) infiltrated with Pf0-1 carrying an empty vector (EV) or AvrRps4 (A4) (B). Ion leakage was also measured in SETI_WT, SETI_*enhanced disease susceptibility 1* (SETI_*eds1*), and SETI_*gh* infiltrated with mock or estradiol (E2) treatment. C. Measurements

were taken 3dpi. D, E. Ion leakage assays were performed in Col-0, *non-race-specific disease resistance 1* (*ndr1*), and *gh* infiltrated with Pf0-1 carrying empty vector or AvrRpt2 (D). Ion leakage was also measured in estradiol (E2) inducible AvrRpt2 and Avrrpt2x*gh* infiltrated with mock or estradiol (E2). E. Measurements were taken 24h post-infiltration. Different letters indicate statistically significant differences (Tukey's HSD test, $p \leq 0.05$).

The *sard1 cbp60g* mutant does not enhance susceptibility to necrotrophic fungi

Necrotrophic pathogens exploit host cell death to promote infection[32,33]. Given the enhanced HR in *gh* mutants, we tested whether this would render plants more vulnerable to the necrotrophic fungus *Botrytis cinerea*. Unexpectedly, *gh* plants displayed lesion sizes comparable to WT Col-0 **(Figure 3).**

In contrast, eds5 mutants, an established SA-deficient background, showed significantly larger lesions, consistent with their increased susceptibility to *B. cinerea* (**Figure 3**). Previous work demonstrated that SA-deficient mutants, including *eds5*, undergo enhanced ETI-associated cell death and ion leakage in response to effectors such as AvrRpt2[34], which correlates with increased vulnerability to necrotrophs. Based on this precedent, we expected *gh* mutants to mirror this phenotype. Instead, *gh* mutants retained WT-like resistance to *B. cinerea* despite their stronger HR.

These findings reveal that enhanced HR in *gh* does not translate into increased susceptibility to necrotrophs, in contrast to SA-deficient backgrounds. This suggests that the cell death program in *gh* is qualitatively distinct, potentially representing a regulated immune-associated pathway that is uncoupled from the necrotrophy-promoted cell death observed in *eds5* and similar mutants.

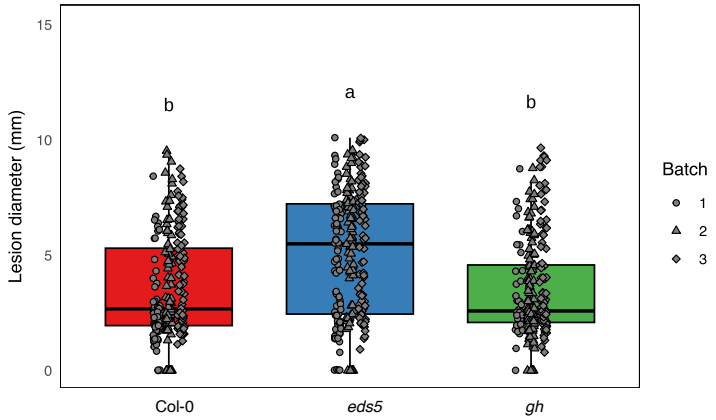

Figure 3. CBP60g and SARD1 do not contribute to resistance against the necrotrophic pathogen *Botrytis cinerea*. The indicated genotypes of Col-0, *enhanced disease susceptibility* 5 (*eds5*) and *cbp60g sard1* (*gh*) were droplet-inoculated with *B. cinerea* B05.10, and lesion diameter were measured 72-96 h post-inoculation. Different letters denote statistically significant differences (Tukey's HSD test, $p \leq 0.05$).

The *sard1 cbp60g* mutant disrupts early transcriptional responses to ETI

Early response genes (ERGs)[35,36] are rapidly induced downstream of both pattern-recognition receptors and NLRs, and many are downregulated in the *gh* double mutant. To dissect the transcriptional programs controlled by CBP60g and SARD1, we performed RNA-seq on Col-0 and *gh* plants challenged with Pf0-1 EtHAn:AvrRps4^{KRVYmutant} (PTI) and Pf0-1EtHAn:AvrRps4^{WT} (PTI+ETI)[37].

Across all conditions, we detected 12,174 differentially expressed genes (DEGs, FDR < 0.01, |$\log_2$ fold change| ≥ 1) (**Figure 4**). Hierarchical clustering grouped these DEGs into 10 major clusters (**Figure 4A**), highlighting widespread reprogramming of the immune transcriptome upon the loss of CBP60g and SARD1.

Cluster 5 was particularly notable: genes in this group were strongly induced during PTI and PTI+ETI in Col-0 but showed markedly attenuated expression in *gh* (**Figure 4**). Gene Ontology (GO) analysis revealed enrichment for defense and metabolic pathways (**Figure 5A**), including salicylic acid (SA) biosynthesis (*ICS1* and *PBS3*), N-hydroxypipecolic acid (NHP) biosynthesis (*ALD1*, *SARD4* and *FMO1*), the hypersensitive response (HR), and core immune regulators (*EDS1* and *PAD4*). Transcription factors from immunity associated families (WRKYs, ERFs and NACs) were also prominent, indicating a broad defect in immune reprogramming in the *gh* mutant.

Cluster 8 showed a similar loss of induction in *gh* and was enriched for hormone- and metabolism-related genes (**Figure 5B**), including pathways linked to ethylene (ET), jasmonic acid (JA), and abscisic acid (ABA). These data suggest that CBP60g and SARD1 not only control canonical immune regulators but also orchestrate the metabolic adjustments that accompany immune activation.

Together, these findings establish CBP60g and SARD1 as central integrators of ETI-induced transcription with some involvement in PTI-induced transcription. Their absence compromises the activation of both immune signalling and metabolic pathways, highlighting their dual role in coordinating transcriptional and physiological reprogramming during plant immunity.

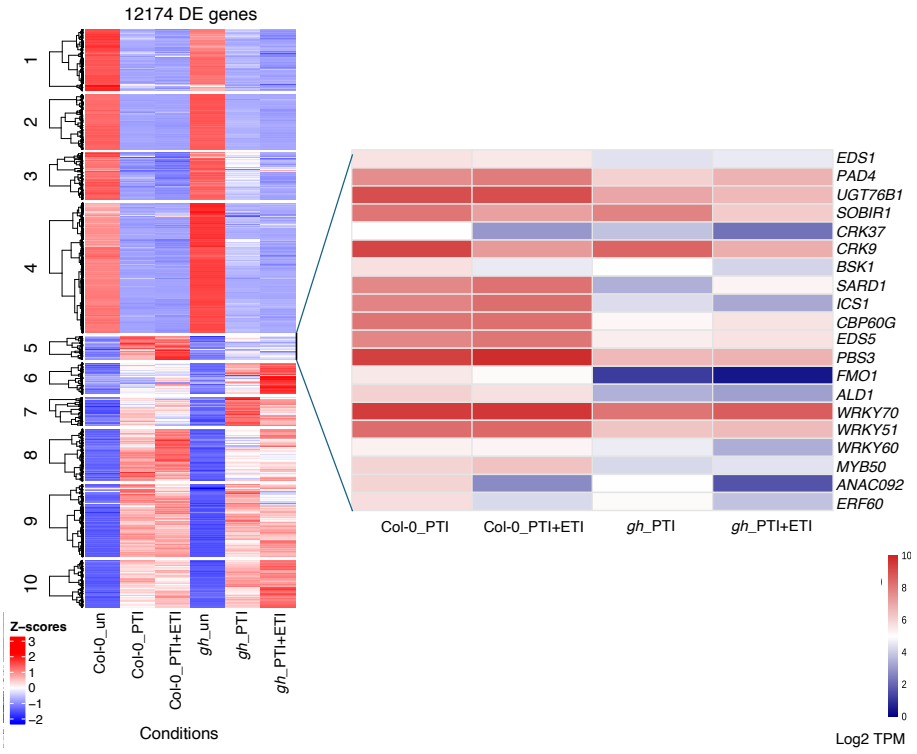

Figure 4. CBP60g/SARD1-dependent transcriptional changes during immune activation. Five- to six-week-old Col-0 and *cbp60g sard1* (*gh*) mutant plants were infiltrated with Pf0-1 carrying either an empty vector or AvrRps4. Leaf samples were collected 4 h post infiltration (hpi) for RNA-seq analysis. The left heatmap shows normalized expression (Z-score) of differentially expressed genes (false discovery rate [FDR] < 0.01; log2 fold change ≥ 1). The right heatmap highlights expression patterns of key immune genes from cluster 5 which showed compromised expression in *gh* mutants following immune activation.

Dual regulatory roles of CBP60g and SARD1 in the plant immune transcriptome

In addition to their well-established roles as positive regulators of immunity, our transcriptome-scale analysis revealed that CBP60g and SARD1 also exert negative regulatory control over specific gene modules.

Hierarchical clustering identified clusters 6 and 10, which contained genes upregulated in the *gh* mutant compared with Col-0, suggesting these genes are normally constrained by CBP60g and SARD1 (**Figure S4A, S4B, Table 1**). GO enrichment associated these clusters with defense responses, calcium signalling, cell death, and cellular organization, indicating that CBP60g and SARD1 help prevent widespread mis-regulation of physiological and cellular processes.

Importantly, these functions link CBP60g and SARD1 to the control of immune intensity and spatial localization. By repressing signalling modules closely tied to programmed cell death, CBP60g and SARD1 may prevent excessive or ectopic immune activation that could be detrimental to the host. Expression analysis further showed that several well-characterized negative regulators, including members of the Nudix hydrolase family (*NUDTs*), *BON1 ASSOCIATED PROTEIN 1* (*BAP1*), BONZAI 3 (*BON3*), and *LESION SIMULATING DISEASE 1* (*LSD1*), were significantly reduced in *gh* (**Figure S4C**). While some of these genes were previously identified as CBP60g and SARD1 binding targets[12], our results demonstrate their functional mis-regulation in the mutant background, providing a transcriptome-level view of how CBP60g and SARD1 integrate both positive and negative arms of immune regulation.

Beyond CBP60g and SARD1 dependent pathways, our data also uncovered modules that appear largely independent of these factors. Cluster 9, for instance, was only modestly affected in *gh* (**Figure 4**) and showed minimal overlap with the SARD1 ChIP-seq dataset [12], in contrast to the strong overlap observed for clusters 5 and 8 (**Figure 5C, Table 2**). Motif enrichment of cluster 9 highlighted families such as WRKY, MYB, ANAC, ETHYLENE RESPONSE FACTOR (ERF), BASIC LEUCINE ZIPPER (bZIP), and BASIC-HELIX-LOOP-HELIX (bHLH), with WRKY motifs being the most enriched (**Figure 5D, Table 3**). These findings

indicate that additional transcription factor networks operate in parallel to CBP60g and SARD1 to drive ETI-associated transcriptional reprogramming.

Together, these results support a model in which CBP60g and SARD1 function as master integrators of the immune transcriptome, coordinating both activation and repression of defense programs. At the same time, the persistence of CBP60g and SARD1independent modules underscores a layered regulatory architecture that balances robust defense activation with the containment of self-damaging responses.

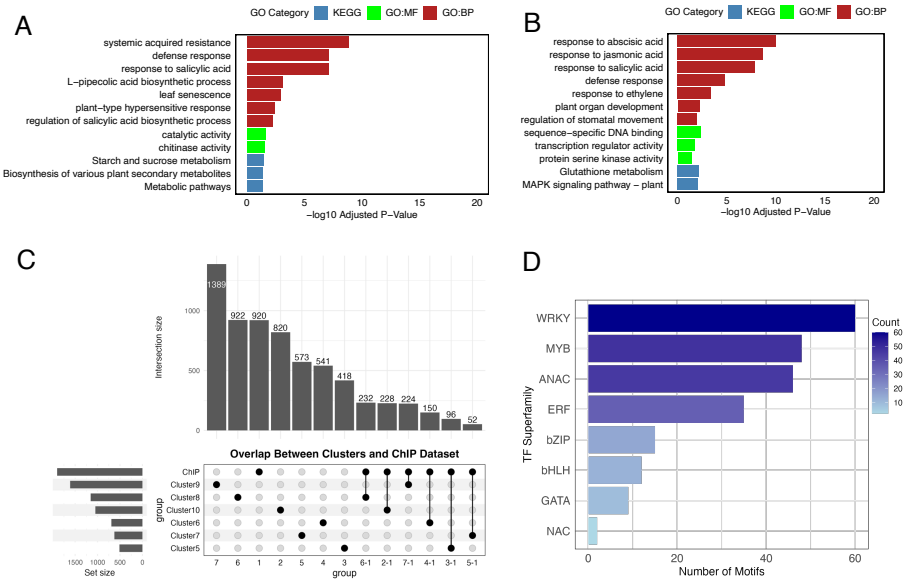

Figure 5. Functional analysis of CBP60g/SARD1-dependent and independent gene clusters.

A-B. Gene Ontology (GO) enrichment analysis of clusters 5 and 8 was performed using g:Profiler. Enriched GO terms are categorized into biological processes (GO:BP), cellular components (GO:KEGG), and molecular functions (GO:MF) (FDR ≤ 0.05, Benjamini–Hochberg correction). C. UpSet plot showing overlap of

differentially expressed genes (DEGs) from various clusters with the SARD1 ChIP-seq dataset reported by Sun et al. (2015). Cluster 9 exhibits minimal overlap with the ChIP-seq dataset. D. Bar graph depicting enrichment of transcription factor motifs in cluster 9 with representation from all major classes such as WRKYs, MYBs, ANACs, ERFs etc.

Overexpressing of *NUDT7* only partially suppresses enhanced ETI-associated HR in *cbp60g sard1* mutants

We hypothesized that the enhanced HR in *gh* plants arises from the misregulation of transcriptional repressors, leading to an imbalance between immune activation and suppression. Previous studies suggested that CBP60g and SARD1 finetune ETI in part by promoting the expression of negative regulators, including members of the Nudix hydrolase family[38]. Nudix hydrolases hydrolyse nucleoside diphosphates linked to other moieties (X), thereby maintaining nucleotide homeostasis and modulating stress responses[39]. This enzymatic activity is conserved across all domains of life, with 29 homologs identified in Arabidopsis (**Figure S4D**), underscoring their central role in cellular regulation.

To explore their contribution to ETI regulation, we profiled Nudix hydrolase family members in responses to Pf0-1 EtHAn:AvrRps4 (**Figure S4D**). Among them, *NUDT7* was the most strongly induced in Col-0 but showed markedly reduced induction in *gh* (**Figure 6A**), indicating that CBP60g and SARD1 are required for ETI-dependent transcriptional activation of this key negative regulator. Earlier findings have also pointed out *NUDT7* as negative regulator of cell death[40–42]. Consistent with these reports, more recently *NUDT7* has been shown to suppress TIR-only protein RESPONSE TO THE BACTERIAL TYPE III EFFECTOR PROTEIN HOPBA1 (RBA1)-mediated cell death in *Nicotiana benthamiana*[43], supporting its conserved role as a negative regulator of immune-associated HR.

To test whether restoring *NUDT7* expression could compensate for the loss of CBP60g and SARD1, we generated *NUDT7* overexpression (*NUDT7*^{OE}) lines in both SETI_WT and SETI_*gh* backgrounds (**Figure S5A**). Upon infiltration with Pf0-1 EtHAn_AvrRps4, *NUDT7*^{OE} plants exhibited reduced HR compared with their non-transgenic counterparts, confirming a suppressive role for *NUDT7* (**Figures 6B, S5B, S5C**). However, in the *gh* background the enhanced HR was only partially suppressed, indicating that *NUDT7* overexpression alone cannot restore immune homeostasis that is caused by the loss of CBP60g and SARD1.

These results demonstrate that although NUDT7 contributes to buffering ETI-associated cell death, the severe HR phenotype in *gh* mutants reflects broader misregulation of multiple negative immune regulators beyond NUDT7. Thus, CBP60g and SARD1 act at the network level to balance immune activation with transcriptional repression, and loss of this dual control cannot be compensated by a single negative regulator.

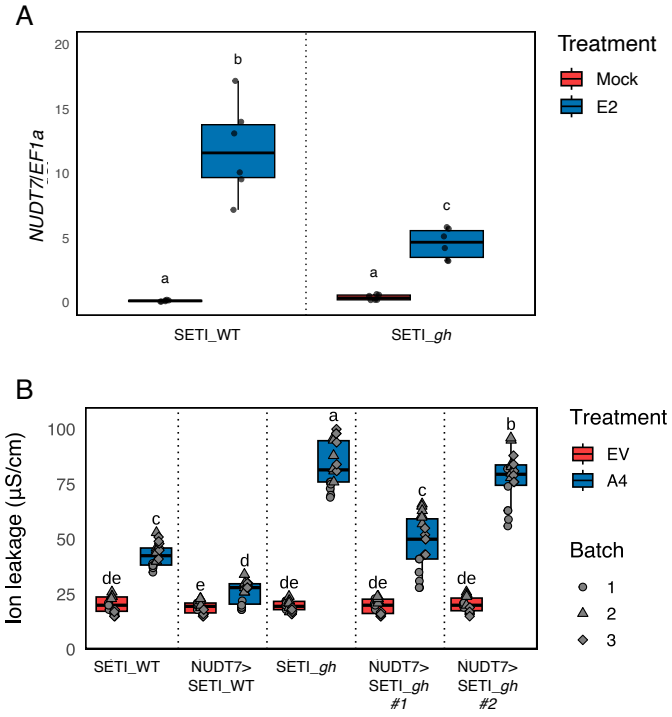

Figure 6. Contribution of NUDT7 to ETI-induced cell death. A. Five-week-old SETI_WT and SETI_*gh* plants were infiltrated with mock or 50 µM estradiol (E2). Samples were collected 4 h post infiltration (hpi) for RNA extraction and qPCR analysis. *NUDT7* expression levels are shown relative to *EF1α*. Different letters indicate significant differences (Tukey's HSD test, $p \leq 0.05$). B. Ion leakage assays of the indicated genotypes infiltrated with Pf0-1 carrying either an empty vector (EV) or AvrRps4 (A4). Measurements were taken 24 hpi. Statistical differences are denoted by different letters (Tukey's HSD test, $p \leq 0.05$).

Discussion

CBP60g and SARD1 are widely recognized as transcriptional activators of plant immunity, acting upstream of SA biosynthesis and systemic signalling. Here, we show that their contribution extends across both TNL- and CNL-mediated ETI, as *cbp60g sard1* (*gh*) double mutants displayed reduced resistance to bacterial carrying AvrRps4 and AvrRpt2. Notably,

while SARD1 directly binds to promoters of *EDS1* and *PAD4*, both of which encode central components of TNL signalling, it does not bind to *NDR1*, encoding the CNL adaptor, and *NDR1* expression is unchanged in *gh* compared to the WT. The observation that both pathways are equally compromised suggests that CBP60g/SARD1 also regulate shared downstream immune modules that act as convergence points between NLR classes, in addition to their established role in SA biosynthesis.

Although CBP60g and SARD1 bind promoters of PTI-associated genes and are transcriptionally induced upon PAMP treatment, *gh* mutants did not exhibit altered resistance against the *hrcC*$^{-}$ mutant, which elicits canonical PTI. These findings argue that CBP60g and SARD1 are not essential for baseline PTI outputs. Instead, they likely function as transcriptional hubs that bridge PTI and ETI, enabling mutual potentiation of these two immune layers. This is consistent with our SETI-based transcriptomic profiling, which indicates that CBP60g and SARD1 control early immune gene reprogramming in an ETI-specific context.

One of the most striking features of the *gh* mutant is its exaggerated hypersensitive response (HR) upon ETI activation, despite reduced resistance. This phenotype sharply contrasts with most previously characterized HR regulators, which often show constitutive defense activation, pleiotropic developmental defects, or spontaneous lesion formation. Unlike *dnd1*, *hlm1*, or *lsd1*, *gh* plants grow normally and lack constitutive immunity, making them a valuable genetic model to uncouple cell death from resistance. Interestingly, while *eds5* mutants (also SA-deficient) exhibit enhanced susceptibility to the necrotrophic pathogen *Botrytis cinerea, gh* plants do not, despite comparable reductions in SA accumulation and enhanced HR[8,44]. This suggests that HR in *gh* is qualitatively distinct from that in other SA-deficient mutants and may not be exploited by necrotrophs.

Transcriptomic profiling revealed that CBP60g and SARD1 exert both positive and negative transcriptional control directly or indirectly. Clusters 5 and 8, strongly induced in Col-0 but attenuated in *gh*, included genes required for SA and NHP biosynthesis (*ICS1, PBS3, ALD1, FMO1, SARD4*), the *EDS1/PAD4* module, and numerous defense-related transcription factors, corresponding closely to known CBP60g and SARD1 binding targets. By contrast, clusters 6 and 10 were upregulated in *gh* and enriched for genes involved in Ca^{2+} signalling, cellular organization, and cell death execution, indicating that CBP60g and SARD1 normally constrain HR-promoting programs. Cluster 9, which was minimally affected in *gh* and showed little overlap with SARD1 ChIP targets, was enriched for WRKY, MYB, ANAC, ERF, bZIP, and bHLH motifs, suggesting CBP60g and SARD1 independent transcriptional programs that sustain residual ETI. Together, these findings support a model in which CBP60g and SARD1 function as dual regulators, promoting defense gene activation while simultaneously restraining runaway cell death, such that their absence both weakens essential defense modules and releases repression on HR-associated pathways, producing the paradoxical phenotype of reduced resistance but enhanced HR.

We further tested this model by examining Nudix hydrolases, a family of nucleotide-metabolizing enzymes implicated in immune homeostasis. Among them, *NUDT7* was strongly induced upon ETI in Col-0 but showed markedly reduced expression in *gh*. Overexpression of *NUDT7* suppressed HR in both WT and *gh* backgrounds, but could not fully restore homeostasis in *gh*, demonstrating that loss of CBP60g and SARD1 disrupts multiple layers of negative regulation. This highlights that immune homeostasis depends on a combinatorial network of repressors, rather than on individual factors alone.

Our results broaden the view of CBP60g and SARD1 from SA-dependent activators to network-level integrators that balance immune activation and suppression. The exaggerated HR yet reduced resistance of *gh* mutants reveal that these two immune outputs, which can be associated in some contexts, can also be genetically and mechanistically separated. Similar uncoupling between hypersensitive cell death and disease resistance has been reported previously. For example, RRS1/RPS4- and RPP1-mediated immunity can confer effective resistance in the absence of AvrRps4-induced HR, and genetic analyses have shown that cell death and resistance can originate from distinct signalling routes downstream of TIR-NLR activation[45]. Consistent with these observations at a broader scale, [46]showed that a majority of ETI-eliciting effectors across the *Pseudomonas syringae* pan-genome trigger effective defense without inducing macroscopic HR, demonstrating that HR is not an obligatory output of ETI in Arabidopsis. Future studies combining high-resolution temporal profiling, network modelling, and metabolomic analyses will be critical to identify upstream signals and downstream executioners of this atypical (independent of resistance) HR. More broadly, the dual roles of CBP60g and SARD1 underscore how plants achieve robust pathogen defense while minimizing self-inflicted damage, a principle of immune regulation with both mechanistic and translational significance.

Acknowledgments

HC and PD acknowledge European Research Council Starting Grant “R-ELEVATION” (grant agreement: 101039824). JDGJ was supported by the Gatsby Charitable Foundation (UK).

Competing interests

The authors declare no competing interests.

Author contributions

PD conceptualized and oversaw the inception of the research project. The experimental work was collaboratively conducted by HC, H-JS, and BPMN. Data analysis and figure generation were performed by HC and PD. JDGJ was involved throughout the project, providing valuable discussions that significantly shaped the research HC and PD wrote the initial manuscript draft. All co-authors contributed to subsequent revisions. The final manuscript was prepared by HC and PD and was approved for submission by all authors.

Data and code availability

- The RNA-seq data for this study have been deposited in the European Nucleotide Archive (ENA) at EMBL-EBI under EMBL-EBI: PRJEB34958.
- All codes are available via GitHub: https://github.com/chhilla/HR_gh

Materials and Methods

Plant material and growth conditions

Arabidopsis thaliana accessions Col-0 and a β-estradiol (E2) inducible Super-ETI line (SETI_WT), were used as the wild-type controls in this study. Mutants of *eds1-2*, eds1-12, *sard1-1 cbp60g-1* that were used in this study have been previously described[8,47,48]. Mutants of *eds1-2* and *sard1-1 cbp60g-1* were crossed with SETI_wt to generate SETI_*eds1-2* and SETI_*gh* plants respectively. NUDT7^{OE} overexpression plants in different genetic backgrounds were generated by transforming *AtRBCS1A::gDNANUDT7*-mEGFP-tHSP18.2 construct generated through In-fusion cloning into the SETI_WT and SETI_*gh* plants. Plants were grown at 21°C under long-day conditions (16 h light, 8 h dark), and at 50% humidity.

Bacterial strains and growth conditions

Pseudomonas syringae pv. tomato (*Pst*) DC3000 EV (carrying empty vector) grown on the King's B medium plates containing 25 μg mL^{-1} rifampicin, and 50 μg mL^{-1} kanamycin and *Pst* DC3000 *hrcC*$^{-}$ were grown on the King's B medium plates containing 25 μg mL^{-1} rifampicin. *Pseudomonas fluorescens* engineered with a Type III secretion system (Pf0-1 'EtHAn' strains) expressing empty vector or AvrRpt2 was grown on the King's B medium plates with 50 μg mL^{-1} kanamycin, 34 μg mL^{-1} Chloramphenicol and 5 μg mL^{-1} tetracycline. *Pseudomonas fluorescens* engineered with a Type III secretion system (Pf0-1 'EtHAn' strains) expressing AvrRps4 was grown on the King's B medium plates with 10 μg mL^{-1} Gentamycin, 34 μg mL^{-1} Chloramphenicol and 5 μg mL^{-1} tetracycline. All the Pseudomonas strains were grown on plates at 28°C for 2 days for further inoculum preparation.

Hypersensitive cell death response phenotyping in Arabidopsis

Pseudomonas fluorescens engineered with a Type III secretion system (Pf0-1 'EtHAn' strains) expressing one of the effectors (AvrRps4 or AvrRpt2), or pVSP61 empty vector were grown on selective KB plates for 24 h at 28 °C[28,36]. Bacteria were harvested from the plates, resuspended in infiltration buffer (10 mM $MgCl_2$), and the concentration was adjusted to OD600=0.2 (108 CFU mL^{-1}). The abaxial surfaces of 5-week-old Arabidopsis leaves were hand infiltrated with a 1 mL needleless syringe. Cell death was monitored 3dpi after infiltration.

Electrolyte leakage assay

Two leaves of 5-week-old *Arabidopsis* plants were hand infiltrated using a 1-mL needleless syringe with 50 μM E2 dissolved in Milli-Q water or Pf0-1 'EtHAn' strain carrying AvrRps4 or AvrRpt2 dissolved in 10mM $MgCl_2$ (OD_{600}=0.2). DMSO in Milli-Q water or 10mM $MgCl_2$ was used as mock treatment. Leaf discs were collected with a 7-mm diameter cork borer from

infiltrated leaves on paper towels. Leaf discs were dried and transferred into 2 mL of deionised water in 12-well plates (2 leaf disks per well. The plate was incubated for 30 min in a growth chamber with controlled conditions at 21°C under long-day conditions (16-h light/8-h dark) with a light intensity of 120-150 µmol m^{-2}. The water was replaced after incubation with 2 mL of deionised water. Electrolyte leakage was measured with Pocket Water Quality Meters (LAQUAtwin-EC-33; Horiba) calibrated at 1.41 mS/cm. Around 100 µL of the sample was used to measure conductivity at the indicated time points. ANOVA (p-value ≤ 0.05) was used for identifying significant factors. Tukey-HSD-Test ($p \leq 0.05$) was used to determine differences between treatment and lines. A detailed statistical summary is available on GitHub: https://github.com/chhilla/HR_gh.

Bacterial growth assay

Pseudomonas syringae pv. tomato (*Pst*) strain DC3000 carrying pVSP61 empty vector or AvrRps4 and *Pst* DC3000 *hrcC*$^{-}$ was grown on selective King's B (KB) medium plates. Bacteria were harvested from the plates, resuspended in infiltration buffer (10 mM $MgCl_2$), and the concentration was adjusted to an optical density of 0.001 at 600 nm [OD_{600}=0.001, representing ~5×10^5 colony-forming units (CFU) mL^{-1}]. Bacteria were infiltrated into abaxial surfaces of 5-week-old Arabidopsis leaves with a 1 mL needleless syringe. For quantification, leaf samples were harvested with a 6 mm diameter cork borer (Z165220; Merck-Sigma-Aldrich), resulting in leaf discs with an area of 0.283 cm^2. Two leaf discs per leaf were harvested as a single sample. For each condition, four samples were collected immediately after infiltration as 'day 0' samples to ensure no significant difference introduced by unequal infiltrations, and six samples were collected at 3 dpi as 'day 3' samples to compare the bacterial growth between different genotypes, conditions, and treatments. For 'day 0',

samples were ground in 200 µL of infiltration buffer and spotted (10 µL per spot) on selective KB medium agar plates to grow for 48 h at 28 °C. For 'day 3', samples were ground in 200 µL of infiltration buffer, serially diluted (5, 50, 500, 5000, and 50 000 times), and spotted (6 µL per spot) on selective KB medium agar plates to grow for 48 h at 28 °C. The number of colonies (CFU per drop) was monitored, and bacterial growth was represented as CFU cm^{-2} of leaf tissue. All results are plotted using ggplot2 in R[49], ANOVA (p-value ≤ 0.05) was used for identifying significant factors. Tukey-HSD-Test (p-value ≤ 0.05) was used to determine differences between treatment and lines. A detailed statistical summary is available on GitHub: https://github.com/chhilla/HR_gh.

Lesion diameter measurement

B. cinerea strain B05.10 was grown as described previously[50] and used for inoculations as described by[51]. Arabidopsis wild type and mutant plants were droplet inoculated with *B. cinerea* at 2.5×10^5 spores/mL in 5 µL of 6 g/L potato dextrose broth, and lesion diameter was measured after 72-96 h. ANOVA (p-value ≤ 0.05) was used for identifying significant factors. Tukey-HSD-Test (p-value ≤ 0.05) was used to determine differences between treatment and lines. A detailed statistical summary is available on GitHub: https://github.com/chhilla/HR_gh.

ROS burst assay

Leaf discs (6 mm diameter) were collected from 5-week-old plants using a cork borer and placed abaxial side down in 96-well plates containing 200 µL of deionized water. Plates were incubated overnight in the dark. The following day, 200 µL of a reaction mixture containing 20 mM luminol (Sigma-Aldrich, A8511), 0.02 mg mL^{-1} horseradish peroxidase (Sigma-Aldrich, P6782), and 100 nM flg22 was added to each well. Reactive oxygen species (ROS) production was quantified using TECAN microplate reader. ANOVA (p-value ≤ 0.05) was used for identifying

significant factors. Tukey-HSD-Test (p-value ≤ 0.05) was used to determine differences between treatment and lines. A detailed statistical summary is available on GitHub: https://github.com/chhilla/HR_gh.

Reverse transcription-quantitative PCR (RT-qPCR) for measuring relative gene expression

For gene expression analysis, RNA was isolated from 5-week-old Arabidopsis leaves and used for subsequent RT–qPCR analysis. RNA was extracted with a VeZol-pure total RNA isolation Kit (RC202-01; Vazyme) and treated with RNase-free DNase (4716728001; Merck-Roche). Reverse transcription was carried out using HiScript III all-in-one RT SuperMix (R333-01; Vazyme). qPCR was performed using a CFX96 Touch™ Real-Time PCR Detection System. Primers for qPCR analysis of *NUDT7* are (F:5'-CTTGCAAGCTAAGTGGATGC-3'; R: 5'-GCGATACTTTAAGGCGCTTG-3')[12]. The elongation factor 1α (EF1α) primers (F: 5'-CAGGCTGATTGTGCTGTTCTTA-3'; R: 5'-GTTGTATCCGACCTTCTTCAGG-3') were used as an internal control. Data were analysed using the double delta Ct method[52]. All results are plotted using ggplot2 in R. A detailed statistical summary is available on GitHub: https://github.com/chhilla/HR_gh.

RNA-seq raw data processing, alignment, quantification of expression, and data visualization

Pseudomonas fluorescens engineered with a Type III secretion system (Pf0-1 'EtHAn' strains) expressing AvrRps4 and AvrRps4KRVY135-138AAAA was infiltrated in 5- to 6-week-old *cbp60g sard1* double mutant *and* wild-type (Col-0) Arabidopsis leaves using a 1 mL needleless syringe. For RNA-seq analysis, two leaves per plant were collected at 4 hours post infiltration (hpi) as one biological replicate. Untreated samples were included as controls. Total RNA was extracted from three biological replicates using the Zymo RNA extraction kit.

The RNA sample was sequenced by Novogene. Raw reads were trimmed into 390 bp clean reads by the Novogene bioinformatics service. At least 12 million paired-end clean reads for each sample were provided by Novogene for RNA-seq analysis. All reads passed FastQC before the following analyses. All clean reads were mapped to a comprehensive Reference Transcript Dataset for Arabidopsis Quantification of Alternatively Spliced Isoforms (AtRTD2_QUASI) containing 82,190 non-redundant transcripts from 34,212 genes via Galaxy and Salmon tools[53,54]. The estimated gene transcript counts were used for differential gene expression analysis and statistical analysis with the 3D RNA-seq software[55]. The low-expressed transcripts were filtered if they did not meet the criteria of ≥3 samples with ≥1 count per million reads. The batch effects between three biological replicates were removed to reduce artificial variance with the RUVSeq method[56]. The expression data were normalised across samples with the TMM (weighted trimmed mean of M-values)[57]. The significance of expression changes in the contrasting groups 'Col-0_kv vs. Col-0_un, groups 'Col-0_a4 vs. Col-0_un', '*gh*_kv vs. *gh*_un' and '*gh*_a4 vs. *gh*_un' were determined by the limma-voom method[58,59]. A gene was defined as a significant differentially expressed gene (DEG) if it had a Benjamini–Hochberg adjusted *p*-value <0.01 and log2[fold change (FC)] ≥ 1 (upregulated) or log2[fold change (FC)] ≤ −1 (downregulated). The GO term analysis was analysed with g:Profiler[60]. Enrichment analysis of transcription factor motifs in the promoters of genes of interest was performed using the AME tool from the MEME Suite[61,62].

Quantification and statistical analysis

All quantitative and statistical analyses were performed using R (version 4.3.1). Data visualization, including boxplots and bar plots, was carried out using the ggplot2 package. Details of the statistical tests applied and

significance thresholds are provided in the corresponding figure legends. RNA-sequencing data were processed and analyzed as described in the RNA-seq analysis section above.

Supplementary Information

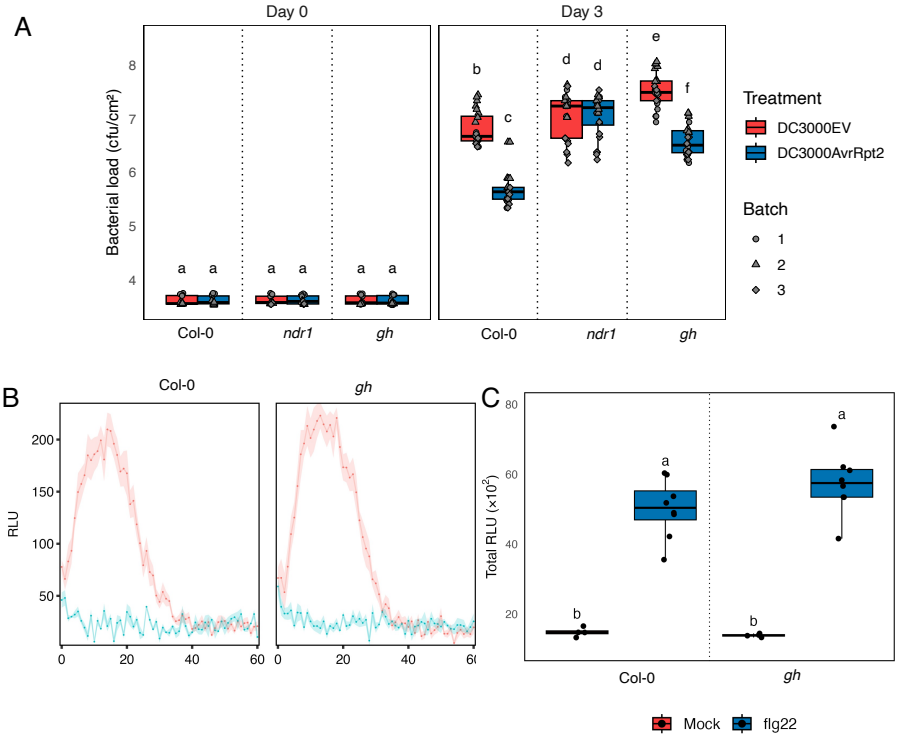

Figure S1. Contribution of CBP60g and SARD1 in PTI and ETI. A. Leaves of Col-0 and the indicated mutant genotypes, *non-race specific disease resistance 1* (*ndr1*) and *cbp60g sard1* (*gh*) were infiltrated with *Pseudomonas syringae* pv. *tomato* DC3000 carrying either an empty vector (EV) or AvrRpt2. Bacterial growth was quantified as colony-forming units (CFU) at 0- and 3-days post-inoculation (dpi). Each data point

represents two pooled leaves from a single plant. Black lines indicate mean values of technical replicates. Statistical differences are indicated by different letters (Tukey's honestly significant difference [HSD] test, p ≤ 0.05). B. Col-0 and *gh* were treated with mock or flg22 and ROS burst is measured. Statistical differences are denoted by different letters (Tukey's HSD test, p ≤ 0.05). C. Total RLU counts in Col-0 and *gh* plants. Statistical differences are denoted by different letters (Tukey's HSD test, $p \leq 0.05$).

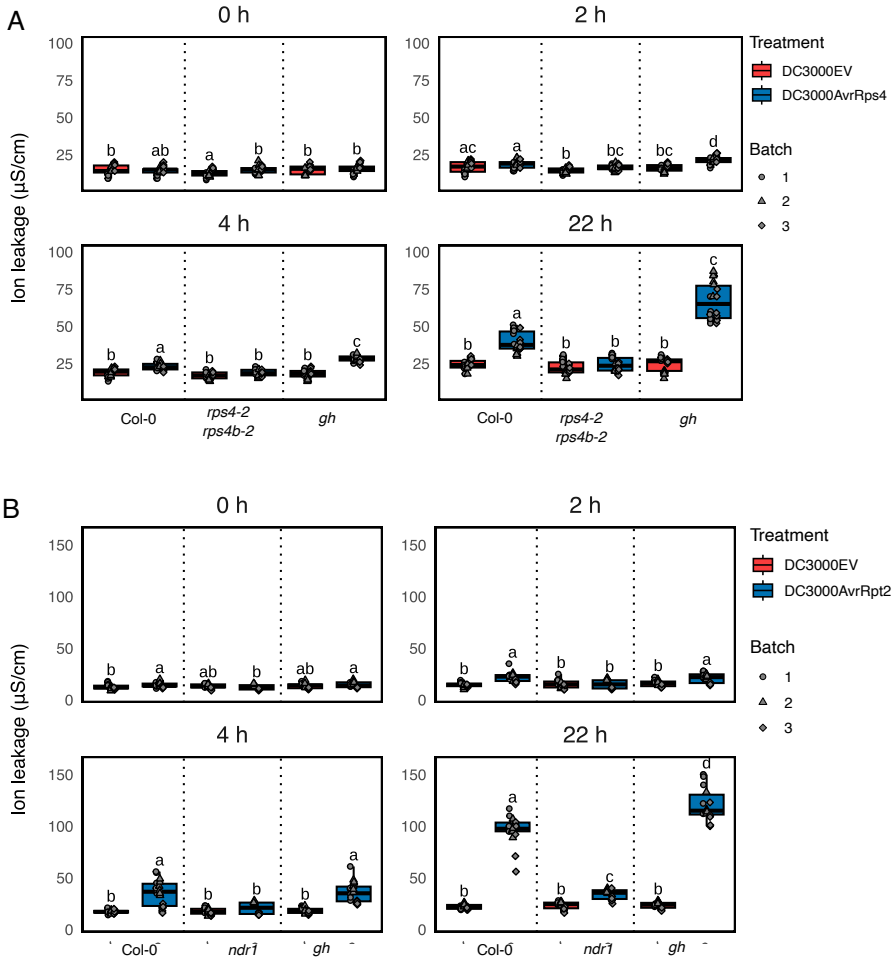

Figure S2. Loss of CBP60g and SARD1 enhances ETIAvrRps4-induced HR. A-B. Ion leakage in indicated mutants infiltrated with *Pseudomonas syringae* DC3000 (empty vector or AvrRps4) and (empty vector or AvrRpt2) measured at interval of 0-22 h post-infiltration. Mutants shown the mutants analysed were *rps4-2 rps4b-2* and *gh* in (A), and *non-ndr1* and *gh* in (B). Different letters indicate statistical significance (Tukey's HSD test, $p \leq 0.05$).

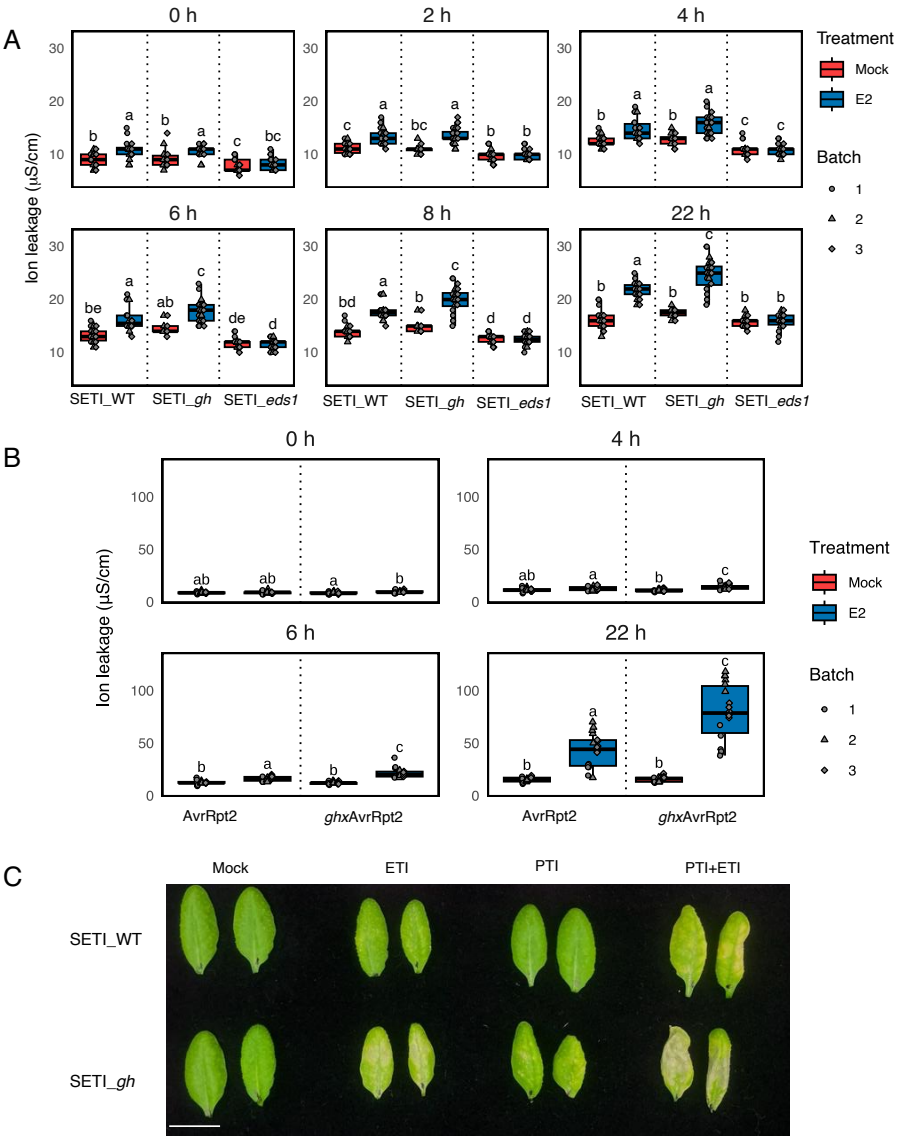

Figure S3. Loss of CBP60g and SARD1 enhances ETI-induced hypersensitive response (HR). A-B. Ion leakage measurements of SETI_WT, SETI_*gh* and SETI_*eds1* infiltrated with mock or estradiol (E2) at the specified time points. Different letters indicate statistically significant differences (Tukey's HSD test, $p \leq 0.05$). C. HR phenotypes of SETI_WT

and SETI_*gh* plants infiltrated with mock, E2 (ETI), DC3000 *hrcC*⁻ (PTI), or PTI+ETI treatments, photographed 3 days post-infiltration. Scale bar = 1 cm.

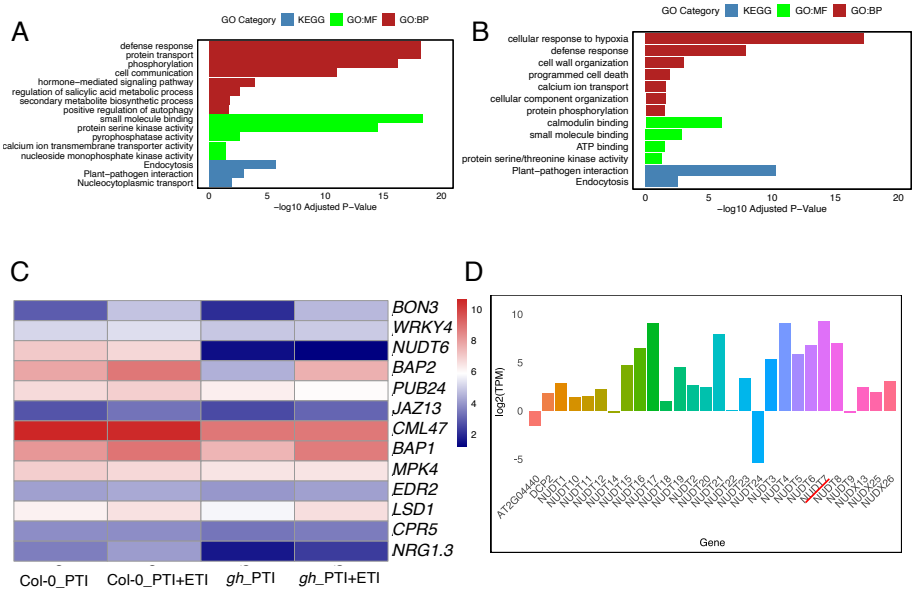

Figure S4. Negative regulation of immune components by CBP60g and SARD1. A-B. GO enrichment analysis of clusters 6 and 10 using g:Profiler, categorized into biological process (GO:BP), cellular component (GO:KEGG), and molecular function (GO:MF) terms (FDR ≤ 0.05, Benjamini–Hochberg correction). C. Heatmap showing expression (Log2TPM) of representative negative immune regulators in WT and *cbp60g sard1* (*gh*) during (PTI) and PTI+ETI. D. Expression profiles of NUDT family members following PTI+ETI treatment. Nudix7 is highlighted with red line.

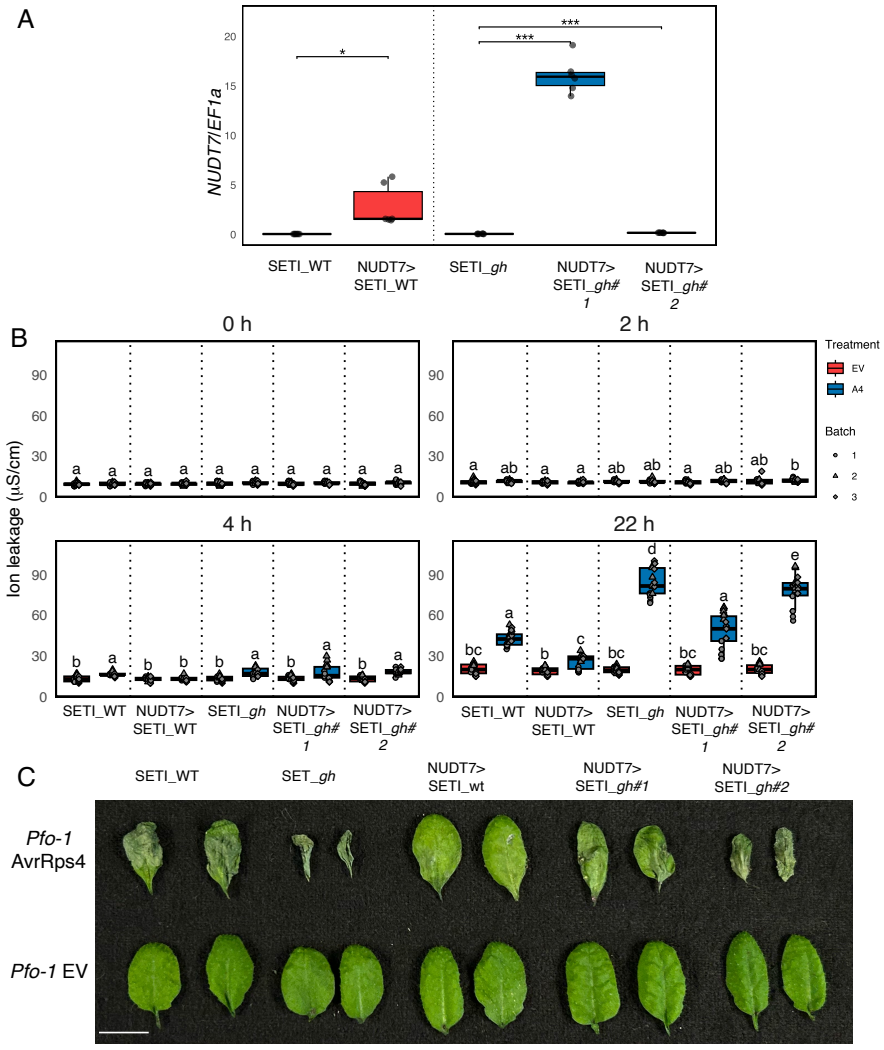

Figure S5. NUDT7 overexpression cannot fully rescue enhanced HR in *cbp60g sard1*. A. Leaves from Five-week-old plants of SETI_WT, SETI_*gh* along with the overexpression lines of NUDT7 in SETI_WT and SETI_*gh* background were harvested for RNA extraction and qPCR. *NUDT7* expression levels are shown relative to *EF1α.* Scale bar = 1 cm. Asterisk indicate significant difference (t-test, $p \leq 0.05$). (#1 and #2 independent lines). B. Ion leakage in indicated mutants infiltrated with

Pseudomonas syringae DC3000 (empty vector or AvrRps4) measured at 0-22 h post-infiltration. Different letters indicate statistical significance (Tukey's HSD test, $p \leq 0.05$). C. HR phenotypes of indicated genotypes infiltrated with *Pf0-1* carrying empty vector or AvrRps4 at 3 days post-infiltration.

Supplemental tables can be accessed online at (https://doi.org/10.1101/2025.06.28.662111).

References

1. Yates, P.L. (1946). Food and agriculture organization of the united nations. Journal of Farm Economics *28*, 54. 10.2307/1232585.

2. Ngou, B.P.M., Jones, J.D.G., and Ding, P. (2022). Plant immune networks. Trends Plant Sci. *27*, 255–273. 10.1016/j.tplants.2021.08.012.

3. Ngou, B.P.M., Ding, P., and Jones, J.D.G. (2022). Thirty years of resistance: Zig-zag through the plant immune system. Plant Cell *34*, 1447–1478. 10.1093/plcell/koac041.

4. Tsuda, K., and Somssich, I.E. (2015). Transcriptional networks in plant immunity. New Phytol. *206*, 932–947. 10.1111/nph.13286.

5. Köster, P., DeFalco, T.A., and Zipfel, C. (2022). Ca2+ signals in plant immunity. EMBO J. *41*, e110741. 10.15252/embj.2022110741.

6. Jiang, Y., and Ding, P. (2023). Calcium signaling in plant immunity: a spatiotemporally controlled symphony. Trends Plant Sci. *28*, 74–89. 10.1016/j.tplants.2022.11.001.

7. Ding, P., and Redkar, A. (2018). Pathogens suppress host transcription factors for rampant proliferation. Trends Plant Sci. *23*, 950–953. 10.1016/j.tplants.2018.08.010.

8. Zhang, Y., Xu, S., Ding, P., Wang, D., Cheng, Y.T., He, J., Gao, M., Xu, F., Li, Y., Zhu, Z., et al. (2010). Control of salicylic acid synthesis and systemic acquired resistance by two members of a

plant-specific family of transcription factors. Proc Natl Acad Sci USA *107*, 18220–18225. 10.1073/pnas.1005225107.

9. Wang, L., Tsuda, K., Truman, W., Sato, M., Nguyen, L.V., Katagiri, F., and Glazebrook, J. (2011). CBP60g and SARD1 play partially redundant critical roles in salicylic acid signaling. Plant J. *67*, 1029–1041. 10.1111/j.1365-313X.2011.04655.x.

10. Truman, W., and Glazebrook, J. (2012). Co-expression analysis identifies putative targets for CBP60g and SARD1 regulation. BMC Plant Biol. *12*, 216. 10.1186/1471-2229-12-216.

11. Truman, W., Sreekanta, S., Lu, Y., Bethke, G., Tsuda, K., Katagiri, F., and Glazebrook, J. (2013). The CALMODULIN-BINDING PROTEIN60 family includes both negative and positive regulators of plant immunity. Plant Physiol. *163*, 1741–1751. 10.1104/pp.113.227108.

12. Sun, T., Zhang, Y., Li, Y., Zhang, Q., Ding, Y., and Zhang, Y. (2015). ChIP-seq reveals broad roles of SARD1 and CBP60g in regulating plant immunity. Nat. Commun. *6*, 10159. 10.1038/ncomms10159.

13. Thordal-Christensen, H. (2020). A holistic view on plant effector-triggered immunity presented as an iceberg model. Cell. Mol. Life Sci. *77*, 3963–3976. 10.1007/s00018-020-03515-w.

14. Balint-Kurti, P. (2019). The plant hypersensitive response: concepts, control and consequences. Mol. Plant Pathol. *20*, 1163–1178. 10.1111/mpp.12821.

15. Künstler, A., Bacsó, R., Gullner, G., Hafez, Y.M., and Király, L. (2016). Staying alive – is cell death dispensable for plant disease resistance during the hypersensitive response? Physiological and Molecular Plant Pathology *93*, 75–84. 10.1016/j.pmpp.2016.01.003.

16. Yu, G.X., Braun, E., and Wise, R.P. (2001). Rds and Rih mediate hypersensitive cell death independent of gene-for-gene resistance to the oat crown rust pathogen Puccinia coronata f. sp. avenae. Mol. Plant Microbe Interact. *14*, 1376–1383. 10.1094/MPMI.2001.14.12.1376.

17. Coll, N.S., Epple, P., and Dangl, J.L. (2011). Programmed cell death in the plant immune system. Cell Death Differ. *18*, 1247–1256. 10.1038/cdd.2011.37.

18. Coll, N.S., Vercammen, D., Smidler, A., Clover, C., Van Breusegem, F., Dangl, J.L., and Epple, P. (2010). Arabidopsis type I metacaspases control cell death. Science *330*, 1393–1397. 10.1126/science.1194980.

19. Yu, I.C., Parker, J., and Bent, A.F. (1998). Gene-for-gene disease resistance without the hypersensitive response in Arabidopsis dnd1 mutant. Proc Natl Acad Sci USA *95*, 7819–7824. 10.1073/pnas.95.13.7819.

20. Balagué, C., Lin, B., Alcon, C., Flottes, G., Malmström, S., Köhler, C., Neuhaus, G., Pelletier, G., Gaymard, F., and Roby, D. (2003). HLM1, an essential signaling component in the hypersensitive response, is a member of the cyclic nucleotide-gated channel ion channel family. Plant Cell *15*, 365–379. 10.1105/tpc.006999.

21. Lorrain, S., Vailleau, F., Balagué, C., and Roby, D. (2003). Lesion mimic mutants: keys for deciphering cell death and defense pathways in plants? Trends Plant Sci. *8*, 263–271. 10.1016/S1360-1385(03)00108-0.

22. Greenberg, J.T., and Yao, N. (2004). The role and regulation of programmed cell death in plant-pathogen interactions. Cell. Microbiol. *6*, 201–211. 10.1111/j.1462-5822.2004.00361.x.

23. Narusaka, M., Shirasu, K., Noutoshi, Y., Kubo, Y., Shiraishi, T., Iwabuchi, M., and Narusaka, Y. (2009). RRS1 and RPS4 provide a dual Resistance-gene system against fungal and bacterial pathogens. Plant J. *60*, 218–226. 10.1111/j.1365-313X.2009.03949.x.

24. Saucet, S.B., Ma, Y., Sarris, P.F., Furzer, O.J., Sohn, K.H., and Jones, J.D.G. (2015). Two linked pairs of Arabidopsis TNL resistance genes independently confer recognition of bacterial effector AvrRps4. Nat. Commun. *6*, 6338. 10.1038/ncomms7338.

25. Kunkel, B.N., Bent, A.F., Dahlbeck, D., Innes, R.W., and Staskawicz, B.J. (1993). RPS2, an Arabidopsis disease resistance locus specifying recognition of Pseudomonas syringae strains expressing the avirulence gene avrRpt2. Plant Cell *5*, 865–875. 10.1105/tpc.5.8.865.

26. Axtell, M.J., and Staskawicz, B.J. (2003). Initiation of RPS2-specified disease resistance in Arabidopsis is coupled to the AvrRpt2-directed elimination of RIN4. Cell *112*, 369–377. 10.1016/s0092-8674(03)00036-9.

27. Huang, W., Wang, Y., Li, X., and Zhang, Y. (2020). Biosynthesis and Regulation of Salicylic Acid and N-Hydroxypipecolic Acid in Plant Immunity. Mol. Plant *13*, 31–41. 10.1016/j.molp.2019.12.008.

28. Thomas, W.J., Thireault, C.A., Kimbrel, J.A., and Chang, J.H. (2009). Recombineering and stable integration of the Pseudomonas syringae pv. syringae 61 hrp/hrc cluster into the genome of the soil bacterium Pseudomonas fluorescens Pf0-1. Plant J. *60*, 919–928. 10.1111/j.1365-313X.2009.03998.x.

29. Sohn, K.H., Hughes, R.K., Piquerez, S.J., Jones, J.D.G., and Banfield, M.J. (2012). Distinct regions of the Pseudomonas syringae coiled-coil effector AvrRps4 are required for activation of immunity. Proc Natl Acad Sci USA *109*, 16371–16376. 10.1073/pnas.1212332109.

30. McNellis, T.W., Mudgett, M.B., Li, K., Aoyama, T., Horvath, D., Chua, N.H., and Staskawicz, B.J. (1998). Glucocorticoid-inducible expression of a bacterial avirulence gene in transgenic Arabidopsis induces hypersensitive cell death. Plant J. *14*, 247–257. 10.1046/j.1365-313x.1998.00106.x.

31. Ngou, B.P.M., Ahn, H.-K., Ding, P., Redkar, A., Brown, H., Ma, Y., Youles, M., Tomlinson, L., and Jones, J.D.G. (2020). Estradiol-inducible AvrRps4 expression reveals distinct properties of TIR-NLR-mediated effector-triggered immunity. J. Exp. Bot. *71*, 2186–2197. 10.1093/jxb/erz571.

32. Derbyshire, M.C., and Raffaele, S. (2023). Till death do us pair: Co-evolution of plant-necrotroph interactions. Curr. Opin. Plant Biol. *76*, 102457. 10.1016/j.pbi.2023.102457.

33. Lai, Z., and Mengiste, T. (2013). Genetic and cellular mechanisms regulating plant responses to necrotrophic pathogens. Curr. Opin. Plant Biol. *16*, 505–512. 10.1016/j.pbi.2013.06.014.

34. Radojičić, A., Li, X., and Zhang, Y. (2018). Salicylic Acid: A Double-Edged Sword for Programed Cell Death in Plants. Front. Plant Sci. *9*, 1133. 10.3389/fpls.2018.01133.

35. Ding, P., Ngou, B.P.M., Furzer, O.J., Sakai, T., Shrestha, R.K., MacLean, D., and Jones, J.D.G. (2020). High-resolution expression profiling of selected gene sets during plant immune activation. Plant Biotechnol. J. *18*, 1610–1619. 10.1111/pbi.13327.

36. Sohn, K.H., Segonzac, C., Rallapalli, G., Sarris, P.F., Woo, J.Y., Williams, S.J., Newman, T.E., Paek, K.H., Kobe, B., and Jones, J.D.G. (2014). The nuclear immune receptor RPS4 is required for RRS1SLH1-dependent constitutive defense activation in Arabidopsis thaliana. PLoS Genet. *10*, e1004655. 10.1371/journal.pgen.1004655.

37. Ngou, B.P.M., Ahn, H.-K., Ding, P., and Jones, J.D.G. (2021). Mutual potentiation of plant immunity by cell-surface and intracellular receptors. Nature *592*, 110–115. 10.1038/s41586-021-03315-7.

38. Sun, T., Liang, W., Zhang, Y., and Li, X. (2018). Negative regulation of resistance protein-mediated immunity by master

transcription factors SARD1 and CBP60g. J. Integr. Plant Biol *60*, 1023–1027. 10.1111/jipb.12698.

39. Kraszewska, E. (2008). The plant Nudix hydrolase family. Acta Biochim. Pol. *55*, 663–671.

40. Bartsch, M., Gobbato, E., Bednarek, P., Debey, S., Schultze, J.L., Bautor, J., and Parker, J.E. (2006). Salicylic acid-independent ENHANCED DISEASE SUSCEPTIBILITY1 signaling in Arabidopsis immunity and cell death is regulated by the monooxygenase FMO1 and the Nudix hydrolase NUDT7. Plant Cell *18*, 1038–1051. 10.1105/tpc.105.039982.

41. Straus, M.R., Rietz, S., Ver Loren van Themaat, E., Bartsch, M., and Parker, J.E. (2010). Salicylic acid antagonism of EDS1-driven cell death is important for immune and oxidative stress responses in Arabidopsis. Plant J. *62*, 628–640. 10.1111/j.1365-313X.2010.04178.x.

42. Wang, H., Lu, Y., Liu, P., Wen, W., Zhang, J., Ge, X., and Xia, Y. (2013). The ammonium/nitrate ratio is an input signal in the temperature-modulated, SNC1-mediated and EDS1-dependent autoimmunity of nudt6-2 nudt7. Plant J. *73*, 262–275. 10.1111/tpj.12032.

43. Yu, D., Song, W., Tan, E.Y.J., Liu, L., Cao, Y., Jirschitzka, J., Li, E., Logemann, E., Xu, C., Huang, S., et al. (2022). TIR domains of plant immune receptors are 2',3'-cAMP/cGMP synthetases mediating cell death. Cell *185*, 2370-2386.e18. 10.1016/j.cell.2022.04.032.

44. Nawrath, C., and Métraux, J.P. (1999). Salicylic acid induction-deficient mutants of Arabidopsis express PR-2 and PR-5 and accumulate high levels of camalexin after pathogen inoculation. Plant Cell *11*, 1393–1404. 10.1105/tpc.11.8.1393.

45. Castel, B., Ngou, P.-M., Cevik, V., Redkar, A., Kim, D.-S., Yang, Y., Ding, P., and Jones, J.D.G. (2019). Diverse NLR immune receptors activate defence via the RPW8-NLR NRG1. New Phytol. *222*, 966–980. 10.1111/nph.15659.

46. Laflamme, B., Dillon, M.M., Martel, A., Almeida, R.N.D., Desveaux, D., and Guttman, D.S. (2020). The pan-genome effector-triggered immunity landscape of a host-pathogen interaction. Science *367*, 763–768. 10.1126/science.aax4079.

47. Falk, A., Feys, B.J., Frost, L.N., Jones, J.D., Daniels, M.J., and Parker, J.E. (1999). EDS1, an essential component of R gene-mediated disease resistance in Arabidopsis has homology to eukaryotic lipases. Proc Natl Acad Sci USA *96*, 3292–3297. 10.1073/pnas.96.6.3292.

48. Ordon, J., Gantner, J., Kemna, J., Schwalgun, L., Reschke, M., Streubel, J., Boch, J., and Stuttmann, J. (2017). Generation of chromosomal deletions in dicotyledonous plants employing a user-friendly genome editing toolkit. Plant J. *89*, 155–168. 10.1111/tpj.13319.

49. Wickham, H. (2016). ggplot2: Elegant Graphics for Data Analysis (Use R!) 2nd ed. (Springer).

50. Stefanato, F.L., Abou-Mansour, E., Buchala, A., Kretschmer, M., Mosbach, A., Hahn, M., Bochet, C.G., Métraux, J.-P., and Schoonbeek, H. (2009). The ABC transporter BcatrB from Botrytis cinerea exports camalexin and is a virulence factor on Arabidopsis thaliana. Plant J. *58*, 499–510. 10.1111/j.1365-313X.2009.03794.x.

51. Schoonbeek, H.-J., Yalcin, H.A., Burns, R., Taylor, R.E., Casey, A., Holt, S., Van den Ackerveken, G., Wells, R., and Ridout, C.J. (2022). Necrosis and ethylene-inducing-like peptide patterns from crop pathogens induce differential responses within seven brassicaceous species. Plant Pathol. *71*, 2004–2016. 10.1111/ppa.13615.

52. Livak, K.J., and Schmittgen, T.D. (2001). Analysis of relative gene expression data using real-time quantitative PCR and the 2(-Delta Delta C(T)) Method. Methods *25*, 402–408. 10.1006/meth.2001.1262.

53. Zhang, R., Kuo, R., Coulter, M., Calixto, C.P.G., Entizne, J.C., Guo, W., Marquez, Y., Milne, L., Riegler, S., Matsui, A., et al. (2022). A high-resolution single-molecule sequencing-based Arabidopsis transcriptome using novel methods of Iso-seq analysis. Genome Biol. *23*, 149. 10.1186/s13059-022-02711-0.

54. Bray, N.L., Pimentel, H., Melsted, P., and Pachter, L. (2016). Near-optimal probabilistic RNA-seq quantification. Nat. Biotechnol. *34*, 525–527. 10.1038/nbt.3519.

55. Guo, W., Tzioutziou, N.A., Stephen, G., Milne, I., Calixto, C.P., Waugh, R., Brown, J.W.S., and Zhang, R. (2021). 3D RNA-seq: a

powerful and flexible tool for rapid and accurate differential expression and alternative splicing analysis of RNA-seq data for biologists. RNA Biol. *18*, 1574–1587. 10.1080/15476286.2020.1858253.

56. Risso, D., Ngai, J., Speed, T.P., and Dudoit, S. (2014). Normalization of RNA-seq data using factor analysis of control genes or samples. Nat. Biotechnol. *32*, 896–902. 10.1038/nbt.2931.

57. Robinson, M.D., and Oshlack, A. (2010). A scaling normalization method for differential expression analysis of RNA-seq data. Genome Biol. *11*, R25. 10.1186/gb-2010-11-3-r25.

58. Law, C.W., Chen, Y., Shi, W., and Smyth, G.K. (2014). voom: Precision weights unlock linear model analysis tools for RNA-seq read counts. Genome Biol. *15*, R29. 10.1186/gb-2014-15-2-r29.

59. Ritchie, M.E., Phipson, B., Wu, D., Hu, Y., Law, C.W., Shi, W., and Smyth, G.K. (2015). limma powers differential expression analyses for RNA-sequencing and microarray studies. Nucleic Acids Res. *43*, e47. 10.1093/nar/gkv007.

60. Kolberg, L., Raudvere, U., Kuzmin, I., Adler, P., Vilo, J., and Peterson, H. (2023). g:Profiler-interoperable web service for functional enrichment analysis and gene identifier mapping (2023 update). Nucleic Acids Res. *51*, W207–W212. 10.1093/nar/gkad347.

61. Bailey, T.L., Johnson, J., Grant, C.E., and Noble, W.S. (2015). The MEME Suite. Nucleic Acids Res. *43*, W39-49. 10.1093/nar/gkv416.

62. McLeay, R.C., and Bailey, T.L. (2010). Motif Enrichment Analysis: a unified framework and an evaluation on ChIP data. BMC Bioinformatics *11*, 165. 10.1186/1471-2105-11-165.

Chapter 5
General Discussion

Himanshu Chhillar[1], Niels Aerts[2], Saskia CM Van Wees[2], Pingtao Ding[1]

1 Institute of Biology Leiden, Leiden University, 2333 BE Leiden, The Netherlands

2 Plant-Microbe Interactions, Department of Biology, Science4Life, Utrecht University, 3508 TB Utrecht, The Netherlands

The content of 5.6 from this chapter were published in this review article: Essays in Biochemistry (2022) Sep 30;66(5):607–620. doi: 10.1042/EBC20210100

5.1 A general overview of challenges in improving plant disease resistance

Plant innate immunity relies on a multilayered defense system involving both cell-surface pattern recognition receptors (PRRs) and intracellular nucleotide-binding leucine-rich repeat receptors (NLRs)[1]. While significant advances have been made in identifying the components and downstream signaling modules associated with both pattern-triggered immunity (PTI) and effector-triggered immunity (ETI), many critical questions remain unanswered[2]. In particular**,** how different NLR signaling branches (*e.g.*, ADR1- versus NRG1-mediated) coordinate distinct immune outputs, such as transcriptional reprogramming versus hypersensitive cell death[3–5], remains incompletely understood. Moreover, the spatio-temporal regulation of ETI across different cell types, and how such regulation contributes to immune specificity, strength, or trade-offs with growth, are emerging as key areas of investigation. While recent studies have begun to characterize individual modules, there is still limited clarity on how these modules function independently, redundantly, or synergistically under various immunogenic contexts. This study provides a multi-dimensional dissection of ETI in plants, integrating functional, spatial, and regulatory insights into how plants orchestrate immune responses with precision and flexibility. Building on a foundation of genetic, transcriptional, and cell-type-resolved approaches, we reveal a modular organization of the ETI network that is contextually specialized across signaling nodes, cell types, and transcriptional regulators.

5.2 Dissecting EDS1 module function under isolated ETI activation

At the core of Toll/interleukin-1 receptor (TIR)-NLR-mediated ETI signaling lies the ENHANCED DISEASE SUSCEPTIBILITY 1 (EDS1) node, which forms mutually exclusive heteromeric complexes with either PHYTOALEXIN DEFICIENT 4 (PAD4) or SENESCENCE-ASSOCIATED

GENE 101 (SAG101) to propagate downstream immune signaling via helper NLRs ACTIVATED DISEASE RESISTANCE 1 (ADR1s) and N REQUIREMENT GENE 1 (NRG1s)[4,6], respectively. Our analyses support a model of unequal redundancy[3,5,7], in which the EDS1-PAD4-ADR1 module predominantly contributes to disease resistance and transcriptional reprogramming, while the EDS1-SAG101-NRG1 module is more tightly linked to cell death (HR). We have employed the synthetic estradiol inducible ETI system i.e. Super ETI (SETI)[8] to isolate ETI specific responses of these modules. The functional divergence becomes especially evident under isolated ETI conditions, where SETI_*pad4* mutants show partial relief of growth inhibition and retain priming capacity **(Chapter 2)**, whereas SETI_*sag101* mutants exhibit more severe defects in HR and immune suppression[9]. These findings not only reinforce the idea of functional bifurcation within ETI signaling nodes but also highlight their synergistic roles in mediating immune robustness (**Chapter 2**). Curiously, the retention of ETI activated priming ability by immune compromised plants such as SETI_*pad4* open new venues for harnessing enhanced resistance in plants through prior learning, even when the immune system is not fully functional (**Chapter 2**).

5.3 Interplay between PTI and ETI

Importantly, our transcriptome data during different immune conditions (PTI, ETI, PTI+ETI) underscore the dominant influence of PTI in shaping early immune landscapes, where co-activation with PTI (PTI+ETI) can mask ETI-specific gene expression due to pathway convergence and cellular response saturation (**Chapter 2**). This suggests that while ETI contributes additional layers of defense**,** its distinct transcriptional signature is best revealed in isolation**.** Notably, the requirement of PTI for NRG1 resistosome formation[10], further illustrates the functional

interdependence between surface-localized and intracellular immune pathways.

5.4 Spatial regulation of immune responses

We further build on our understanding of modular ETI regulation by exploring its spatial dynamics at the single-cell level. While earlier sections of our study demonstrate that PAD4-ADR1 and SAG101-NRG1 modules contribute differentially to transcriptional reprogramming and cell death, respectively, it remained unclear how these immune outputs are orchestrated across the complex cellular architecture of a leaf. Our ETI single-cell transcriptomic atlas paints a compelling picture of broad transcriptional competence but spatially refined execution of immunity. Genes encoding core signaling nodes such as *EDS1*, *PAD4*, *SAG101*, and enzymes in the salicylic acid (SA) biosynthesis pathway are widely expressed across diverse cell types (**Chapter 3**), suggesting a uniform capacity for immune perception and signal propagation.

However, the downstream immune responses especially those involving metabolic branches such as N-hydroxypipecolic acid (NHP) and jasmonic acid (JA) pathways display marked cell-type-specific expression patterns, indicating that tissue identity imposes critical regulatory constraints. This tissue-intrinsic logic of immunity is further shaped by differential transcription factor activity, such as specific induction of WRKY8 in pavement cells and the upregulation of trihelix DNA-binding factors in hydathodes. Together, these findings challenge the previously assumed notion of homogeneous immune activation and instead support a model wherein cell-type-specific chromatin accessibility, transcription factor availability, and structural vulnerabilities collectively dictate the amplitude and nature of immune responses.

Importantly, the functional relevance of this spatial heterogeneity becomes particularly evident in the context of nonhost resistance (NHR). Although CBP60g and SARD1 are pathogen-responsive transcription factors and established master regulators of immune gene expression[11,12], our data show that their absence in specific outer tissue layers such as the epidermis or hydathodes allows haustorial entry by non-adapted pathogens (**Chapter 3**), underscoring that immune competence alone is not sufficient because precise spatial execution of transcriptional programs is essential for effective resistance**.** This provides direct evidence that cell-type-specific transcriptional regulation underlies a layered immune architecture**,** one that ensures maximal immune responsiveness at the most vulnerable tissue interfaces.

5.5 CBP60G and SARD1 as toolkit to uncouple disease resistance and cell death

This spatial dependence also complements the broader role of CBP60g and SARD1 in maintaining immune balance across tissues. In addition to their roles in activating SA biosynthesis, CBP60g and SARD1 also serve as key modulators of immune homeostasis (**Chapter 4**). The *cbp60g sard1* (*gh*) mutant exhibits an uncoupling of HR from disease resistance without any growth defects, a phenomenon rarely observed. Elevated HR in *gh* mutants, despite reduced SA levels and compromised ETI, points to transcriptional misregulation of genes encoding negative immune regulators (*e.g.*, NUDIX HYDROLASE 7 (*NUDT7*), *BON1 ASSOCIATED PROTEIN 1* (*BAP1*), *LESION SIMULATING DISEASE 1* (*LSD1*))[13–15], suggesting an imbalance in immune suppression **(Chapter 4**). These findings not only extend the functional repertoire of CBP60g/SARD1 beyond SA control but also provide a model for studying immune activated programmed cell death in plants.

Together, our findings converge on a modular model of ETI, wherein uniformly initiated immune signaling is interpreted through layers of spatial, functional, and transcriptional logic**.** The PAD4-ADR1 and SAG101-NRG1 branches act as parallel and partially redundant modules tuned to distinct immune outputs; cell-type-specific TFs provide regulatory precision; and PTI-ETI cross-talk modulates overall signal amplitude. This layered architecture ensures not only effective defense but also minimizes collateral damage and preserves growth under stress. The exaggerated HR observed in *gh* mutants where heightened cell death occurs in the absence of robust disease resistance serves as a striking example of what happens when transcriptional regulation within this modular framework is disrupted. This phenotype illustrates how loss of immune homeostasis can lead to the uncoupling of defense outputs, further emphasizing the need for tight regulatory coordination across all layers of the immune network.

5.6 Future perspectives

While these studies have illuminated modular aspects of ETI signaling and spatial immune execution, a comprehensive understanding of how transcriptional and signaling networks are integrated at the whole-organism and single-cell level remains incomplete. The robustness and specificity of plant immunity are contingent upon finely tuned gene regulatory mechanisms that coordinate responses across diverse cellular and environmental contexts. Yet the integration of these regulatory layers how they interface, under what circumstances they are engaged, and how they collectively shape immune outputs is still poorly understood.

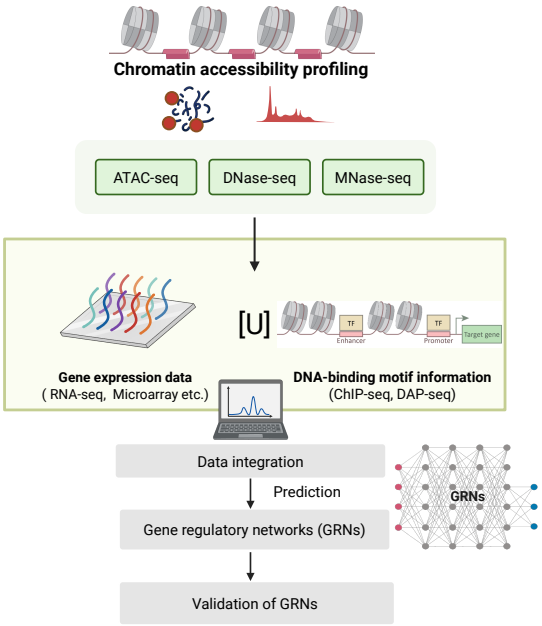

Figure 1. Next-generation toolkit for elucidating immune-responsive GRNs. Integration of data on TF DNA-binding, chromatin accessibility, and gene expression can be employed as a powerful tool to elucidate the highly interconnected gene regulatory networks (GRNs) that determine the plant immune transcriptome, even at single cell resolution. For instance, information related to TF-binding sites can be obtained from chromatin-immunoprecipitation followed by sequencing (ChIP-seq), and DNA affinity purification sequencing (DAP-seq). Information about chromatin status can be derived from methods such as Assay for Transposase-Accessible Chromatin using sequencing (ATAC-seq), micrococcal nuclease digestion with deep-sequencing (MNase-seq), or DNase-I hypersensitive sites sequencing (DNase-seq). Different variants of RNA (e.g. mRNA, miRNA, lncRNA) can be measured by RNA-seq. These data can be integrated to reveal GRNs that shape the plant immune transcriptome. The functionality of these GRNs can be tested and validated by mutant analysis under different conditions or in different tissues or cell types.

To unravel these complexities, future research must embrace a systems biology framework, leveraging the convergence of multi-omics technologies, advanced data integration, and predictive modeling[16,17]. This includes systematic comparisons of diverse immune-stimulatory treatments (e.g., PTI, ETI, and their combinations), coupled with genome-wide assays such as chromatin accessibility profiling (*e.g.*, ATAC-seq), epigenomic mapping (DNA/histone modifications), and transcriptomic analyses encompassing mRNAs, miRNAs, and lncRNAs. By integrating these datasets through computational modeling and machine learning approaches, we can begin to reconstruct the gene regulatory networks (GRNs) that govern immune signaling with both spatial and temporal resolution (**Figure 1**).

In parallel, single-cell technologies will be essential for dissecting GRNs at the resolution of individual cell types. Such approaches can identify cell-autonomous versus non-cell-autonomous responses, reveal transcriptional heterogeneity within tissues, and elucidate how immune signaling propagates across spatial domains. Addressing questions such as which immune responses are inherently cell-type-specific, and how factors like developmental stage, circadian rhythms, abiotic stress, or distance from the infection site influence immunity, will require high-throughput methods tailored for spatial and temporal precision. Tools like laser-capture microdissection, spatial transcriptomics, and dual host-pathogen single-cell profiling represent promising avenues to interrogate the intimate host-pathogen interface *in planta*.

Collectively, such integrative, high-resolution analyses will pave the way for a network-level understanding of plant immunity one that accounts for both global regulatory dynamics and local cellular context. These insights will not only clarify how plants maintain immune robustness under variable

conditions but will also provide actionable frameworks for rational engineering of crops with enhanced and durable resistance across diverse environmental and pathogen challenges.

Future work should aim to define the temporal dynamics of ETI execution, integrate chromatin accessibility data (*e.g.*, ATAC-seq, ChIP-seq), and expand cross-pathogen functional validation to better understand how these modules adapt to diverse pathogens. By dissecting the immune circuitry at such high resolution, we lay the groundwork for engineering durable and spatially targeted immune responses in crops a promising step toward achieving sustainable agriculture.

References

1. Jones, J.D.G., and Dangl, J.L. (2006). The plant immune system. Nature *444*, 323–329. 10.1038/nature05286.

2. Jones, J.D.G., Staskawicz, B.J., and Dangl, J.L. (2024). The plant immune system: From discovery to deployment. Cell *187*, 2095–2116. 10.1016/j.cell.2024.03.045.

3. Lapin, D., Kovacova, V., Sun, X., Dongus, J.A., Bhandari, D., von Born, P., Bautor, J., Guarneri, N., Rzemieniewski, J., Stuttmann, J., et al. (2019). A Coevolved EDS1-SAG101-NRG1 Module Mediates Cell Death Signaling by TIR-Domain Immune Receptors. Plant Cell *31*, 2430–2455. 10.1105/tpc.19.00118.

4. Sun, X., Lapin, D., Feehan, J.M., Stolze, S.C., Kramer, K., Dongus, J.A., Rzemieniewski, J., Blanvillain-Baufumé, S., Harzen, A., Bautor, J., et al. (2021). Pathogen effector recognition-dependent association of NRG1 with EDS1 and SAG101 in TNL receptor immunity. Nat. Commun. *12*, 3335. 10.1038/s41467-021-23614-x.

5. Saile, S.C., Jacob, P., Castel, B., Jubic, L.M., Salas-Gonzáles, I., Bäcker, M., Jones, J.D.G., Dangl, J.L., and El Kasmi, F. (2020). Two unequally redundant "helper" immune receptor families mediate Arabidopsis thaliana intracellular "sensor" immune receptor functions. PLoS Biol. *18*, e3000783. 10.1371/journal.pbio.3000783.

6. Wagner, S., Stuttmann, J., Rietz, S., Guerois, R., Brunstein, E., Bautor, J., Niefind, K., and Parker, J.E. (2013). Structural basis for signaling by exclusive EDS1 heteromeric complexes with SAG101

or PAD4 in plant innate immunity. Cell Host Microbe *14*, 619–630. 10.1016/j.chom.2013.11.006.

7. Wu, Z., Li, M., Dong, O.X., Xia, S., Liang, W., Bao, Y., Wasteneys, G., and Li, X. (2019). Differential regulation of TNL-mediated immune signaling by redundant helper CNLs. New Phytol. *222*, 938–953. 10.1111/nph.15665.

8. Ngou, B.P.M., Ahn, H.-K., Ding, P., Redkar, A., Brown, H., Ma, Y., Youles, M., Tomlinson, L., and Jones, J.D.G. (2020). Estradiol-inducible AvrRps4 expression reveals distinct properties of TIR-NLR-mediated effector-triggered immunity. J. Exp. Bot. *71*, 2186–2197. 10.1093/jxb/erz571.

9. Chhillar, H., Yeh, P.-M., Nguyen, H.H., Jones, J.D., and Ding, P. (2024). Modular mechanisms of immune priming and growth inhibition mediated by plant effector-triggered immunity. BioRxiv. 10.1101/2024.02.01.578334.

10. Feehan, J.M., Wang, J., Sun, X., Choi, J., Ahn, H.-K., Ngou, B.P.M., Parker, J.E., and Jones, J.D.G. (2023). Oligomerization of a plant helper NLR requires cell-surface and intracellular immune receptor activation. Proc Natl Acad Sci USA *120*, e2210406120. 10.1073/pnas.2210406120.

11. Zhang, Y., Xu, S., Ding, P., Wang, D., Cheng, Y.T., He, J., Gao, M., Xu, F., Li, Y., Zhu, Z., et al. (2010). Control of salicylic acid synthesis and systemic acquired resistance by two members of a plant-specific family of transcription factors. Proc Natl Acad Sci USA *107*, 18220–18225. 10.1073/pnas.1005225107.

12. Sun, T., Zhang, Y., Li, Y., Zhang, Q., Ding, Y., and Zhang, Y. (2015). ChIP-seq reveals broad roles of SARD1 and CBP60g in regulating plant immunity. Nat. Commun. *6*, 10159. 10.1038/ncomms10159.

13. Ge, X., Li, G.-J., Wang, S.-B., Zhu, H., Zhu, T., Wang, X., and Xia, Y. (2007). AtNUDT7, a negative regulator of basal immunity in Arabidopsis, modulates two distinct defense response pathways and is involved in maintaining redox homeostasis. Plant Physiol. *145*, 204–215. 10.1104/pp.107.103374.

14. Yang, H., Li, Y., and Hua, J. (2006). The C2 domain protein BAP1 negatively regulates defense responses in Arabidopsis. Plant J. *48*, 238–248. 10.1111/j.1365-313X.2006.02869.x.

15. Dietrich, R.A., Richberg, M.H., Schmidt, R., Dean, C., and Dangl, J.L. (1997). A novel zinc finger protein is encoded by the Arabidopsis LSD1 gene and functions as a negative regulator of plant cell death. Cell *88*, 685–694. 10.1016/s0092-8674(00)81911-x.

16. Leong, R., He, X., Beijen, B.S., Sakai, T., Goncalves, J., and Ding, P. (2025). Unlocking gene regulatory networks for crop resilience and sustainable agriculture. Nat. Biotechnol. *43*, 1254–1265. 10.1038/s41587-025-02727-4.

17. Aerts, N., Chhillar, H., Ding, P., and Van Wees, S.C.M. (2022). Transcriptional regulation of plant innate immunity. Essays Biochem. *66*, 607–620. 10.1042/EBC20210100.

Summary

Plants possess a sophisticated innate immune system composed of two major defense layers: pattern-triggered immunity (PTI) and effector-triggered immunity (ETI). Rather acting as independent pathways, PTI and ETI are highly interconnected and mutually reinforcing, together generating robust and durable immune responses. Over the past decades, extensive research has elucidated key components of plant immune architecture and signalling. However, the complexity and interconnectedness of immune signalling mean that key gaps remain in our understanding of the organisation and execution of ETI The research described in this thesis employs genetics and transcriptomics to define how ETI signalling is partitioned across distinct pathways and leaf cell types in *Arabidopsis thaliana* (Arabidopsis).

Chapter 1 provides an overview of the organizational principles underlying plant immunity, from pathogen perception at the cell surface and intracellular immune receptors to downstream signalling cascades and transcriptional reprogramming. Particular emphasis is placed on the regulatory layers that shape immune output, including calcium signaling and the CALMODULIN-BINDING PROTEIN 60 (CBP60) family of transcription factors, CBP60g and SYSTEMIC ACQUIRED RESISTANCE DEFICIENT 1 (SARD1)**,** which are central regulators of salicylic acid (SA)-dependent immunity. Although recent studies have demonstrated that PTI and ETI synergize to amplify immune responses, this interdependence has made it difficult to disentangle ETI-specific signalling. Because natural pathogen infection invariably activates PTI prior to ETI, dissecting ETI in isolation has remained a major experimental challenge. To overcome this limitation, this thesis employs a synthetic, estradiol-inducible ETI (SETI)

system, enabling precise activation and analysis of ETI signaling in absence of confounding PTI inputs.

Chapter 2 uses this inducible ETI system to dissect the functional contributions of two partially redundant signaling branches in Arabidopsis TIR-NLR–mediated immunity. We demonstrate that the two ENHANCED DISEASE SUSCEPTIBILITY 1 (EDS1) associated modules, EDS1-PHYTOALEXIN DEFICIENT 4 (PAD4)-ACTIVATED DISEASE RESISTANCE 1 (ADR1) and EDS1-SENESCENCE-ASSOCIATED GENE 101 (SAG101)-N REQUIREMENT GENE 1 (NRG1), play distinct roles during ETI execution. The PAD4-ADR1 is involved in disease resistance while NRG1-SAG101 branch is primarily responsible for triggering the hypersensitive response (HR), a localized form of programmed cell death. These results establish that disease resistance and HR represent separable outputs of ETI, rather than obligatorily coupled consequences of the same signalling process.

To uncover the transcriptional basis of this functional separation, we performed global transcriptome profiling in SETI_*pad4*, SETI_*sag101*, and SETI_*pad4 sag101* backgrounds following PTI, ETI, and combined PTI+ETI activation. These analyses revealed that PAD4 is the dominant driver of immune-induced transcriptional reprogramming, whereas the contribution of SAG101 becomes evident mainly in the SETI_*pad4 sag101* double mutant, highlighting a context-dependent redundancy between the two signalling branches. Furthermore, we identified node-specific gene regulatory signatures, with distinct sets of defense-related genes preferentially controlled by the PAD4–ADR1 or SAG101–NRG1 modules. Importantly, this chapter also demonstrates that immune priming can be retained even if immune signaling is partially compromised, indicating that plants can maintain immune memory without fully engaging

all ETI branches. This finding has practical implications for crop improvement, as it suggests that durable disease resistance may be achieved while minimizing the fitness costs associated with excessive immune activation.

Chapter 3 extends the concept of ETI modularity from signalling pathways to cellular and spatial organization. Using single-cell RNA sequencing (scRNA-seq), we resolved immune ETI-induced transcriptional responses at the level of individual leaf cell types. Although ETI activation is initiated broadly across the tissue, its transcriptional execution varies substantially between cell identities. A conserved core defense program is activated in most cell types, representing a shared ETI backbone, while additional immune modules are selectively deployed in specific cell types, reflecting differences in developmental state, chromatin accessibility, and transcription factor availability.

Comparison of single-cell ETI-responsive genes with bulk RNA-seq data confirms that these transcriptional programs represent authentic ETI outputs rather than artifacts of cell isolation. We further classify ETI-responsive genes into “generalists”, expressed across multiple cell types, and “specialists”, restricted to one or a few cell types. This distinction reveals a hierarchical immune organization in which broadly distributed defenses coexist with highly localized, cell-type-specific immune functions.

A key finding of this chapter is that transcription factors CBP60g and SARD1 are preferentially induced in epidermal pavement cells, the plant’s first physical barrier against pathogen invasion. Functional analyses show that loss of these regulators compromises the epidermis ability to restrict pathogen entry, even when inner tissues retain immune competence. These results demonstrate that effective ETI requires not only robust

signaling but also precise spatial deployment of immune regulators across tissue layers.

Chapter 4 focuses on CBP60g and SARD1 as central transcriptional regulators that enable plants to balance immune activation with cellular viability during ETI. Through genetic analysis, inducible ETI activation, and transcriptome profiling, we show that these transcription factors function not merely as positive regulators of SA-mediated immunity, but as master coordinators that integrate immune-promoting and immune-restraining programs.

The *cbp60g sard1* double mutant provides a striking genetic uncoupling of ETI outputs: ETI induction triggers exaggerated HR, yet pathogen resistance is markedly reduced. This demonstrates that HR is neither sufficient nor required for effective pathogen restriction, challenging the long-standing assumption that stronger cell death necessarily correlates with stronger immunity. Notably, the absence of major developmental defects in this mutant allows immune-specific phenotypes to be interpreted without confounding pleiotropic effects. Transcriptome analyses reveal that CBP60g and SARD1 simultaneously activate defense genes while maintaining expression of negative immune regulators, including Nudix hydrolases, thereby preventing uncontrolled or self-destructive immune activation. Their regulatory role can thus be understood as establishing a dynamic equilibrium that permits strong pathogen control while safeguarding cellular integrity.

In the concluding **Chapter 5**, these findings are integrated into a broader conceptual framework of plant immunity, and future research directions are discussed. Collectively, this thesis demonstrates that ETI is not a uniform or binary response, but a modular, tunable, and spatially coordinated immune system. By elucidating how core immune signaling

nodes interface with central transcriptional regulators across distinct cellular contexts, this work provides a foundation for developing strategies to engineer disease-resistant crops that maintain growth and yield, an essential goal for sustainable agriculture and plant biotechnology.

Samenvatting

Planten beschikken over een geavanceerd aangeboren immuunsysteem dat bestaat uit twee hoofdverdedigingslagen: pattern-triggered immunity (PTI) en effector-triggered immunity (ETI). PTI en ETI fungeren eerder als onafhankelijke routes; ze zijn sterk met elkaar verbonden en versterken elkaar wederzijds, waarbij ze samen robuuste en duurzame immuunresponsen genereren. In de afgelopen decennia heeft uitgebreid onderzoek belangrijke componenten van de immuunarchitectuur en signaaloverdracht van planten aan het licht gebracht. De complexiteit en onderlinge verbondenheid van immuunsignalering zorgen echter ervoor dat er belangrijke gaten blijven bestaan in ons begrip van de organisatie en uitvoering van ETI. Het onderzoek dat in deze scriptie wordt beschreven, gebruikt genetica en transcriptomics om te bepalen hoe ETI-signalering is verdeeld over verschillende pathway en bladceltypen bij *Arabidopsis thaliana* (Arabidopsis).

Hoofdstuk 1 geeft een overzicht van de organisatorische principes die ten grondslag liggen aan plantimmuniteit, van de perceptie van pathogeen aan het celoppervlak en intracellulaire immuunreceptoren tot downstream signaalcascades en transcriptionele herprogrammering. Bijzondere nadruk ligt op de regulerende lagen die de immuunoutput vormgeven, waaronder calciumsignalering en de CALMODULIN-BINDING PROTEIN 60 (CBP60) familie van transcriptiefactoren, CBP60g en SYSTEMIC ACQUIRED RESISTANCE DEFICIENT 1 (SARD1), die centrale regulatoren zijn van salicylzuur (SA)-afhankelijke immuniteit. Hoewel recente studies hebben aangetoond dat PTI en ETI samenwerken om immuunresponsen te versterken, heeft deze onderlinge afhankelijkheid het moeilijk gemaakt om ETI-specifieke signalering te ontwarren. Omdat tijdens natuurlijke pathogene infectie PTI onvermijdelijk activeert vóór ETI,

is het dissectieren van ETI in isolatie een grote experimentele uitdaging gebleven. Om deze beperking te overwinnen, maakt deze scriptie gebruik van een synthetisch, estradiol-induceerbaar ETI (SETI)-systeem, waardoor nauwkeurige activatie en analyse van ETI-signalering mogelijk is zonder verstorende PTI-inputs.

Hoofdstuk 2 gebruikt dit induceerbare ETI-systeem om de functionele bijdragen van twee gedeeltelijk redundante signaaltakken in Arabidopsis TIR-NLR-gemedieerde immuniteit te analyseren. We tonen aan dat de twee ENHANCED DISEASE SUSCEPTIBILITY 1 (EDS1) geassocieerde modules, EDS1-PHYTOALEXINE DEFICIENT 4 (PAD4)-ACTIVATED DISEASE RESISTANCE 1 (ADR1) en EDS1- SENESCENCE-ASSOCIATED GENE 101 (SAG101)-N REQUIREMENT GENE 1 (NRG1)) een verschillende rol spelen tijdens de uitvoering van ETI. De NRG1-SAG101-tak is voornamelijk verantwoordelijk voor het triggeren van de hypersensitive response (HR), een gelokaliseerde vorm van geprogrammeerde celdood. Deze resultaten stellen vast dat ziekteresistentie en HR scheidbare outputs van ETI zijn, in plaats van verplicht gekoppelde gevolgen van hetzelfde signaalproces.

Om de transcriptionele basis van deze functionele scheiding te achterhalen, voerden we globale transcriptomprofilering uit in SETI_*pad4*, SETI_*sag101* en SETI_*pad4 sag101* achtergronden na PTI-, ETI- en gecombineerde PTI+ETI-activatie. Deze analyses toonden aan dat PAD4 de dominante drijfveer is van immuun-geïnduceerde transcriptionele herprogrammering, terwijl de bijdrage van SAG101 vooral duidelijk wordt in de dubbele *mutant SETI_pad4 sag101,* wat een contextafhankelijke redundantie tussen de twee signaaltakken benadrukt. Daarnaast identificeerden we node-specifieke genregulatiesignaturen, met verschillende sets defensie-gerelateerde genen die bij voorkeur worden

gecontroleerd door de PAD4-ADR1 of SAG101-NRG1 modules. Belangrijk is dat dit hoofdstuk ook aantoont dat immuunpriming behouden kan blijven, zelfs als de immuunsignalering gedeeltelijk verzwakt is, wat aangeeft dat planten het immuungeheugen kunnen behouden zonder volledig alle ETI-takken te activeren. Deze bevinding heeft praktische gevolgen voor de verbetering van het gewas, omdat het suggereert dat duurzame ziekteresistentie kan worden bereikt terwijl de fitheidskosten die gepaard gaan met overmatige immuunactivatie worden geminimaliseerd.

Hoofdstuk 3 breidt het concept van ETI-modulariteit uit van signaalroutes naar cellulaire en ruimtelijke organisatie. Met behulp van single-cell RNA-sequencing (scRNA-seq) losten we immuun-ETI-geïnduceerde transcriptieresponsen op op het niveau van individuele bladceltypen. Hoewel ETI-activatie breed over het weefsel wordt geïnitieerd, varieert de transcriptie-uitvoering aanzienlijk tussen celidentiteiten. Een geconserveerd kernverdedigingsprogramma wordt in de meeste celtypen geactiveerd en vertegenwoordigt een gedeelde ETI-ruggengraat, terwijl aanvullende immuunmodules selectief worden ingezet in specifieke celtypen, wat verschillen weerspiegelt in ontwikkelingstoestand, chromatine-toegankelijkheid en beschikbaarheid van transcriptiefactoren.

Vergelijking van enkelcel ETI-responsieve genen met bulk RNA-seq-data bevestigt dat deze transcriptieprogramma's authentieke ETI-output vertegenwoordigen in plaats van artefacten van celisolatie. We classificeren ETI-responsieve genen verder in "generalisten", tot expressie gebracht over meerdere celtypen, en "specialisten", beperkt tot één of enkele celtypen. Dit onderscheid onthult een hiërarchische immuunorganisatie waarin breed verspreide verdedigingen naast sterk gelokaliseerde, celtype-specifieke immuunfuncties bestaan.

Een belangrijke bevinding van dit hoofdstuk is dat transcriptiefactoren CBP60g en SARD1 bij voorkeur worden geïnduceerd in epidermale wegtakcellen, de eerste fysieke barrière tegen pathogeneninvasie van de plant. Functionele analyses tonen aan dat het verlies van deze regulatoren het vermogen van de epidermis om de toegang van pathogeen te beperken aantast, zelfs wanneer het binnenste weefsel immuuncompetentie behoudt. Deze resultaten tonen aan dat effectieve ETI niet alleen robuuste signalering vereist, maar ook een precieze ruimtelijke inzet van immuunregulatoren over weefsellagen.

Hoofdstuk 4 richt zich op CBP60g en SARD1 als centrale transcriptieregulatoren die planten in staat stellen immuunactivatie in balans te brengen met cellulaire levensvatbaarheid tijdens ETI. Door genetische analyse, induceerbare ETI-activatie en transcriptomprofilering tonen we aan dat deze transcriptiefactoren niet alleen functioneren als positieve regulatoren van SA-gemedieerde immuniteit, maar ook als meestercoördinatoren die immuunbevorderende en immuunbeperkende programma's integreren.

De *cbp60g sard1* dubbele mutant zorgt voor een opvallende genetische ontkoppeling van ETI-outputs: ETI-inductie veroorzaakt een overdreven HR, maar de weerstand tegen ziekteverwekkers is aanzienlijk verminderd. Dit toont aan dat HR noch voldoende noch vereist is voor effectieve pathogeenbeperking, waarmee de lang bestaande aanname wordt uitgedaagd dat sterkere celdood noodzakelijkerwijs correleert met een sterkere immuniteit. Opmerkelijk is dat het ontbreken van grote ontwikkelingsdefecten in deze mutant het mogelijk maakt immuunspecifieke fenotypes te interpreteren zonder pleiotrope effecten te verstoren. Transcriptoomanalyses tonen aan dat CBP60g en SARD1 tegelijkertijd verdedigingsgenen activeren terwijl ze de expressie van

negatieve immuunregulatoren, waaronder Nudix-hydrolasen, behouden, waardoor ongecontroleerde of zelfdestructieve immuunactivatie wordt voorkomen. Hun regulerende rol kan dus worden begrepen als het vestigen van een dynamisch evenwicht dat sterke pathogeencontrole mogelijk maakt terwijl de celintegriteit wordt beschermd.

In het afsluitende **hoofdstuk 5** worden deze bevindingen geïntegreerd in een breder conceptueel kader van plantimmuniteit, en worden toekomstige onderzoeksrichtingen besproken. Gezamenlijk toont deze scriptie aan dat ETI geen uniforme of binaire respons is, maar een modulair, afstembaar en ruimtelijk gecoördineerd immuunsysteem. Door te verduidelijken hoe kern immuunsignaalknooppunten samenwerken met centrale transcriptieregulatoren over verschillende cellulaire contexten, biedt dit werk een basis voor het ontwikkelen van strategieën om ziekteresistente gewassen te ontwikkelen die groei en opbrengst behouden, een essentieel doel voor duurzame landbouw en plantenbiotechnologie.

Curriculum Vitae

Himanshu Chhillar (born 5 March 1997, Haryana, India) obtained his BSc in Life Sciences from the University of Delhi (2014–2017) and his MSc in Botany from Jamia Hamdard University, New Delhi (2017–2019). In 2022, he began his doctoral research under the supervision of Dr. Pingtao Ding at the Institute of Biology Leiden (IBL), Faculty of Science, Leiden University, the Netherlands, where he focused on understanding how plants coordinate immune responses at the transcriptional and cellular level. During his PhD, he investigated effector-triggered immunity (ETI) using an inducible immune activation system, enabling him to dissect ETI-specific transcriptional programs independent of pathogen variability. His work provided mechanistic insights into how ETI reshapes the plant immune transcriptome in a cell- types specific manner, identifying key components involved in pathogen restriction. He further demonstrated that plants with a compromised immune system can still be primed to mount effective resistance against pathogens. Collectively, these findings contribute to a deeper understanding of how plants mount an optimum immune response without any trade-offs and have potential implications for improving crop resistance and food security. Himanshu's work has resulted in several peer-reviewed publications and preprints, which have collectively received over 1,000 citations to date, as well as invited presentations at international meetings, including the Utrecht Plant Immunity Minisymposium (Netherlands) and the ZMBP Plant Innate Immunity Symposium (Germany). His work was recognized with the EPSO Young Plant Scientist Award (2025). In addition to his research, he has supervised four MSc and two HBO students, supporting them through structured project development, regular feedback, and presentation training, while fostering an inclusive and collaborative learning environment. He has also contributed to advanced MSc courses at the IBL, including Innate Immune Systems and Advanced Molecular Genetics and Biotechnology. He is currently continuing this line of research as a postdoctoral researcher under the supervision of Dr. Pingtao Ding at the IBL, with the aim of translating fundamental insights into strategies for enhancing crop disease resistance.